An analysis of pion-nucleon scattering at intermediate and high energies

Peter J. Ogden

AN ANALYSIS OF PION-NUCLEON SCATTERING

AT

INTERMEDIATE AND HIGH ENERGIES

AN ANALYSIS OF PION-NUCLEON SCATTERING

AT

INTERMEDIATE AND HIGH ENERGIES

THESIS SUBMITTED TO THE

UNIVERSITY OF DURHAM.

BY

PETER J. OGDEN B.Sc.(DUNELM)

FOR THE DEGREE OF DOCTOR OF PHILOSOPHY

DEPARTMENT OF PHYSICS
UNIVERSITY OF DURHAM

DATE: AUGUST, 1971

TO

MY PARENTS

ABSTRACT

A phenomenological analysis of pion nucleon scattering at intermediate and high energies is presented.

The intermediate energy range (2-5 GeV) is discussed in terms of a 'new' phase shift analysis which has been constructed from a series of single energy fits to an energy dependent model partial wave analysis. This 'new' phase shift solution exhibits a similar resonance structure to the energy dependent model but enjoys a much better fit to the scattering data, comparable with previous single energy analyses. We discuss the difficulties encountered in previous single energy analyses and illustrate the advantages and feasibility of the energy dependent analysis in which the partial waves satisfy the required smoothness criteria, by construction.

The high energy scattering data is discussed with reference to the Regge pole model and we exploit the analytic properties of the scattering amplitudes by the use of the Continuous Moment Sum Rules (C.M.S.R.). The sum rules provide a set of consistency equations between the high energy Regge parameters and the low and intermediate energy data which is represented by the phase shifts.

In previous analyses of the C.M.S.R., the energy at which they are evaluated has been taken as 2 GeV which corresponded to the maximum energy of available phase shift data. 2 GeV is a long way from the region where we expect the Regge representation to be valid and the saturation of the C.M.S.R. with only those trajectories identified in the high energy region is not obvious, since we may expect lower lying trajectories to be important at these energies.

We construct the C.M.S.R. at a higher cut off (5 GeV) from the 'new' phase shift solution and compare the results from a simultaneous analysis of the scattering data and C.M.S.R. at the two cut offs.

Several differences are apparent between the two analyses in particular we show that it is not possible to construct the A'^{-} and B^{+} amplitudes at 2 GeV via the C.M.S.R. without considering trajectories other than those identified in the high energy scattering region. We present evidence for a new vacuum trajectory which we associate with the η_{0+} (700) meson and this single vacuum trajectory alone constructs the amplitude B^{+} at high energies.

The total cross-section data is adequately described by the three trajectories P,P' and ρ in the energy range 5-20 GeV but the extrapolations of their contributions to the energy range (20-70 GeV) does not exhibit the energy dependence of the recent Serpukhov pion-nucleon total cross-section data.

There have been several models to account for this apparent change in behaviour at 20 GeV which involve the addition of further contributions to the conventional Regge pole terms and all these models give an adequate description of the total cross-section data over the whole energy range, which is not surprising considering their increased parameter freedom.

We consider two different possibilities of asymptopia which involve the addition of multi-pomeron cuts and dipole contributions respectively to the P,P',ρ Regge poles and we increase our information input to the analysis by the use of the F.E.S.R. as a series of constraint equations on the parameters of the fit.

We show that the size of the multi-Pomeron cuts identified from the scattering data and the C.M.S.R. are incompatible whereas a dipole solution satisfies both the scattering data and C.M.S.R.. We consider the possibility of Pomeranchuk theorem violation by the inclusion of an odd-signature dipole like term in the amplitude A'^{-} but we are unable to reach a decisive conclusion on the possible violation because of the large experimental errors on the Serpukhov data.

ACKNOWLEDGEMENTS

I should like to express my thanks to my supervisor Professor B. H. Bransden for his friendly guidance and assistance throughout this work and to the members of the Physics and Mathematics Departments in the University of Durham for many stimulating conversations.

In particular, I should like to mention Dr. P. D. B. Collins and Dr. A. D. Martin (who introduced me to the subject) and Mr. M. J. Symons for his many comments on this work.

I am most grateful to Mr. D. J. Harrison for his assistance in the preparation and execution of several programmes and to my patient typist Mrs. S. Robson.

I should also like to thank Mrs. Catherine R. Ogden for her valuable assistance, especially in the preparation of this thesis and the Science Research Council for the award of a research studentship enabling me to carry out this work.

PREFACE

Part of the work reported here has been done in collaboration with Professor B. H. Bransden and is published (Nuclear Physics B26 (1971) p.511-524).

No part of the work presented in this thesis has previously been submitted for a degree in this or any other University.

C O N T E N T S

continued ... /

continued ...

INTRODUCTION

At our present level of understanding, there are four basic interactions which are characterised by their relative strengths. If we take the strength of the strong interaction as one unit, then its relation in strength to the other three interactions, electromagnetic, weak and gravitational is given by the ratio $1 : 10^{-2} : 10^{-13} : 10^{-39}$.

The strong interaction forces provide the binding forces in nuclei, they are short range forces $\sim 10^{-13}$ cm. and beyond this the range of the interaction falls off exponentially. The electromagnetic interaction force is a long range force with the well known inverse square law behaviour. It is the electromagnetic force which binds the electrons in an atom to the nucleus and at these distances the strong interactions are negligible. The weak interactions are also short range forces, but from the foregoing their magnitude is reduced by a factor of 10^{-13} over strong interaction forces. Certainly weak interactions can not compete when strong interactions are possible, however, selection rules forbid certain strong interaction transitions and these interactions can proceed via the weak interaction. The gravitational force has the same inverse square law behaviour as the electromagnetic interaction, but from its relative magnitude compared to the other three interactions, it enters very little into our considerations of elementary particle reactions at sub-atomic distances.

This differentiation in types of interaction provides the first division in the classification of particles, those which interact via strong interactions, known as hadrons and those which do not, known as leptons and photon.

There are further classifications of the elementary particles which are associated with the various symmetries of the interactions. There are certain conservation laws which appear to be satisfied by all the interact-

ions, among these is the space-time symmetry of 'Lorentz invariance', which implies energy, momentum and angular momentum are conserved. Other quantum numbers which appear to be conserved are charge Q, baryon number B and lepton number L.

With any elementary particle we have an associated type of statistics, depending on whether the state vector describing a system of identical particles is symmetric or antisymmetric under the interchange of any two particles. The statistics describe a fundamental property of the particles; particles for which the state vector is symmetric are called 'bosons' and antisymmetric 'fermions'. There is a simple connection between the particle statistics and spin which gives bosons integral spin and fermions half-odd integral spin.

Hadrons include both fermions and bosons. Those hadrons which are also fermions are termed baryons, the lightest of these is the proton, and those which are also bosons are termed meson of which the pion is a spin zero meson.

There are other symmetries which may not be exact for all interactions but are satisfied by strong interactions. Charge conjugation operator C replaces particles by their anti-particles, parity operator P corresponds to space inversion and the operator T defines time reversal. The symmetries associated with these operators C, P and T is such that all strong interactions are invariant under a combination of all three taken together.

It has long been observed that the neutron and proton although differing in charge are indistinguishable in strong interactions. This property of the strong interaction is termed 'charge independence'. As further strongly interacting particles have been observed these too occurred in multiplets of differing charge but with similar strong interaction properties. The symmetry associated with charge independence is the symmetry of

the group SU(2). With each SU(2) multiplet, there are two corresponding quantum numbers I and I_3 (I is the total isotopic spin, analgous to J for ordinary spin and I_3 indicates the position of a particle in a multiplet in analogy with J_z for ordinary spin). I_3 or the 'z' component of isotopic spin is related to the charge Q by the following relation:

$$Q = I_3 + Y/2 \qquad Y = B+S \qquad \text{I}$$

where B is the baryon number, Y the hypercharge and S the strangeness quantum number

It would be very fortunate if there was a basic theoretical model which covered such a large range of interaction strengths, a priori, no distinction in the types of interaction would be necessary. The theoretical treatment of the electromagnetic interaction using the formalism of quantum field theory is based on the construction of an interaction Hamiltonian, the fine structure constant and electron mass appearing as fundamental constants of the theory.

Attempts to construct an interaction Hamiltonian, which could be applied in a field theoretic framework to describe strong interactions, have so far been unsuccessful. The approach which has enjoyed most success in describing the strong interactions of elementary particles is based on the unitarity, analyticity and crossing of the so-called S matrix. Because of its short range, any strong interaction can be regarded as a transition between an ingoing state $|i\rangle$ and an outgoing state $|f\rangle$, each describing a system of non interacting physical particles. The amplitude for such a transition is denoted by

$$S_{fi} = \langle f|S|i\rangle \qquad \text{II}$$

The S matrix is constructed of all possible transition amplitudes and so in principle each element is a directly observable quantity. The 'conservation

of probability' require that the S-matrix is unitary, i.e.

$$\sum_n S^{\dagger}_{fn} S_{ni} = \delta_{fi} \qquad \text{III}$$

The S matrix as postulated, is a powerful tool in the understanding of elementary particle reactions, but as it stands it is incomplete. In an analogy with potential scattering, "the force giving rise to the interaction is not defined".

The exact nature of the strong interaction force is still an unsolved problem, but several hypotheses are available. Consider a scattering process in which all the particles are

$$a + b \rightarrow c + d \qquad (1)$$

strongly interacting (for simplicity consider the spinless case). The scattering process is described by a single amplitude which is a function of two independent variables, e.g. centre of mass energy and scattering angle. An important consequence of the analyticity of the S-matrix is 'crossing' whereby the processes (1), (2) and (3) are related and can be described by a single amplitude.

$$a + b \rightarrow c + d \qquad (1)$$
$$\bar{d} + b \rightarrow c + \bar{a} \qquad (2)$$
$$\bar{c} + b \rightarrow \bar{a} + d \qquad (3)$$

It is customary to define three new invariants s, t and u which correspond to the squares of the centre of mass energies for processes (1), (2) and (3) respectively. To each process there is a certain range of values of the respective invariant for which the scattering process corresponds to a physical energetically possible one. These physical ranges of the variables s, t and u are non-overlapping, so that an analytic continuation must

be defined to relate the scattering amplitudes in each region.

The Mandelstam representation defines a prescription for continuation, the scattering amplitude is assumed to be the same analytic function of s, t and u, with only those singularities demanded by imposing unitarity in each process channel (1), (2) and (3), for all three processes. This is referred to as the 'Maximal Analyticity of the first kind' of the S-matrix, - the singularities resulting from unitarity in one channel, help to determine the form of the amplitude in the physical region of the other channels. These crossed channel singularities, in analogy with potential scattering, provide the 'force' for the strong interaction.

Maximal analyticity of the S-matrix implies that all other singularities can be found, given the poles but it does not restrict the number of poles introduced into the S matrix. The question is how much information, how many particle masses and couplings, if any, must be introduced into the theory. A self-consistent picture of hadron physics would have all the hadron couplings and masses ultimately related and all 'particles' would be composite {i.e. generated by other singularities of the amplitude}. However if they are 'elementary particles' {analgous to the electron in Q.E.D.} can they be distinguished from composite particles? The answer to the problem is bound up with the angular momentum properties of the S-matrix.

Consider the contribution to the s-channel amplitude of the process (1) from the exchange of a particle mass m, spin α in the crossed channel. At high energies, elementary field theory indicates that the contribution behaves like

$$A(s,t) \sim \frac{S^{\alpha}}{t-m^2} \qquad \text{IV}$$

It can be shown by combining the unitarity and analyticity of partial wave amplitudes that the amplitude describing high energy forward scattering must

satisfy the 'Froissart Bound' given in equation V

$$|A(s,t=0)| < \text{const.}\, s\, (\log s)^2 \quad s \to \infty \qquad \text{V}$$

Certainly the behaviour of the scattering amplitude at high energies, from the exchange of a fixed spin $\alpha = 2$ particle in the forward direction $[t = 0]$, violates this bound. The problem has arisen because the spin of the particle is assumed to be a constant, not only when the particle is produced and is real ($t=m^2$) but also when it is exchanged and is virtual ($t<0$). In terms of the Mandelstam representation particles with spin greater than one cannot be represented simply by pole terms.

A possible way out of the difficulty was proposed by Chew and Frautschi, who translated some results of T. Regge in potential scattering to the relativistic situation. The amplitude is expressed in terms of its singularities in the complex angular momentum plane (ℓ-plane), these singularities are supposed to be poles giving contributions to the amplitudes of the form Equation VI

$$A(s,t) = \beta(t) \frac{P_{\alpha(t)}(\text{Cos}\theta)}{\sin \pi\, \alpha(t)} + B(s,\text{Cos}\theta) \qquad \text{VI}$$

where α and β are the positions and residue of the pole in the complex plane. As the centre of mass energy 't' varies, the pole moves in the complex ℓ plane along a trajectory $\ell = \alpha(t)$ and when ℓ passes through the physical integral values we have a bound state pole. The problem, arising from high spin particles, is then averted by requiring $\alpha(t) < 1$ in the s channel physical region $\{t < 0 \quad s > 0\}$.

It is now generally believed that the strong interaction forces are due to the exchange of these 'Regge Poles'. Such a prescription gives definite predictions for the behaviour of the high energy scattering amplitude and the Regge hypothesis has been successful in the correlation of much

high energy scattering data.

Most of the interest in Regge theory has centred on the phenomenological implications of Regge theory rather than its relation to the fundamental dynamical principles. In fact it can be argued that our understanding of the fundamental dynamics lying behind the success of Regge phenomenology has made very little if any real progress since the introduction of Regge's ideas into the S-matrix. Such a situation is not surprising when we hope to arrive at the dynamics through phenomenology and the latter is in no way complete.

CHAPTER 1

GENERAL KINEMATICS

In high energy scattering experiments, a beam of charged particles is scattered off a fixed proton or neutron target. In a diagramatic representation of the scattering event, for a non-production two body process, there are two particles entering the interaction region in the initial state and two particles emerging in the final state.

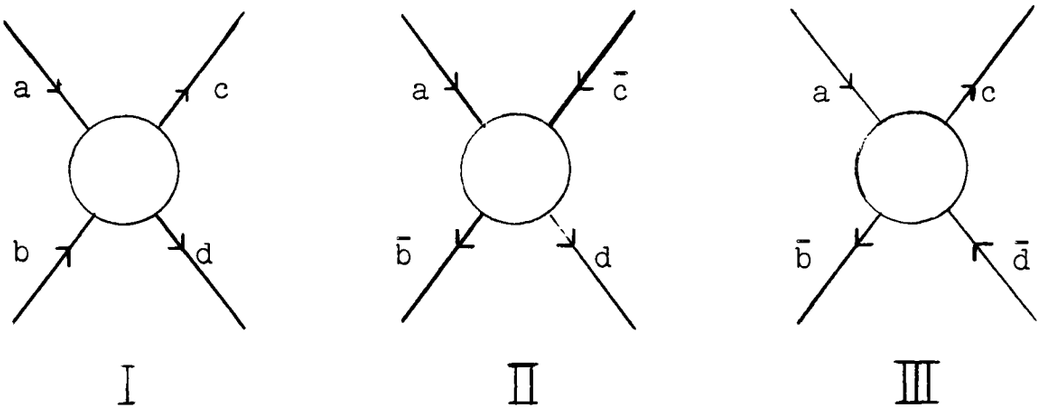

FIG.1

The single diagram can describe the three processes I, II and III

$$a + b \rightarrow c + d \qquad \text{I}$$
$$a + \bar{c} \rightarrow \bar{b} + d \qquad \text{II}$$
$$a + \bar{d} \rightarrow c + \bar{b} \qquad \text{III}$$

It is convenient to label all the particle momenta as ingoing and pa, pb, pc, pd denote the four momenta of particles a, b, c, d respectively.

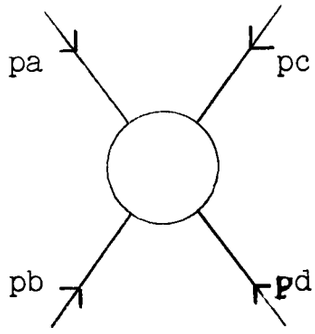

FIG.2

The following three invariants s, t and u [1] [2] are defined as below, where the second equality in each case follows from energy momentum conservation:

$$pa + pb + pc + pd = 0 \qquad 1.1$$

$$\begin{aligned} s &= -(pa+pb)^2 = -(pc+pd)^2 && (a) \\ t &= -(pa+pc)^2 = -(pb+pd)^2 && (b) \qquad 1.2 \\ u &= -(pa+pd)^2 = -(pc+pb)^2 && (c) \end{aligned}$$

It is usual to discuss the scattering process in a particular frame of reference, the two most used being the centre of mass frame (c.m. system) and the laboratory frame (lab. system).

CENTRE OF MASS FRAME

In the centre of mass frame the total three momentum of the ingoing particles is zero and hence also of the outgoing.

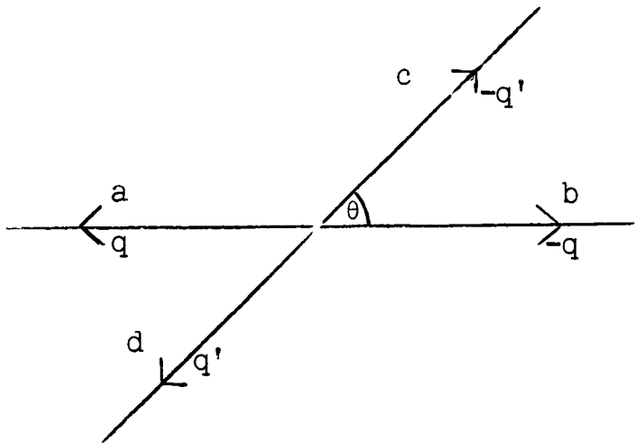

FIG. 3

The three momenta of the ingoing particles are denoted by q and -q and similarly those of the outgoing by q' and -q'. Writing the four momenta explicitly.

$$\begin{aligned} pa &= (-Ea, q) & pc &= (Ec, -q') \\ pb &= (-Eb, -q) & pd &= (Ed, q') \end{aligned} \qquad 1.3$$

where Ea, Eb, Ec, Ed denote the centre of mass energies of the particles. The mass shell constraints require that:

$$\begin{aligned} -pa^2 &= Ea^2 - q^2 = ma^2 \\ -pb^2 &= Eb^2 - q^2 = mb^2 \\ -pc^2 &= Ec^2 - q'^2 = mc^2 \\ -pd^2 &= Ed^2 - q'^2 = md^2 \end{aligned} \qquad 1.4$$

where ma, mb, mc, md denote the particle masses. The invariants s, t and u, expressed in terms of the foregoing are given in equations 1.5

$$\begin{aligned} s &= -(pa+pb)^2 = (Ea+Eb)^2 \\ t &= -(pa+pc)^2 = (Ea-Ec)^2 - (q-q')^2 \\ u &= -(pa+pd)^2 = (Ea-Ed)^2 - (q+q')^2 \end{aligned} \qquad 1.5$$

LABORATORY FRAME

In the laboratory frame the target particle is at rest. The energy, three momenta of the incident and outgoing particles are denoted by W_L, q_L and W_L', q_L' respectively.

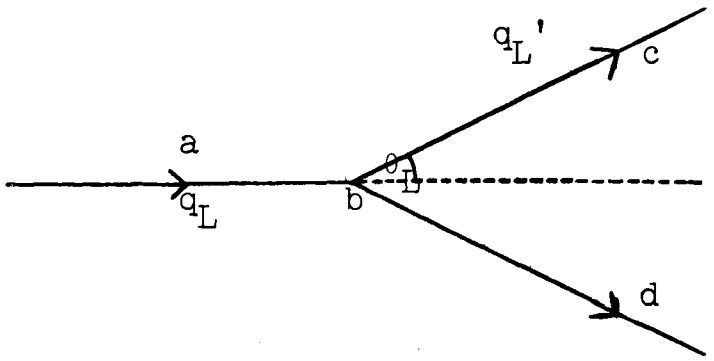

FIG.4

The four vectors pa, pb, pc, pd are written explicitly as

$$pa = (-W_L, q_L) \qquad pc = (W_L', -q_L')$$
$$pb = (-Mb, 0) \qquad pd = (W_L + Mb - W_L', q_L' - q_L) \qquad 1.6$$

The invariants s and t are given in terms of the laboratory parameters in equations 1.7

$$s = -(pa+pb)^2 = (W_L+Mb)^2 - q_L^2 = Ma^2 + Mb^2 + 2W_L\, Mb$$
$$t = -(pa+pc)^2 = -2W_L\, W_L' + 2Ma^2 + 2q_L q_L' \cos\theta_L \qquad 1.7$$

q_L and θ_L (the laboratory scattering angle) are expressed in terms of the centre of mass parameters by equating the invariants as defined in each frame of reference. Simple manipulation yields

$$q_L = \frac{W}{Mb}\, q_{cm} \qquad 1.8$$

where $W = \sqrt{s}$ is the centre of mass energy.

PION-NUCLEON SCATTERING - KINEMATICS - MANDELSTAM REPRESENTATION

The basic principles of crossing and analyticity as outlined in the Introduction indicate that the three processes 1, 2 and 3 can be described by the same analytic function of the Mandelstam invariants s, t and u.

$$\pi^- p \rightarrow \pi^- p \quad \ldots\ldots 1$$

$$\pi^+ p \rightarrow \pi^+ p \quad \ldots\ldots 2$$

$$\pi^+ \pi^- \rightarrow p \bar{p} \quad \ldots\ldots 3$$

If the pion mass and nucleon mass are denoted by μ and M then from the considerations of general kinematics only two of the

$$s + t + u = 2M^2 + 2\mu^2 = \Sigma \qquad 1.9$$

Mandelstam variables are independent.

In the centre of mass frame of process 1, the invariants can be written from equations 1.5 as

$$s = (\sqrt{M^2+q^2} + \sqrt{\mu^2+q^2})^{1/2} = W^2$$

$$t = -2q^2 (1-\cos\theta) \qquad 1.10$$

$$u = \frac{((W+M)^2 - \mu^2)((W-M)^2 - \mu^2)}{4s}$$

where q and θ are the centre of mass momenta and scattering angle respectively. From the inversion of equations 1.10 these quantities are written as:

$$q^2 = \frac{1}{4s} (s - (M+\mu)^2)(s - (M-\mu)^2)$$

$$\cos\theta = \frac{1}{4sq^2} (s^2 + s(2t-\Sigma) + (M^2-\mu^2)^2) \qquad 1.11$$

In the laboratory frame, from equations 1.7 the invariant s is written

$$s = M^2 + \mu^2 + 2M\,W_L \qquad 1.12$$

where W_L is the pion laboratory energy.

The range of the variables s, t and u, which correspond to a physical, energetically possibible process, is termed the 'physical region' for that process. A Mandelstam [3] diagram can be constructed for the three invariants in two dimensions by drawing the axes s = 0, t = 0 and u = 0 to form an equilateral triangle. Fig.5.

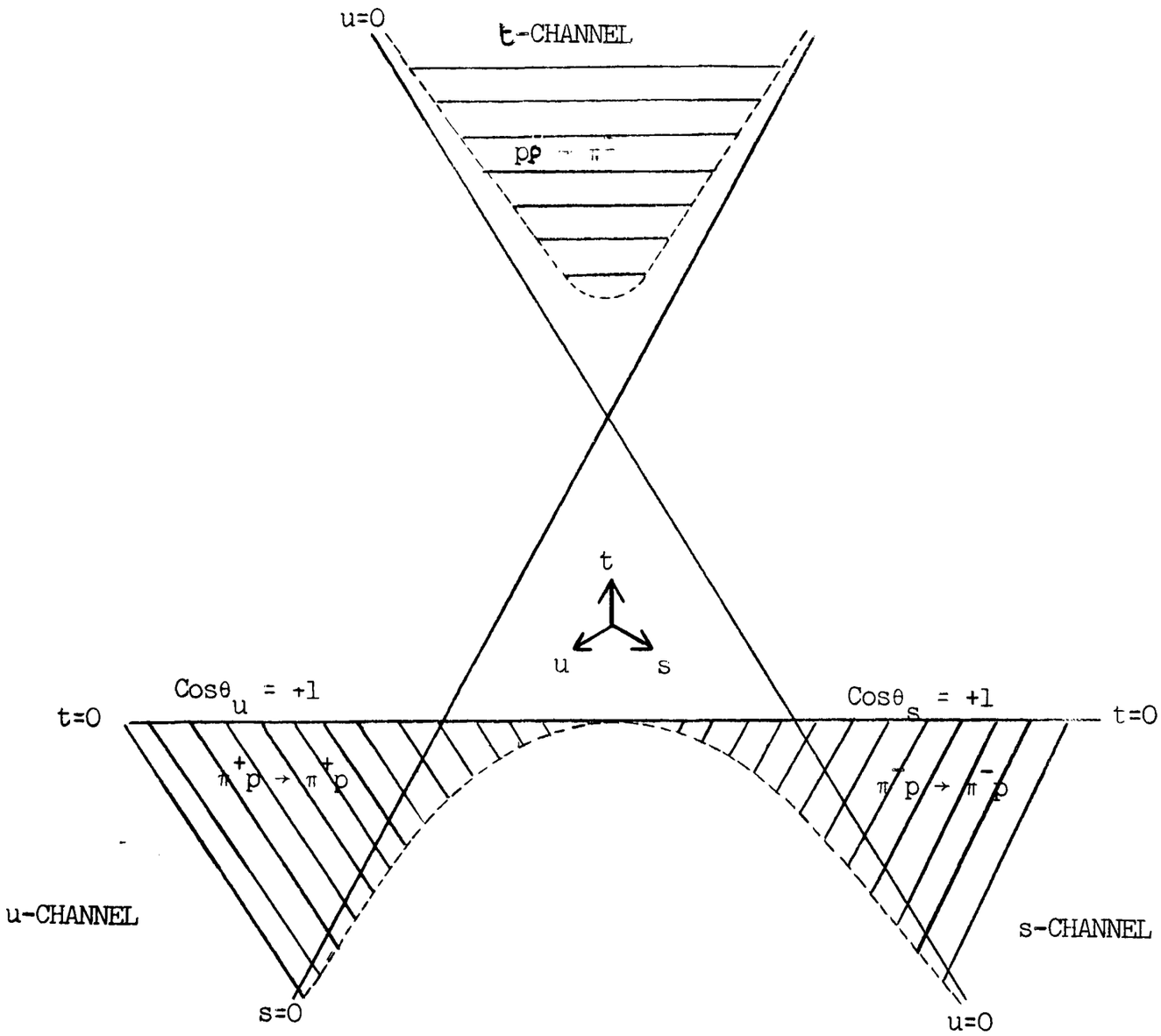

FIG.5

The s-channel physical region is defined for $q_s \geq 0$ and $-1 \leq \cos\theta_s < 1$. The values of the invariants for this range are:

$$\pi^- p \to \pi^- p \qquad s \geq (M+\mu)^2 - 4q_s^2 \leq t \leq 0 \quad \ldots\ldots 1$$

Similarly the physical regions of process 2 is given by

$$\pi^+ p \to \pi^+ p \qquad u \geq (M+\mu)^2 \qquad t \leq 0 \quad \ldots\ldots 2$$

and the physical regions of process 3:

$$\pi\bar{\pi} \to p\bar{p} \qquad t \geq 4M^2 \qquad s \leq 0 \qquad u \leq 0 \quad \ldots\ldots 3$$

SCATTERING AMPLITUDES - T MATRIX

The S matrix element $\langle f|s|i\rangle$ is the probability amplitude for an initially observed free particle state $|i\rangle$ to be observed as the final free particle state $|f\rangle$. There are two distinct ways in which this result can come about: the first is that the particles do not interact at all, the amplitude for this being simply $\langle f|i\rangle$; the other way is through an actual interaction of the particles and the amplitude for this is denoted by 'i' times the so called T matrix element $\langle f|T|i\rangle$. The total amplitude is written as a sum of these separate amplitudes.

$$\langle f|S|i\rangle = \langle f|i\rangle + i\,\langle f|T|i\rangle \qquad 1.13$$

The aggregate of T matrix elements defines an operator T in terms of which Equation 1.13 can be written

$$S = 1 + i\,T \qquad 1.14$$

For pion nucleon scattering the S matrix can be written [4]

$$S = \delta fi - i(2\pi)^4 \, \delta^4 \, (p_2+q_2-p_1-q_1) \left[\frac{M^2}{4E_1E_2W_1W_2}\right] \bar{U}_2 \, T \, U_1 \qquad 1.15$$

where p_1E, p_2E_2 denote the four momenta and energy of the ingoing and outgoing nucleon and q_1W_1, q_2W_2 denote the four momenta and energy of the ingoing and outgoing pion.

U_1 and U_2 are the spinors in the intial and final state. Momentum conservation: $p_1 + q_1 = p_2 + q_2$ permits only three independent four vectors to be constructed

$$P = \tfrac{1}{2} (p_1+p_2), \; Q = \tfrac{1}{2} (q_1+q_2), \; K = \tfrac{1}{2} (q_1-q_2) = \tfrac{1}{2} (p_2-p_1) \qquad 1.16$$

The mass shell constraints (see equation 1.4) allow two scalars only to be constructed from P, Q and K, and these are:

$$\nu = \frac{P.Q}{M} \quad , \quad K^2 \qquad 1.17$$

Consequently the T matrix can be expressed as a function of $\nu + K^2$ only.

Since the T matrix must be invariant under Lorentz transformations, it is necessary to express it in terms of invariants constructed from the independent four vectors P, Q and K and the Dirac matrices γ^u where:

$$\begin{aligned} \{i \, \gamma.p_1 + M\} \, u_1 &= 0 \\ \{i \, \gamma.p_2 + M\} \, u_2 &= 0 \end{aligned} \qquad 1.18$$

The invariants constructed from $i \, \gamma.P$, and $i \, \gamma.K$ can be taken through the matrix element until they act on the final and initial state spinors, Equation 1.15, where from equation 1.18, they give a constant. {The spinor normalisation is $\bar{u}_2u_2 = \bar{u}_1u_1 = 1$}.

The only independent scalar that can be constructed is $i \, \gamma.Q$ and the T matrix is written:

$$T = -A + i\gamma_5 Q\, B \qquad 1.19$$

where A and B are invariant scalar functions of ν and K^2 {simply related to s and t}. A is independent of the nucleon spin and B is associated with nucleon spin by the factor $\gamma_5 Q$.

HELICITY AMPLITUDES

The free particle states $|i\rangle$ and $|f\rangle$ in equation 1.13 are constructed from the combination of non-interacting single particle states. A single particle state can be labelled by $|j,m\ ;\ \bar{p},\tau\rangle$ where m is the particle mass, $\bar{p}$ the momentum, j the total spin and τ the spin index. These vectors correspond to an irreducible representation of the Lorentz Group and represent the direct product: [2]

$$|j,m\ ;\ \bar{p},\tau\rangle = |\bar{p},m\rangle \otimes |j,\tau\rangle = |P\rangle \otimes |\alpha\rangle \qquad 1.20$$

where α labels the states of the little group of P.

It is necessary to correlate the spin index with the direction of spin of the particles. It is not possible to construct simultaneous eigenstates of the momentum operator with the z component of spin since,

$$[\vec{p}.\vec{\tau}] \neq 0 .$$

However it is possible to construct simultaneous eigenstates of the momentum operator and the projection of spin along the direction of motion.

$$\text{i.e.} \quad J.P\ |m,j\ ;\ \bar{p},\tau\rangle = \tau|p|\ |m,j\ ;\ \bar{p},\tau\rangle$$

and $$\lambda = \frac{\vec{J}.\vec{P}}{|p|} \quad \text{is termed the helicity.} \qquad 1.21$$

A non-interacting two particle state can be described by the direct product

of two single particle state vectors. For simplicity the notation is abbreviated to

$$|p_1 p_2 \; ; \; \lambda_1 \lambda_2\rangle = |m_1, j_1 \; ; \; p_1 \lambda_1\rangle \otimes |m_2, j_2 \; ; \; p_2 \lambda_2\rangle \qquad 1.22$$

where $\lambda_1 \lambda_2$ are the helicities in the initial and final states and $p_1 p_2$ are now the four momenta of the particles respectively.

The two particle states in the centre of mass system are labelled by $|p\ \theta\ \phi,\ \lambda_1 \lambda_2\rangle$ where $p_1 = -p_2 = p$ and θ and ϕ define the direction of the relative momentum.

It is possible to remove any dependence on P from the vectors $|\alpha\rangle$ by defining the new vectors:

$$|\theta\ \phi, \lambda_1 \lambda_2\rangle = \left[\frac{q}{4\sqrt{s}}\right]^{1/2} |\alpha\rangle \qquad 1.23$$

such that the centre of mass state vectors are given by

$$|p\ \theta\ \phi, \lambda_1 \lambda_2\rangle = \left[\frac{4\sqrt{s}}{q}\right]^{1/2} |p\rangle \otimes |\theta\ \phi, \lambda_1 \lambda_2\rangle \qquad 1.24$$

If the S matrix is written as a direct product then since the state

$$S = I \otimes S_p$$

vectors $|i\rangle$ and $|f\rangle$ have a direct product representation

$$\langle f|S|i\rangle = \langle P_f|P_i\rangle \langle \alpha_f|S_p|\alpha_i\rangle \qquad 1.25$$

The T matrix can also be written as a direct product such that

$$T = I \otimes T_p$$

$$\langle f|S|i\rangle = \langle f|i\rangle + i\langle P_f|P_i\rangle \langle \alpha_f|T_p|\alpha_i\rangle \qquad 1.26$$

and the Lorentz Invariant T matrix elements are written as

$$\langle \alpha_f | T_p | \alpha_i \rangle = \frac{4\sqrt{s}}{(qq')^{1/2}} \langle \theta'\phi', \lambda' | T_p | \theta\ \phi, \lambda \rangle \qquad 1.27$$

where $\lambda\lambda'$ are the net helicities in the initial and final states and $(\theta\phi)$, $(\theta'\phi')$ label the directions of the momenta q,q' respectively.

The choice of the coordinate axes in the centre of mass frame relative to which the polar angles $\theta\ \phi$, $\theta'\phi'$ are measured is arbitrary and a convenient choice is one which makes the polar angles in the initial state zero. The T matrix element can then be written as

$$T_{\lambda'\lambda}(s,t) = \langle \theta'\ \phi', \lambda' | T_p | 0\ 0, \lambda \rangle \qquad 1.28$$

and in the case of elastic scattering, helicity amplitudes $g_{\lambda'\lambda}(\theta\phi)$ are defined such that

$$g_{\lambda'\lambda}(\theta\ \phi) = \frac{2\pi}{q} \langle \theta\ \phi, \lambda' | T_p | 0\ 0, \lambda \rangle \qquad 1.29$$

and the differential cross-section is then

$$\left[\frac{d\sigma}{d\Omega}\right]_{cm} = |g_{\lambda'\lambda}(\theta,\phi)|^2 \qquad 1.30$$

HELICITY AMPLITUDES-CROSSING

The crossing postulate requires that the s channel centre of mass T matrix elements should be the same analytic functions of the invariants as the t channel elements apart from the need to rotate the helicities from the direction of motion in one centre of mass system to the other. It is customary to define s and t channel relativistic helicity amplitudes $f^s_{\lambda(s)}(s,t)$, $f^t_{\lambda(t)}(s,t)$ where $\lambda(s)$, $\lambda(t)$ label the helicities in each channel

by:

$$f^{s}_{\lambda(s)}(s,t) = 8\pi\sqrt{\frac{s\, q_s}{q_s'}}\; g_{\lambda(s)}\,(\theta_s,\phi_s)$$

$$f^{t}_{\lambda(t)}(t,s) = 8\pi\sqrt{\frac{t\, q_t}{q_t'}}\; g_{\lambda(t)}\,(\theta_t,\phi_t) \qquad 1.31$$

and q_s, q_s' and q_t, q_t' are the initial and final state momenta in the s and t channels respectively. The crossing relation is then written:

$$f^{s}_{\lambda(s)}(s,t) = \sum_{\lambda(t)} M^{\lambda(t)}_{\lambda(s)}\,(s,t)\, f^{t}_{\lambda(t)}(t,s) \qquad 1.32$$

where $M^{\lambda(t)}_{\lambda(s)}\,(s,t)$ is the crossing matrix. Because of the orthogonality of the crossing matrix the differential cross sections are written:

$$\left[\frac{d\sigma}{d\Omega}\,(s,t)\right]_{cm} = \frac{1}{64\pi^2 s}\;\left|f^{s}_{\lambda(s)}(s,t)\right|^2 = \frac{1}{64\pi^2 s}\;\left|i^{t}_{\lambda(t)}(s,t)\right|^2 \qquad 1.33$$

PION NUCLEON AMPLITUDES - PARTIAL AMPLITUDES

The helicity amplitudes have a simple decomposition [5] in terms of partial amplitudes. The term partial wave amplitude is reserved to describe a matrix element between parity eigenstates and the helicity states are not parity eigenstates. The partial decomposition of the helicity amplitudes as given by Jacob and Wick is:

$$g_{\lambda'\lambda}\,(s,t) = \frac{e^{i(\lambda-\lambda')\phi}}{2q}\;\sum_{J}\,(2J+1)\; T_{\lambda'\lambda}{}^{J}(s)\; d_{\lambda\,\lambda'}{}^{J}(\theta) \qquad 1.34$$

where θ and ϕ define the direction of the relative momentum.

The helicity subscripts for s-channel pion-nucleon scattering are written as $\pm^{*}$; '+' corresponding to when the spin is in the direction

of motion and '-' when it isn't. The net helicity in the initial state is $\lambda = \frac{1}{2}$ and in the final state $\lambda' = \pm\frac{1}{2}$.

It would appear that there are several partial amplitudes but by parity conservation

$$T^{j}_{++} = T^{j}_{--} \quad \text{and} \quad T^{j}_{+-} = T^{j}_{-+} \qquad 1.35$$

There are then two independent helicity amplitudes g_{++}, g_{+-} and the corresponding relativistic amplitudes are f_{++}, f_{+-} where the normalisation is given in equations 1.31. The partial wave decompositions are then:

$$g_{++}(s,t) = q^{-1} \sum_{j} (j+\tfrac{1}{2})\, T^{j}_{++}(s)\, d^{J}_{\frac{1}{2}\,\frac{1}{2}}(\theta)$$

$$g_{+-}(s,t) = q^{-1}\, e^{-i\phi} \sum_{j} (j+\tfrac{1}{2})\, T^{j}_{+-}(s)\, d^{J}_{-\frac{1}{2}\,\frac{1}{2}}(\theta) \qquad 1.36$$

PARITY EIGENSTATES

S-channel pion-nucleon scattering is described in terms of partial wave amplitudes and since the helicity states are not parity eigenstates, it is necessary to take combinations of the helicity partial amplitudes which correspond to definite parity states. The partial wave amplitudes then are

$$T_{j-} = T^{j}_{++} + T^{j}_{+-}$$

$$T_{j+} = T^{j}_{++} - T^{j}_{+-} \qquad 1.37$$

where j+ and j- label the definite parity states.

In this basis the restrictions imposed by unitarity take on a simple form:

$$|S_{J\pm}|^2 \leqslant 1 \qquad 1.38$$

If $S_{J\pm}$ are parameterised by $\eta_{J\pm}\, e^{2i\delta_{j\pm}}$ $\quad 0 \leqslant \eta_{J\pm} \leqslant 1$, where η and δ are referred to as the elasticity and phase shift respectively, then the unitarity restriction is satisfied and the partial wave amplitudes can be written as:

$$\frac{T_{J\pm}}{2q} = f_{J\pm} = \frac{\eta_{J\pm}\, e^{2i\delta_{j\pm}} - 1}{2iq} \qquad 1.39$$

The total parity conserving amplitudes f_1 and f_2 are written in terms of the helicity amplitudes as

$$\begin{aligned} g_{++} &= \left[f_1+f_2\right] \text{Cos } \theta/2 \\ g_{+-} &= \left[f_1-f_2\right] \text{Sin } \theta/2\, e^{-i\phi} \end{aligned} \qquad 1.40$$

and manipulation yields the following partial wave decompositions.

$$\begin{aligned} f_1 &= \sum_{\ell} \left[f_{\ell+}\, P'_{\ell+1}(\text{Cos}\theta) - f_{\ell-}\, P'_{\ell-1}(\text{Cos}\theta)\right] \\ f_2 &= \sum_{\ell} \left[f_{\ell-} - f_{\ell+}\right] P_{\ell}'\,(\text{Cos}\theta) \end{aligned} \qquad 1.41$$

where the following associations have been made

$$\begin{aligned} f_{j-} &= f_{\ell+} \\ & \qquad \pm \text{ refer to } j = \ell \pm \tfrac{1}{2} \\ f_{j+} &= f_{(\ell+1)-} \end{aligned} \qquad 1.42$$

INVARIANT AMPLITUDES

An alternative to the helicity amplitudes g_{++}, g_{+-} are the invariant

amplitudes A and B. From equation 1.19 the scattering T matrix can be written as:

$$\bar{U}(p_2)\ \{-A + i\gamma.QB\}\ U(p_1) \qquad 1.43$$

where $\bar{U}(p_2)$, $U(p_1)$ are two-component Pauli-spinors, quantisised along a fixed direction, which describe the spin states of the ingoing and outgoing nucleon.

The s and t channel helicity amplitudes are obtained by evaluating this expression in the respective centre of mass frames and this allows the invariant amplitudes to be expressed in terms of the parity conserving amplitudes, f_1 and f_2:

$$A = 4\pi \left[f_1 \left[\frac{W+M}{E+M}\right] - f_2 \left[\frac{W-M}{E-M}\right] \right]$$

$$B = 4\pi \left[f_1 \left[\frac{1}{E+M}\right] + f_2 \left[\frac{1}{E-M}\right] \right] \qquad 1.44$$

$$E = (M^2+q^2)^{1/2}$$

The invariant amplitudes, as will be demonstrated, have simple crossing and analytic properties. The only rule is that the invariant amplitudes be non-singular except where they have the dynamical poles of the Mandelstam representation.

ISOSPIN RELATIONS

So far the charge of the pion and the nucleon have been neglected. The introduction of charge implies that there are as many amplitudes to be considered, as there are possible charge configurations in the initial and final

states allowed by the conservation of charge. However the charge independence of strong interactions limits the number of amplitudes.

The decomposition of the physical pion-nucleon states in terms of the isospin states of the π-N system can be represented diagramatically.

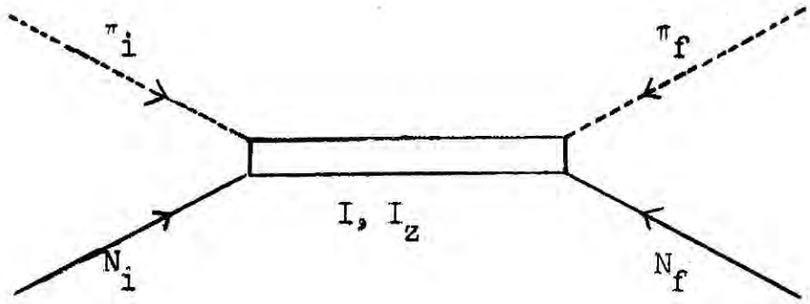

FIG.6

where the intermediate state carries isospin I with third component I_z.

For pion-nucleon scattering there are six possible charge states

$$|p\,\pi^+\rangle,\ |p\,\pi^-\rangle,\ |p\,\pi^0\rangle,\ |n\,\pi^-\rangle,\ |n\,\pi^+\rangle,\ |n\,\pi^0\rangle$$

The possible isospin exchanges are $I = \frac{1}{2}$, $I = \frac{3}{2}$ and all six charge amplitudes can be expressed in terms of the scattering amplitudes $F_{1/2}$, $F_{3/2}$ corresponding to the two isospin states.

$$\begin{aligned}
&\langle\pi^+p|T|\pi^+p\rangle = \langle\pi^-n|T|\pi^-n\rangle = F_{1/2} \\
&\langle\pi^-p|T|\pi^-p\rangle = \langle\pi^+n|T|\pi^+n\rangle = \tfrac{1}{3}F_{3/2} + \tfrac{2}{3}F_{1/2} \qquad 1.45 \\
&\langle\pi^0n|T|\pi^-p\rangle = \langle\pi^0p|T|\pi^+n\rangle = \tfrac{\sqrt{2}}{3}\left[F_{3/2} - F_{1/2}\right]
\end{aligned}$$

Alternatively the physical pion-nucleon states can be decomposed in terms of the exchanged isospin states.

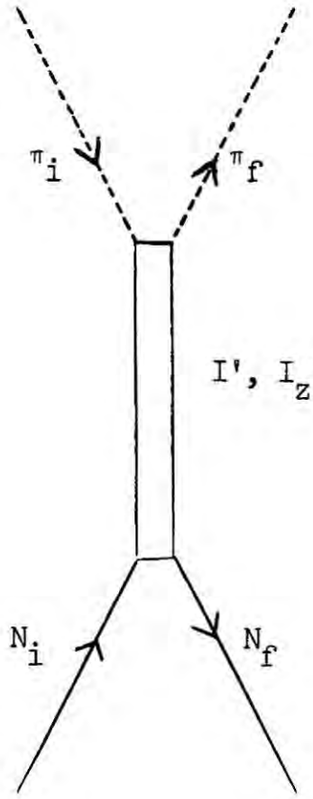

FIG.7

From isospin conservation at the pion vertex I' = 0, 1, 2 whilst from isospin conservation at the nucleon vertex I' = 0 or 1 only. The physical pion states can be decomposed in terms of the independent exchange amplitudes F_0, F_1 corresponding to isospin 0 and 1 respectively

$$\begin{aligned} \langle \pi^+ p|T|\pi^+ p\rangle &= F_0 - \frac{1}{\sqrt{6}} F_1 \\ \langle \pi^- p|T|\pi^- p\rangle &= F_0 + \frac{1}{\sqrt{6}} F_1 \\ \langle \pi^0 n|T|\pi^- p\rangle &= \frac{F_1}{\sqrt{3}} \end{aligned} \qquad 1.46$$

CROSSING INVARIANT AMPLITUDES

$$\pi^- p \to \pi^- p \qquad 1$$

$$\pi^+ p \to \pi^+ p \qquad 2$$

$$\pi^+ \pi^- \to p\bar{p} \qquad 3$$

The basic principles of analyticity and crossing symmetry specify that the above processes are described by the same analytic functions of the Mandelstam variables s,t,u. The relation between the relativistic amplitudes for the processes 1,2,3 obtained by analytic continuation is termed crossing symmetry. The path of continuation for the crossing relation from the s channel process 1 to the u channel process 2 is shown in Fig.8 [6]

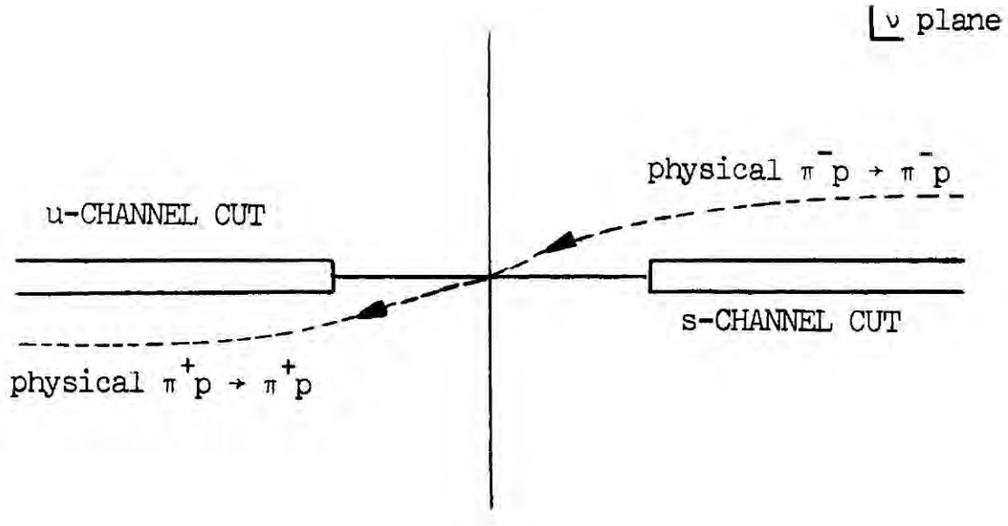

FIG.8

The s ⇔ u crossing relation can be written

$$T_{\pi^- p}(-\nu+i0,t) = T^*_{\pi^+ p}(\nu+i0,t) \qquad 1.47$$

where ν is the symmetric variable,

$$\nu = \frac{s-u}{4M} \qquad 1.48$$

and $\nu \pm i0$ indicates that the limit is taken from the upper (lower) half-plane on to the branch-cut. The labels π^+p, π^-p indicate that these are the amplitudes for the elastic processes $\pi^+p \to \pi^+p$, $\pi^-p \to \pi^-p$ respectively.

Similar crossing relations can be established that involve process 3 for which t is the square of the centre of mass energy.

The T matrix can be expressed in terms of the independent invariant amplitudes A and B, Equation (1.19). The B amplitude is associated with nucleon spin by the factor $\gamma.Q$ but the A amplitude is independent of the nucleon spin. Crossing symmetry thus applies separately to A and $(\gamma.Q)B$.

If the following symmetric and antisymmetric combinations are constructed, Equations (1.49) then the $s \leftrightarrow u$ crossing relations

$$A^{(+)}_{(\nu,t)} = \tfrac{1}{2}\left[A_{\pi^-p}(\nu,t) + A_{\pi^+p}(\nu,t)\right] \quad B^{(+)}_{(\nu,t)} = \tfrac{1}{2}\left[B_{\pi^-p}(\nu,t) + B_{\pi^+p}(\nu,t)\right]$$

$$A^{(-)}_{(\nu,t)} = \tfrac{1}{2}\left[A_{\pi^-p}(\nu,t) - A_{\pi^+p}(\nu,t)\right] \quad B^{(-)}_{(\nu,t)} = \tfrac{1}{2}\left[B_{\pi^-p}(\nu,t) - B_{\pi^+p}(\nu,t)\right] \qquad 1.49$$

for these combinations are given in equations (1.50)

$$A^{(+)}(\nu,t) = A^{(+)}(-\nu,t) \qquad A^{(-)}(\nu,t) = -A^{(-)}(-\nu,t)$$

$$B^{(+)}(\nu,t) = -B^{(+)}(-\nu,t) \qquad B^{(-)}(\nu,t) = B^{(-)}(-\nu,t) \qquad 1.50$$

Further from equations (1.46) it can be seen that these symmetric and antisymmetric amplitudes correspond to the t channel isospin amplitudes, with isospin 0 and 1.

CROSS-SECTIONS

The 'relativistic' helicity amplitudes are normalised such that the differential cross-section for the s-channel process is given by:

$$\frac{d\sigma}{dt}(s,t) = \frac{1}{64\pi sq^2}\left[|f^s_{++}|^2 + |f^s_{+-}|^2\right] \qquad 1.51$$

where f^s_{++}, f^s_{+-} are the s-channel helicity amplitudes. The orthogonality of the crossing matrix for the helicity amplitudes [Equat.1.33] leads to the alternative expression:

$$\frac{d\sigma}{dt}(s,t) = \frac{1}{64\pi sq^2}\left[|f^t_{++}|^2 + |f^t_{+-}|^2\right] \qquad 1.52$$

where f^t_{++}, f^t_{+-} are the t-channel helicity amplitudes continued in the variables s,t to the s channel physical region.

In terms of the invariant amplitudes A and B the differential cross-section is given by

$$\frac{d\sigma}{dt}(s,t) = \frac{1}{\pi s}\left(\frac{M}{4q}\right)^2\left[\left(1-\frac{t}{4M^2}\right)|A'|^2 - \frac{t}{4M^2}\left(\frac{4M^2p_L + st}{4M^2-t}\right)|B|^2\right] \qquad 1.53$$

A' is given by Singh [7]

$$A' = A + \frac{\nu}{1-t/4M^2}\,B \qquad 1.54$$

and the variables have their usual meanings as defined in equations 1.10, 1.11 [p_L is the pion lab momenta given by $p_L = \sqrt{W_L^2 - M^2}$ where ω_L is defined in equation 1.12]. The polarisation P(s,t) defined relative to the normal pi × pf, where pi and pf are initial and final pion momenta, is given by

$$P(s,t) = -\frac{\sin\theta}{16\pi s^{1/2}}\,\frac{\mathrm{Im}\,(A'\,B^*)}{d\sigma/dt} \qquad 1.55$$

and by the optical theorem, the total cross-section δ_T is given by

$$\sigma_T(s) = \frac{\text{Im } A'(s,t=0)}{p_L} \qquad 1.56$$

CHAPTER 11

SECTION A

INTRODUCTION

In Chapter 1 the partial wave decompositions of the pion-nucleon amplitudes, which can be used to describe the s-channel scattering process in terms of direct channel resonances appearing in a particular wave, were constructed. However it was indicated in the Introduction, that it would be the crossed channel singularities that determine the high energy s-channel physical region scattering. As an approximate 'rule of thumb' it is expected that the singularities nearest to the physical region of a given channel exert maximal influence on the scattering. The t channel singularities are expected to be important at $\text{Cos}\theta_s = +1$ [see Fig.5], corresponding to the forward direction in the s-channel, and the u-channel singularities at $\text{Cos}\theta_s = -1$ which corresponds to the backward direction.

For pion-nucleon scattering the possible t channel exchange are mesons and the u-channel exchanges are baryons. Fig.9 illustrates how these crossed channel exchanges build the s channel picture of pion-nucleon scattering.

FIG.9

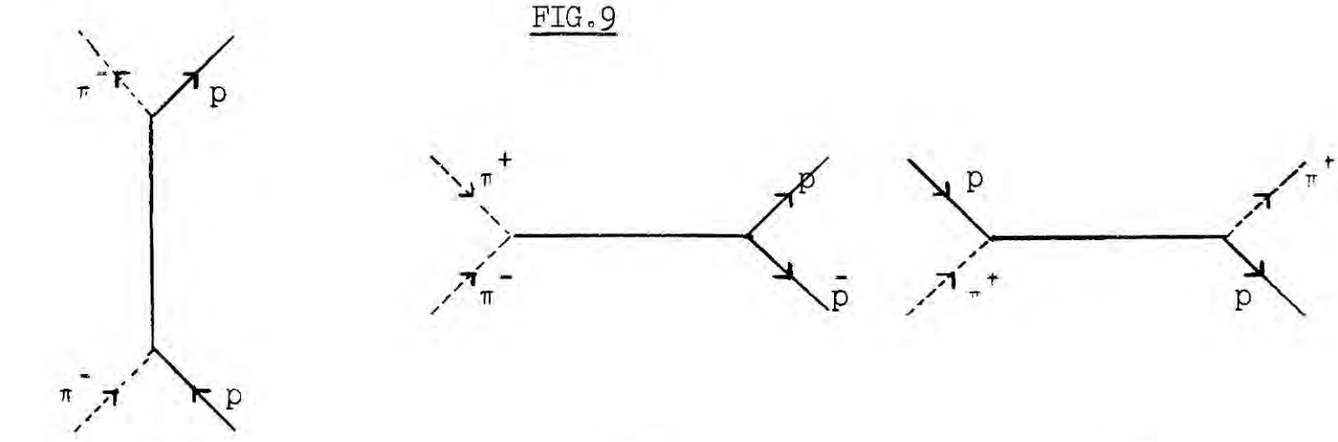

(a) (b) (c)

DIRECT CHANNEL RESONANCES MESON EXCHANGE BARYON EXCHANGE

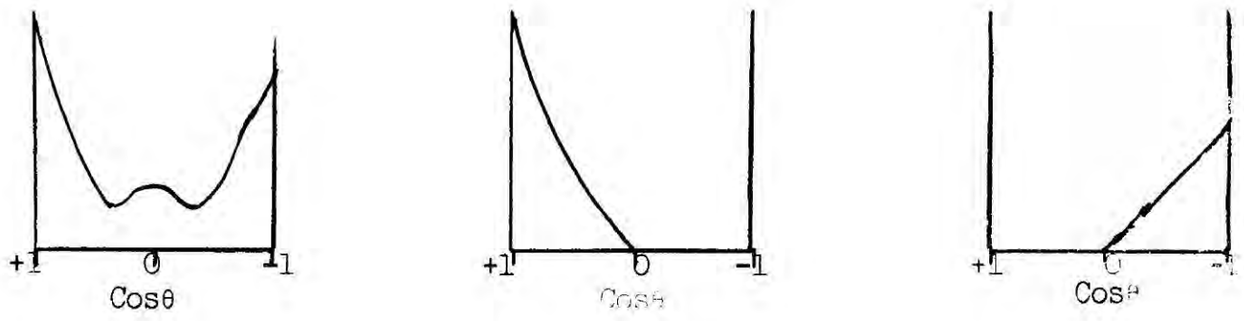

MESON EXCHANGES

The meson exchanges occur in the t-channel which corresponds to the crossed channel process $\pi\bar{\pi} \to N\bar{N}$.

In the t channel physical region

$$t = 4[k_t^2 + \mu^2] = 4[p_t^2 + M^2]$$

$$s = -2k_t\, p_t\, \mathrm{Cos}\theta_t + 2M^2 + 2\mu^2 - 2(k_t^2+\mu^2)^{1/2}\,(p_t^2+M^2)^{1/2} \qquad 2.1$$

$$z_t = \mathrm{Cos}\theta_t = \frac{-(s-u)}{4k_t\, p_t}$$

where k_t and p_t are the pion and nucleon centre of mass momenta and θ_t is the c.m. scattering angle

The decomposition for $\pi\bar{\pi} \to N\bar{N}$ in terms of the invariant amplitudes is written:

$$\bar{u}(p_2)\,[-A + i\gamma.Q\, B]\, u(p_1)$$

and the t channel helicity amplitudes are obtained by evaluating this expression in the corresponding t channel c.m. frame. In terms of the invariant amplitudes they are:

$$f_{++}(t,s) = (t-4M^2)^{-1/2}\,[(4M^2-t)\,A + M(s-u)\,B]$$

$$f_{+-}(t,s) = \frac{2\sqrt{t}\, p_t\, k_t\, \mathrm{Sin}\,\theta_t}{(t-4M^2)^{1/2}}\, B \qquad 2.2$$

The amplitudes A and B have only the dynamical singularities required by the Mandelstam representation but the helicity amplitudes f_{++}, f_{+-} have also kinematic singularities arising from threshold factors etc. To analytically continue the amplitudes, they must be singularity free [8] and the singularity free t channel amplitudes are:

$$\tilde{f}_{++}(t,s) = (4M^2-t)A + M(s-u)B$$

$$\tilde{f}_{+-}(t,s) = B \qquad 2.3$$

The partial amplitude [9] expansions of $\tilde{f}_{++}$, $\tilde{f}_{+-}$ are from equation 1.34

$$\tilde{f}_{++}(t,s) = \sum_J (2J+1)\, f^J_{++}(t)\, P_J(z_t)$$

$$\tilde{f}_{+-}(t,s) = -\sum_J (2J+1)\, f^J_{+-}(t)\, \frac{P_J'(z_t)}{[J(J+1)]^{1/2}} \qquad 2.4$$

One of the shortcomings of the partial wave expansion is its limited range of validity in Cos θ_t or equivalently t. By extending the concept of a partial amplitude from the physical values of J, to a general value of J lying in the complex plane, a representation of the scattering amplitude can be obtained which is valid in the entire t plane.

In the complex J-plane the even and odd J valued amplitudes must be treated separately. Physically this is due to the presence of exchange forces and in analogy with potential scattering the total potential can be written:

$$\text{Total Potential} = \underbrace{V_1(r)}_{\text{direct potential}} + \underbrace{(-1)^J V_2(r)}_{\text{exchange potential}}$$

The even and odd J are separated by the introduction of the 'signature' quantum number $\tau = (-1)^J$ and the Legendre function is given by:

$$P_J(\text{Cos } \theta_t) = \tfrac{1}{2}\left[P_J(\text{Cos } \theta_t) + \tau\, P_J(-\text{Cos } \theta_t)\right] \qquad 2.5$$

In the complex J plane the sum over J of the partial amplitudes in equation 2.4 can be replaced by a contour integral over the path C_1 Fig.10 where $\tilde{f}_{++}(J,t)$, $\tilde{f}_{+-}(J,t)$ are the continuation to complex J values of the partial

amplitudes $\tilde{f}^{J}_{++}(t)$, $\tilde{f}^{J}_{+-}(t)$ respectively. (defined by the Froissart-Gribov projection.)

$$\tilde{f}_{++}(t,s) = \frac{i}{4}\int_{C_1} dJ(2J+1)\frac{\tilde{f}_{++}(J,t)}{\sin \pi J}\left[P_J(-\cos\theta_t) + \tau P_J(\cos\theta_t)\right] \qquad 2.6$$

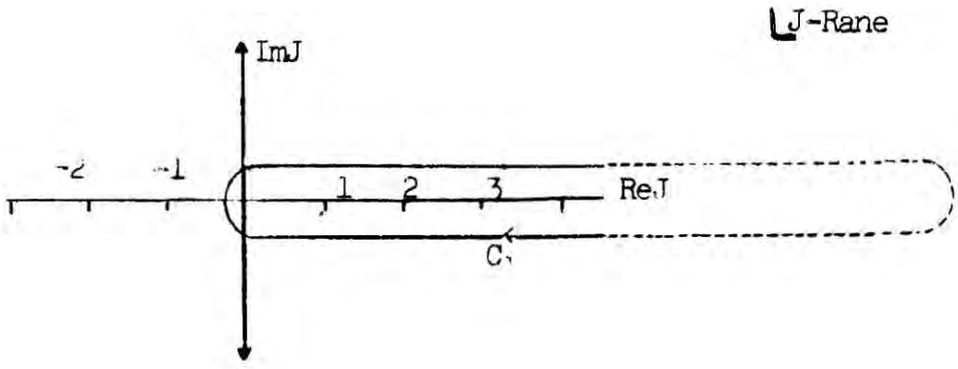

FIG.10

The contour C_1 is chosen to include the positive integers and zero but to avoid any singularities of $\tilde{f}_{++}(J,t)$. The integral transform Equation 2.6 [10] is referred to as a Sommerfeld-Watson transform and a similar expression can be written for the t channel amplitude $\tilde{f}_{+-}$.

Carlson's theorem [11] shows that the analytic continuation defined above is unique under the following conditions

(1) $\tilde{f}_{++}(J,t)$ is regular in ReJ > A {where A is a real finite constant}.

(2) $\tilde{f}_{+-}(J,t)$ is $< \exp(k|J|)$ $\{k < \pi\}$ for ReJ > A

(3) $\tilde{f}_{+-}(J,t)$ is uniquely defined by its values at an infinite sequence of positive integers J = N+1, N+2.

Since $\tilde{f}_{++}(J,t)$ is regular in ReJ > A, the contour C_1 can be displaced to C_2 with a line parallel to the imaginary axis through the point ReJ = A and a semi-circle at infinity without including any singularities of $\tilde{f}_{++}(J,t)$. FIG.11.

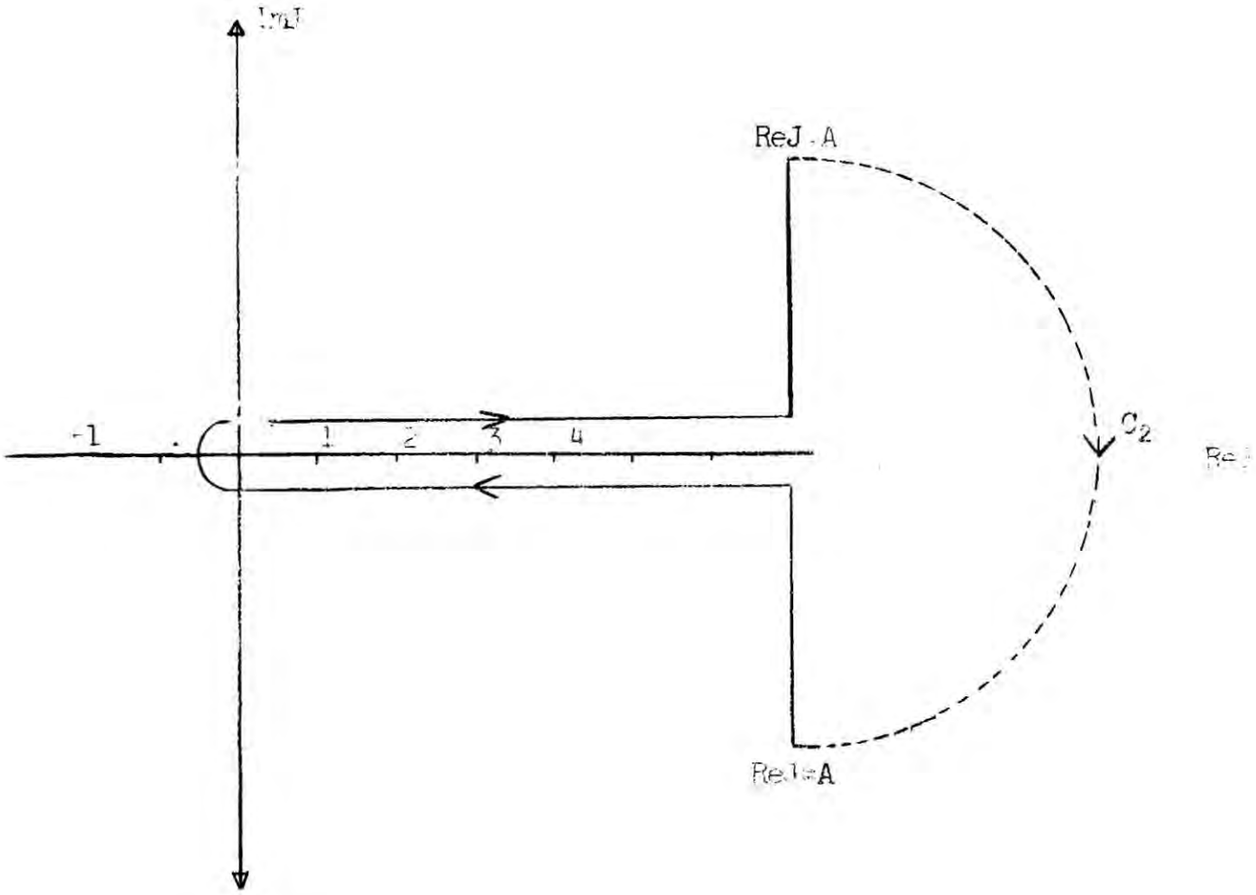

FIG.11

If $\tilde{f}_{++}(J,t)$ is a meromorphic function of J at least as far left as Re J = -½, then as the line ReJ = A is moved to the left, singularities of $\tilde{f}_{++}(J,t)$ will be encountered which are expected to be poles and branch cuts. For the present it is assumed that the only singularities are poles and in analogy with potential scattering they are called Regge poles. [12]

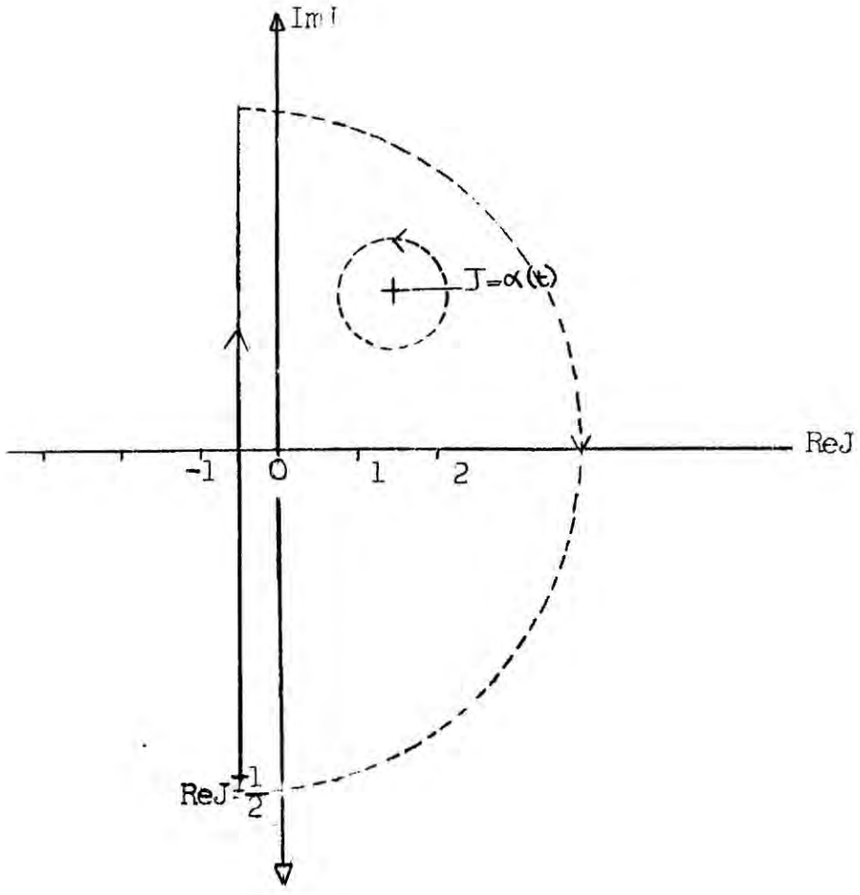

FIG.12

The position and residue of the pole in $\tilde{f}_{++}(J,t)$ are denoted by $\alpha(t)$ and $\beta_{++}(t)$ respectively. Since α is a function of t, then $J = \alpha(t)$ will define a 'trajectory' in the complex J plane as t is varied.

If the single pole term is represented by:

$$\tilde{f}_{++}(J,t) = \frac{\beta_{++}(t)}{J-\alpha(t)} \qquad 2.7$$

then it can be shown that the contribution from the semi-circle at infinity is zero [13] and from Cauchy's theorem the following representation for the amplitude is obtained.

$$\tilde{f}_{++}(t,s) = \frac{i}{4}\int_{-\frac{1}{2}-i\infty}^{-\frac{1}{2}+i\infty} dJ(2J+1)\,\frac{\tilde{f}_{++}(J,t)}{\sin \pi J}\left[P_J(-z_t)+\tau\, P_J(z_t)\right] -$$

$$- \pi \sum_{\substack{\text{Regge}\\ \text{Poles}}} (\alpha(t)+\tfrac{1}{2})\,\beta_{++}(t)\left[\frac{1+\tau\, e^{-i\pi\alpha(t)}}{\sin \pi\alpha(t)}\right] P_{\alpha(t)}(-z_t) \qquad 2.8$$

The integral is referred to as the 'background integral' and the importance

of the above representation is apparent when the behaviour of $\tilde{f}_{++}(t,s)$ is considered as $-z_t \to \infty$.

The asymptotic ($-z_t \to \infty$) expansion of the Legendre function can be written (ERDELYI 1953) [14]

$$P_\alpha(-z_t) \sim \frac{\Gamma(\alpha+\frac{1}{2})}{\Gamma(1+\alpha)} \frac{(-2\,z_t)^\alpha}{\Gamma(\frac{1}{2})} + \frac{\Gamma(-\alpha-\frac{1}{2})}{\Gamma(1-\alpha)} \frac{(-2\,z_t)^{-\alpha-1}}{\Gamma(\frac{1}{2})} \qquad 2.9$$

For Re $\alpha > -\frac{1}{2}$ the first term dominates but for Re $\alpha < -\frac{1}{2}$ the second term dominates. In the background integral equation ReJ = $-\frac{1}{2}$; and hence this integral vanishes as $z_t^{-\frac{1}{2}}$, $[-z_t \to \infty]$ and the amplitude can be expressed as a simple sum of Regge poles.

$$\tilde{f}_{++}(t,s) = -\pi \sum (\alpha+\tfrac{1}{2})\, \beta_{++} \frac{1+\tau\, e^{-i\pi\alpha}}{\sin \pi\alpha} P_\alpha(-z_t) \qquad 2.10$$

If Re $\alpha < -\frac{1}{2}$, the background integral must first be pushed to the left of $J = -\frac{1}{2}$ and in the Regge pole amplitude the function $\frac{P_\alpha(-z_t)}{\sin \pi\alpha}$ is replaced by $\frac{-Q_{-\alpha-1}(-z_t)}{\pi \cos \pi\alpha}$ [15]. The form of the asymptotic expansion remains the same as above however.

EXCHANGE AMPLITUDES

To calculate s-channel scattering due to t channel exchanges the Regge amplitudes must be continued to the region $t \leq 0$, $s \geq (M+\mu)^2$. The Regge pole approximation to the complete amplitude is valid for $-z_t \gg 1$ and this corresponds to the high energy, small t physical region of the s-channel. Equation 2.1

Writing $$P_\alpha(-z_t) \underset{-z_t \to \infty}{\sim} \frac{\Gamma(\alpha+\frac{1}{2})}{\Gamma(1+\alpha)} \frac{(-2z_t)^\alpha}{\Gamma(\frac{1}{2})} \qquad 2.11$$

the t-channel helicity amplitudes are then:

$$\tilde{f}_{++} = \frac{\Gamma(\alpha+3/2)}{\Gamma(1+\alpha)} \beta_{++} \frac{1+\tau\, e^{-i\pi\alpha}}{\mathrm{Sin}\ \pi\alpha} \left[\frac{-2z_t}{2p_t\ k_t}\right]^{\alpha} \qquad 2.12$$

A 'threshold barrier factor' $\left[\frac{p_t\ k_t}{s_o}\right]^{\alpha}$ is extracted and the residue γ_{++} is constructed to have zeros at $\alpha = -3/2, -1/2$ etc. to cancel the unphysical poles of $\Gamma(\alpha+3/2)$.

$$\beta_{++} = \frac{1}{\Gamma(\alpha+3/2)} \gamma_{++} \left[\frac{p_t\ k_t}{s_o}\right]^{\alpha} \qquad 2.13$$

This leads to the final form for the t-channel helicity amplitudes

$$\tilde{f}_{++}(s,t) = \gamma_{++}\, R(s,t) \qquad 2.14$$

$$\text{where } R(s,t) = \frac{1}{\Gamma(1+\alpha)} \frac{1+\tau\, e^{-i\pi\alpha}}{\mathrm{Sin}\ \pi\alpha} \left[\frac{s-u}{2\ s_o}\right]^{\alpha} \qquad 2.15$$

Similarly it can be shown that

$$\tilde{f}_{+-}(s,t) = \alpha\, \gamma_{+-} \frac{R(s,t)}{(-4M\ p_t\ k_t\ \mathrm{Cos}\ \theta_t)} \qquad 2.16$$

INVARIANT EXCHANGE AMPLITUDES

The connection between the t channel kinematic singularity free helicity amplitudes and the invariant amplitudes A and B motivates the customary use of the amplitude A' as expressed in equation 1.54.

The invariant amplitudes then have the following Regge representations

$$A' = \frac{\gamma'_{++}}{\Gamma(1+\alpha)} \left[\frac{1+\tau\, e^{-i\pi\alpha}}{\mathrm{Sin}\ \pi\alpha}\right] \left[\frac{\nu}{\nu_o}\right]^{\alpha}$$

$$B = \frac{\alpha\, \gamma'_{+-}}{\Gamma(1+\alpha)} \left[\frac{1+\tau\, e^{-i\pi\alpha}}{\mathrm{Sin}\ \pi\alpha}\right] \left[\frac{\nu}{\nu_o}\right]^{\alpha-1} \qquad 2.17$$

where γ'_{++}, γ'_{+-} are the residue functions. The pole at $t = 4M^2$ in A' is a

long way from the s-channel physical region ($t<0$) and does not affect the analysis.

SECTION B

INTRODUCTION

The central theme of Regge pole theory is the connection between particle classification and high energy scattering. The Van-Hove Durand [16] [17] model shows how a Regge pole exchange amplitude could arise in a Feynman-type field theory, from the single exchanges of particles on trajectories. The physical interpretation of Regge poles is apparent in this model, the crossed channel Regge poles represent the collective amplitude due to single exchanges of all particles that lie on the trajectory.

A trajectory corresponds to a physical particle when it crosses an alternate integral value of J for positive energy. Thus Regge trajectories connect particles which differ in spin by two units but have otherwise the same quantum numbers [18]. Since most of the resonances which have been positively identified have masses at the most of a few GeV, it is not surprising that many trajectories have been seen at one physical value of J only. Furthermore, the trajectory $J = \alpha(t)$ determined for $t > 0$ from assignments of resonances as Regge recurrences is a smooth continuation of the trajectory for $t < 0$ that describes scattering due to Regge pole exchange.

PION-NUCLEON TRAJECTORIES

For pion-nucleon scattering in the forward direction the exchanged trajectories are meson trajectories. There are two possible isospin states 0 and 1 for the crossed channel $\pi\bar{\pi} \to N\bar{N}$ and the coupling of the exchanged meson to the $\pi\bar{\pi}$ state restricts the exchanged quantum numbers to $\tau P = +1$ (τ is the signature and P the parity).

TRAJECTORY	PARTICLE	MASS (MeV)	J^P	I^G	SIGNATURE
P				0	+1
P'	f_o	1250	2^+	0^+	+1
P''	f'	1500	2^+	0^+	+1
ρ	ρ	750	1^-	1^+	-1

TABLE 1

Table I shows the possible meson trajectories which contribute to the I = 0, 1 states [19]. Extrapolations of the P', ρ trajectories through these mesons to t = 0 yields $\alpha(t=0) \leqslant 0.6$. If the leading trajectory in pion-nucleon scattering had such a low intercept, the elastic and total cross-sections would decrease rather rapidly with increasing energy. Experimentally the trends of total cross-sections are towards constant limiting values at high energies. This empirical behaviour requires a leading positive signature trajectory with $\alpha(t=0) = 1$ [20]. Thus if this leading trajectory has particle recurrences, it must have a small slope since there are no observed mesons which could be associated with the first $J^P = 2^+$ particle. The small slope then ensures that the first recurrence occurs at high mass where new mesons could be discovered. The label P denoting Pomeron is customarily used to denote this trajectory.

The characteristic slope of the Regge trajectories is of the order of 1 GeV^{-2} with the exception of the Pomeron. This anomaly of the Pomeron has created speculation that the Pomeron may not be in fact a simple Regge pole but rather some more complex singularity.

REGGE PARAMETERISATIONS

From equation 1.39 the pion nucleon amplitudes are expressed in terms of the symmetric and antisymmetric combinations $A'^{(+)}$, $A'^{(-)}$, $B^{(+)}$, $B^{(-)}$. The subscripts π^+p, π^-p and C.E.X. refer to the processes $\pi^+p \to \pi^+p$, $\pi^-p \to \pi^-p$ and $\pi^-p \to \pi^0n$ respectively.

$$A'_{\pi^-p}(\nu,t) = A'^{(+)}(\nu,t) + A'^{(-)}(\nu,t) \qquad B_{\pi^-p}(\nu,t) = B^{(+)}(\nu,t) + B^{(-)}(\nu,t)$$

$$A'_{\pi^+p}(\nu,t) = A'^{(+)}(\nu,t) - A'^{(-)}(\nu,t) \qquad B_{\pi^+p}(\nu,t) = B^{(+)}(\nu,t) - B^{(-)}(\nu,t)$$

$$A'_{CEX}(\nu,t) = \sqrt{2}\, A'^{(-)}(\nu,t) \qquad B_{CEX}(\nu,t) = \sqrt{2}\, B^{(-)}(\nu,t)$$

2.18

$A'^{(+)}$, $B^{(+)}$ involve the isospin I = 0 even signature exchanges P,P' etc. and the amplitudes $A'^{(-)}$, $B^{(-)}$ involve the I = 1 odd signature exchanges ρ

The Regge representations for these amplitudes are:

$$A'^{(+)}(\nu,t) = \sum_{PP'} \gamma^+(\alpha(t),t)\, \xi^+(t)\, (\nu^2-\nu_o^2)^{\alpha(t)/2}$$

$$B^{(+)}(\nu,t) = \sum_{PP'} \beta^+(\alpha(t),t)\, \xi^+(t)\, \nu(\nu^2-\nu_o^2)^{\frac{\alpha(t)-2}{2}}$$

$$A'^{(-)}(\nu,t) = \sum_{\rho} \gamma^-(\alpha(t),t)\, \xi^-(t)\, \nu(\nu^2-\nu_o^2)^{\frac{\alpha(t)-1}{2}} \qquad 2.19$$

$$B^{(-)}(\nu,t) = \sum_{\rho} \beta^-(\alpha(t),t)\, \xi^-(t)\, (\nu^2-\nu_o^2)^{\frac{\alpha(t)-1}{2}}$$

where γ^+ β^+ γ^- and β^- are the residue functions and $\xi^\gamma(t)$ is the signature factor.

The energy dependence of the Regge amplitudes is cast in the above form since they lend themselves easily for use in the continuous moment sum rules and have the correct analytic properties at threshold ($\nu=\nu_o$). In the Regge region proper, then $(\nu^2-\nu_o^2)^{1/2}$ is approximately equal to ν and makes little

difference to the high energy calculations.

SIGNATURE

The phase of a meson Regge pole is completely specified by the trajectory through its signature factor

$$\mathcal{P}^{\tau}(t) = \frac{1+\tau\, e^{-i\pi\alpha}}{\sin \pi\alpha} \qquad 2.20$$

Integral values of $\alpha = J_o$ for which $(-1)^{J_o} = \tau$ are termed 'right signature points' conversely 'wrong signature points' have $(-1)^{J_o} = -\tau$.

WRONG SIGNATURE NONSENSE ZEROS

The essential α dependence of the t channel $\pi\bar{\pi} \to N\bar{N}$ amplitudes is

$$A' \sim \frac{1}{\Gamma(1+\alpha)} \mathcal{P}^{\tau}(t)$$

$$B \sim \frac{\alpha}{\Gamma(1+\alpha)} \mathcal{P}^{\tau}(t) \qquad 2.21$$

Consider a negative signature trajectory $\tau = -1$, A' vanishes at wrong signature points $\alpha = -2, -4 \ldots$ and B vanishes at the wrong signature points $\alpha = 0, -2, -4$ etc. At $\alpha = 0$ the exchanged trajectory acts like a spin zero particle and cannot support a unit of helicity. Hence there is a zero in B which is associated with spin flip and no zero in A'. The point $\alpha = 0$ is therefore a nonsense value of the angular momentum for the B amplitude and a sense value for A'.

Because of the third double spectral function fixed poles may be expected in the signatured amplitudes at wrong signature points. They do not give rise to poles in the physical amplitude because they are cancelled by the zeros of the signature factor [21]. However if such poles are also present

in the residues of Regge poles they will cancel the zero of the signature factor which was assumed above. The fixed poles do not modify the energy dependence of the asymptotic amplitude; their only effect is to modify the behaviour of the residue of the moving pole. In the case of $\pi\bar{\pi}$ - $N\bar{N}$ the behaviour of the B amplitude equation 2.21 would be modified to

$$B \sim \frac{\Gamma[\alpha(t).C+D]}{\Gamma[1+\alpha(t)]} \gamma^{\tau}(t) \qquad 2.22$$

by the presence of a fixed pole at $J = 0$.

GHOST STATES

For right signature points the term $\frac{\gamma^{\tau}(t)}{\Gamma[1+\alpha(t)]}$ is finite except at $\alpha = 0$ for $\tau = 1$ or $\alpha = 1$ for $\tau = -1$. Suppose that $\alpha(t)$ is zero at some $t < 0$ for a $\tau = +1$ signature Regge trajectory, then a 'ghost' state appears which represents a t channel particle with $(\text{mass})^2 < 0$. In the B amplitude the kinematic factor $\alpha(t)$ cancels the pole. However in the A' amplitude the pole gives rise to an infinity in the s-channel scattering. As a minimal requirement the non-flip residue must develop a zero to kill the ghost,

$$\gamma^{+}(\alpha(t),t) \sim \alpha(t)\, C(t) \qquad 2.23$$

where $C(t)$ is some function of t. The residue may acquire additional dynamical factors $(\alpha-J_0)$ at the exceptional points $\alpha = J_0$, $J_0 = 0, -1, -2$ etc.

SENSE NONSENSE RESIDUE ZEROS

The exceptional point $\alpha = 0$ [illegible] is crucial to the Regge interpretation of minima in differential cross-sections. The residue factors for the coupling of the exchanged Regge pole to $\pi\bar{\pi}$, $N\bar{N}$ non spin flip and $N\bar{N}$ spin flip are denoted by f, g and h respectively.

The partial wave expansion of the kinematical singularity free helicity amplitude $\tilde{f}_{+-}(t,s)$ [Equation 2.4] involves a factor $\frac{P_J'(z_t)}{[J(J+1)]^{1/2}}$ which leads to a kinematical factor of $\sqrt{\alpha}$ near $\alpha = 0$ in the residue function.

$$\beta^I(\alpha(t),t) \sim \sqrt{\alpha}\ f.h\ \xi^I(t) \qquad 2.24$$

Similarly the non-flip amplitude residue can be written

$$\gamma^I(\alpha(t),t) \sim f.g\ \xi^I(t) \qquad 2.25$$

The exceptional point $\alpha = 0$ corresponds to a right signature point for an even signature trajectory and a wrong signature point for an odd signature trajectory. The even signature factor $\xi^+(t)$ behaves like $1/\alpha$ and the odd signature factor $\xi^-(t)$ like unity near the point $\alpha = 0$.

The behaviour of the residue factors f,g and h is such that all the helicity amplitudes are free from branch points or poles at $\alpha = 0$. Therefore from equations 2.24, 2.25

$$\begin{aligned} fg &\sim \alpha^n \qquad n = 0,1,2 \\ fh &\sim \alpha^{m/2} \qquad m = 1,3,5 \end{aligned} \qquad 2.26$$

There are many possible solutions for f,g and h which satisfy the analyticity criteria at $\alpha = 0$ in equations 2.26. The mechanisms in common usage correspond to the lowest order solutions of the above equations and these are given in table II.

f	g	h	MECHANISM
1	1	$\sqrt{\alpha}$	SENSE
$\sqrt{\alpha}$	$\sqrt{\alpha}$	1	NONSENSE
$\sqrt{\alpha}$	$\sqrt{\alpha}$	α	CHEW
α	α	$\sqrt{\alpha}$	NO COMPENSATION

TABLE II

The sense mechanism is impossible for right signature points since the $\pi\pi - (N\bar{N})_{\substack{\text{non spin} \\ \text{flip}}}$ amplitude would have a pole at $\alpha = 0$.

The overall α dependence, excluding the signature factor, for the $\pi\bar{\pi} - N\bar{N}$ amplitudes obtained from the various mechanisms is given in Table III.

A'	B	MECHANISM
1	α	SENSE
α	α	NONSENSE
α	α^2	CHEW
α^2	α^2	NO COMPENSATION

TABLE III

In the derivation of the spin flip Regge amplitudes equation 2.16 a sense

mechanism was assumed for simplicity and the nonsense mechanism corresponds to the previous consideration of ghost killing factors. A similar treatment can be given for the exceptional points $\alpha = -1, -2$ etc.

T-DEPENDENCE OF RESIDUES

The Regge residues $\gamma^{\pm}(\alpha(t),t)$, $\beta^{\pm}(\alpha(t),t)$ can in general depend on t both explicitly, and implicitly through $\alpha(t)$. Present relativistic theory does not provide a calculational basis to determine the residues and it is necessary to rely on empirical parameterisations.

The appropriate sense-nonsense factors are extracted from the residue and the remainder is parameterised by a rapidly varying function of t such as $\int e^{dt}$. The flexibility in the t dependence of the residues is the greates deficiency of the present Regge pole theory. However continuous moment sum rules (see Chapt.3) should resolve some of the difficulties in the residue parameterisations and are certainly a step forward in the determination of Regge residues.

In the derivation of the Regge pole amplitude it was assumed that the only singularities in the complex J plane were poles corresponding to single particle exchange. However there is every reason to believe that cuts, equivalent to multi-particle exchanges are present [23]. In a phenomenological analysis of a high energy scattering process, a few Regge poles are usually sufficient to fit most of the experimental data. The expected s-dependence is known from the contributing trajectories and 'unexpected' effects, with s-dependence incompatible with known trajectories, presumably arises from a cut. This 'ad hoc' usage of cuts permits the introduction of many free parameters and that data fitting is successful is not surprising Further it is difficult to distinguish the pole and cut contributions, since in a finite region the cut can always be represented by a superposition of poles.

REGGE CUTS IN FEYNMAN GRAPHS

Regge cuts can be generated from the iteration of the unitarity equation in the t channel for the full amplitude but retaining a two particle intermediate state only. FIG.13

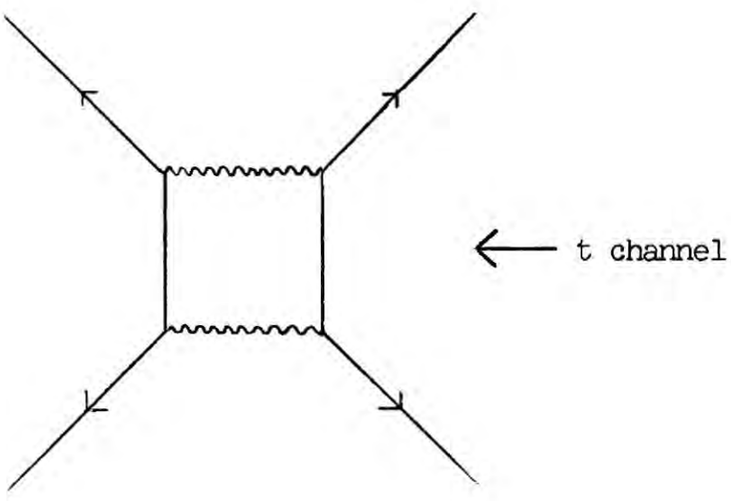

FIG.13

The contribution of these cuts to the double spectral function was first calculated by Amati, Fubini and Stanghellini and they are referred to as AFS cuts or rescattering corrections.[24]

Mandelstam[23] showed that cuts generated by elastic unitarity in Fig.13 are in fact spurious, being cancelled by multi-particle unitarity contributions. To avoid these cancellations, non planar diagrams with a third double spectral function must be considered. FIG.14

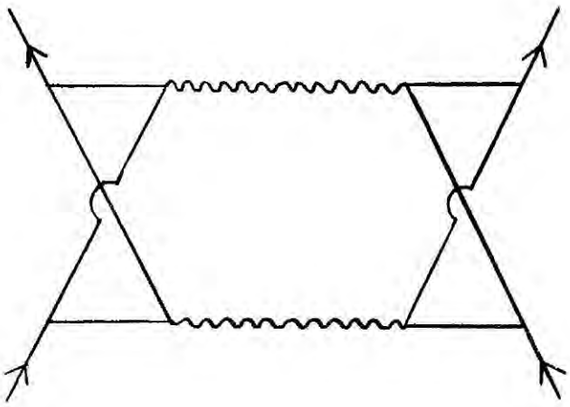

FIG.14

The association of the cuts with the third double spectral function is not surprising since the strongest theoretical evidence for their existence is to shield the Gribov-Pomeranchuk poles, occurring at wrong signature non-sense points, which themselves arise from third double spectral function effects. What perhaps is surprising is that the position in the complex J plane of the cuts arising from non-planar diagrams are in fact the same as the spurious A.F.S. cuts.

CUTS - SOMMERFELD-WATSON TRANSFORM

Cut contributions, if they are present, must be included in the Sommerfeld-Watson Transform equation 2.8. The contour in Fig.15 is deformed to include the cut whose 'right most point' is its branch point $J_c = \alpha_c(t)$. Assuming equation 2.8 and calculating the contribution of the cut only round the contour C_j:

$$\tilde{f}_{cut}(t,s) = -\sum_{j\,cuts} \frac{i}{4} \int_{C_j} dJ(2J+1) \frac{\tilde{f}(J,t)}{\sin \pi J} \left[P_J(-z_t) + \tau P_J(z_t)\right] \qquad 2.27$$

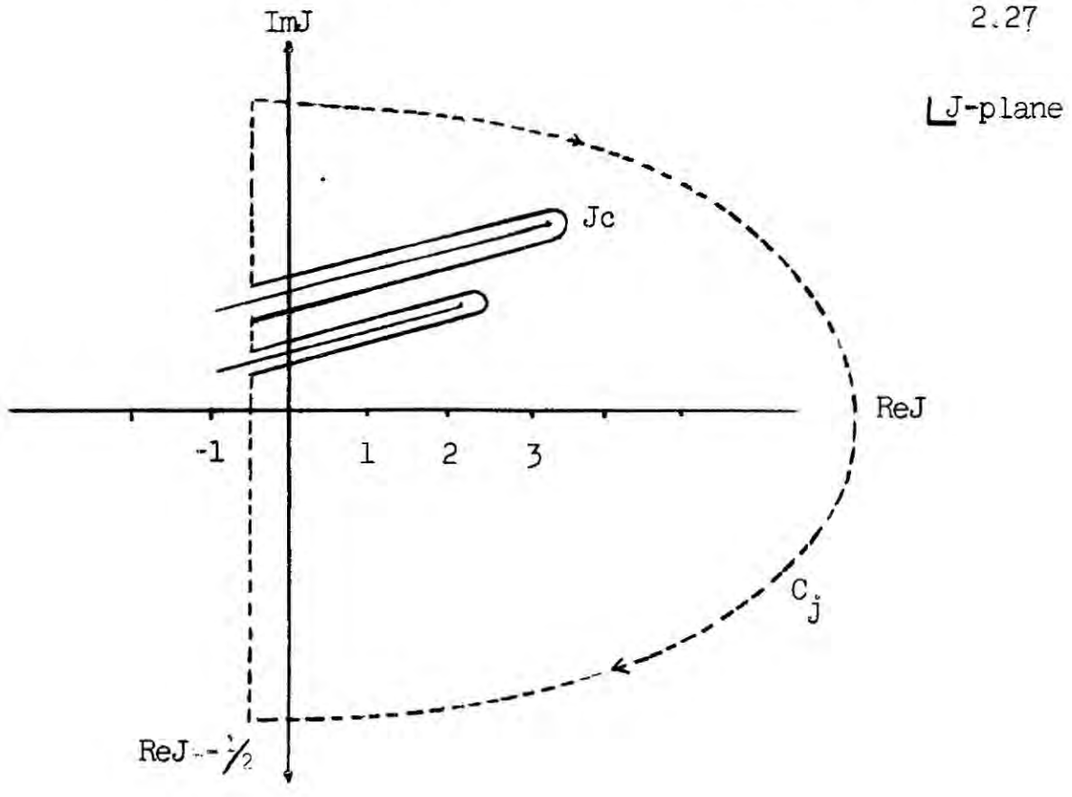

FIG.15

The contour integration involves evaluating $\tilde{f}(J,t)$ above and below the cut where the discontinuity across the cut D(J,t) is given by:

$$D(J,t) = \frac{\tilde{f}(J+i\varepsilon,t) - \tilde{f}(J-i\varepsilon,t)}{2i} \qquad 2.28$$

and $+i\varepsilon$, $-i\varepsilon$ indicate the function is to be evaluated above and below the

cut respectively. The cut amplitude is then given by:

$$\tilde{f}(t,s) = \sum_{j\,\text{cuts}} \frac{1}{2} \int_{\text{background}}^{J_c} (2J+1)\, D(J,t) \left[\frac{1+\tau\, e^{-i\pi J}}{\sin \pi J}\right] P_J(-z_t) \qquad 2.29$$

The position of the branch point in the J plane from the exchange of two trajectories $\alpha_1(t)$, $\alpha_2(t)$ is, as in the A.F.S. calculation

$$J_c = \alpha_c(t) = \text{Max}\left[\alpha_1(t_1) + \alpha_2(t_2) - 1\right] \qquad 2.30$$

where: $2tt_1 + 2tt_2 + 2t_1t_2 - t - t_1^2 - t_2^2 \geq 0$

If these cuts are to shield the Gribov-Pomeranchuk fixed poles [25] then the branch point, at the t-channel threshold, must correspond to the leading wrong signature nonsense point. In the case of two identical spinless particles mass m lying on a trajectory $\alpha(t)$ such that

$$\alpha(m^2) = 0$$

then the highest nonsense point is at -1

$$\alpha_c(m^2) = -1$$

For Example for two identical trajectories equation 2.30 is written

$$\alpha_c(t) = 2\alpha\left[t/4\right] - 1 \qquad 2.31$$

In general, for the exchange of 'n' identical trajectories equation 2.30 becomes

$$\alpha_c(t) = n\alpha\left[\frac{t}{n^2}\right] - n + 1 \qquad 2.32$$

Jones et al. [26] showed that the discontinuity across the cut D(J,t) must vanish at its end point and also be singular there. A simple parameterisation of the discontinuity is then:

$$D(J,t) \underset{J\to\alpha_c(t)}{\sim} [J - \alpha_c(t)]^{\lambda} \qquad 2.33$$

where $\lambda > 0$ and is non integer.

The leading behaviour of the cut contribution from equation 2.29 is in the asymptotic region, (the variable ν is defined in equation 1.48)

$$\tilde{f}(\nu,t) \sim \left[\frac{\nu}{\nu_o}\right]^{\alpha_c(t)} \ln\left[\frac{\nu}{\nu_o}\right]^{-\lambda-1} \qquad 2.34$$

Thus the energy dependence of the cuts essentially differs from a simple pole by the logarithmic factor. One of the difficulties with Regge cuts is the lack of explicit knowledge of the discontinuity function. The standard approach is to incorporate the ideas of the absorption model and Regge eikonal model which allow the calculation of the cut parameters in terms of the input Regge pole parameters.

REGGE ABSORPTION MODEL

In the Reggeised absorption model [27]-[29], the simple Regge pole exchange is modified by elastic scattering in the final and initial states. This situation is equivalent to earlier 'peripheral model calculations' and a similar formulation is adopted. The s-channel partial waves modified by elastic scattering F_{fi}^J are written [Sopkovich (1962)] [30],

$$F_{fi}^J(s) = \sqrt{S_{ff}^J(s)}\, R_{fi}^J(s) \sqrt{S_{ii}^J(s)} \qquad 2.35$$

where R_{fi}^J is the projection of the crossed channel Regge pole exchange and S_{ff}, S_{ii} are the partial wave S matrices for elastic scattering in the final and initial states.

The partial S-matrix can be written

$$S_{ii}^J = 1 + i\, T_{ii}^J \qquad 2.36$$

and in terms of the relativistic amplitudes normalised according to equations 1.31

$$S_{ii}^{J}(s) - 1 + 2i\, k_{ii}(s)\, P_{ii}^{J}(s) \qquad 2.37$$

where $k_{ii}(s) = \frac{q_i}{8\pi\sqrt{s}}$, q_i is the c.m. momentum in the initial state.

A similar expression can be given for $S_{ff}^{J}(s)$ and the square roots in equation 2.35 are expanded so that

$$F_{fi}^{J}(s) = R_{fi}^{J}(s) + i\, k_{ii}(s)\, P_{ii}^{J}(s)\, R_{fi}^{J}(s) + i\, k_{ff}(s)\, P_{ff}^{J}(s)\, R_{fi}^{J}(s) \qquad 2.38$$

Diagramatically this equation can be represented by FIG.16

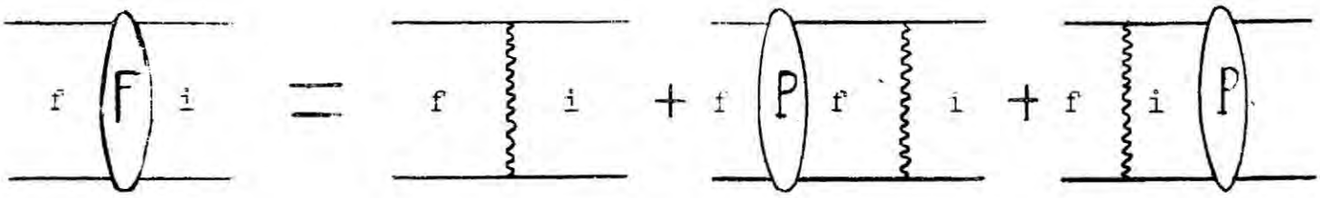

FIG.16

Further, if it is assumed that the elastic scattering is given by the leading Regge pole i.e. Pomeron, then the second and third terms in equation 2.38 are the two particle cut contributions due to the exchange of a Regge pole and the Pomeron. The total amplitude can be written by summing over the partial waves [31]. The expression is somewhat complex and it is derived in APPENDIX A.

REGGE-EIKONAL MODEL [32]

The earliest application of the eikonal model is due to Chou and Yang [33]. To perform the numerical calculations, they used the impact parameter approximation for elastic scattering at high energies. Starting

from the s-channel partial wave expansion of the relativistic amplitudes,

$$F^{s}_{\lambda'\lambda}(s,t) = \sum_{J} (2J+1)\, F^{J}_{\lambda'\lambda}(s)\, d^{J}_{\lambda\lambda'}(\theta) \qquad 2.39$$

the following approximation, valid at large energies and small angles, is made:

$$J + \tfrac{1}{2} = q_s b \qquad 2.40$$

where b is the impact parameter, classically corresponding to the closeness of approach of the particle on the target. The d-functions are written in terms of the Bessel function:

$$d^{J}_{\lambda\lambda'}(\theta) \sim J_{\lambda'-\lambda}\left[(2J+1)\,\mathrm{Sin}\,\frac{\theta}{2}\right]$$

and $\mathrm{Cos}\,\theta = 1 + \frac{t}{2q_s^2}$ gives— $\qquad 2.41$

$$J_{\lambda'-\lambda}\left[(2j+1)\,\mathrm{Sin}\,\frac{\theta}{2}\right] \sim J_{\lambda'-\lambda}\left[b\sqrt{-t}\right]$$

Further, the summation over J is replaced by the integral over the continuous impact parameter b, such that

$$F^{s}_{\lambda'\lambda}(s,t) = \int_0^\infty 2q_s^2\, b\, F^{J}_{\lambda'\lambda}(s)\, J_{\lambda'-\lambda}(b\sqrt{-t})\, db \qquad 2.42$$

The partial wave elements $F^{J}_{\lambda'\lambda}(s)$ are defined in terms of the T matrix elements by

$$F^{J}_{\lambda'\lambda}(s) = \frac{4\pi\sqrt{s}}{q_s}\, T^{J}_{\lambda'\lambda}(s) \qquad 2.43$$

The eikonal phase $\chi(s,b^2)$ is then associated with the phase shift by writing:-

$$F^{J}_{\lambda'\lambda}(s) = \frac{4\pi\sqrt{s}}{iq_s}\left[e^{\chi(s,b^2)} - 1\right]$$

and
$$F^{s}_{\lambda'\lambda}(s,t) = i\,8\pi\, q_s\sqrt{s}\int_0^\infty bdb\left[1 - e^{i\chi(s,b^2)}\right] J_{\lambda'-\lambda}(b\sqrt{-t}) \qquad 2.44$$

This is equivalent to the two dimensional Fourier transform, but the assumption that the partial wave T matrix elements are independent of the azimuthal angle ϕ has been made (i.e. an incident wave front is not altered in direction only phase).

If the exponential in equation 2.44 is expanded then,

$$F_{\lambda'\lambda}(s,t) = 8\pi\, q_s\sqrt{s}\int_0^\infty bdb\left[\chi + i\frac{\chi^2}{2!} - \frac{\chi^3}{3!} \ldots\right] J_{\lambda'-\lambda}(b\sqrt{-t}) \qquad 2.45$$

and if the eikonal phase is now given by the Fourier transform of the relevant t channel Regge pole amplitude which provides the potential, then the first term in equation 2.45 is just the Regge pole amplitude itself $R_{\lambda',\lambda}(s,t)$.

$$R_{\lambda'\lambda}(s,t) = 8\pi\, q_s\sqrt{s}\int_0^\infty bdb\,\chi(s,b^2)\, J_{\lambda'-\lambda}(b\sqrt{-t})$$

and
$$\chi(s,b^2) = \frac{1}{8\pi\, q_s\sqrt{s}}\int_0^\infty \frac{dt}{2}\, R_{\lambda'\lambda}(s,t)\, J_{\lambda'-\lambda}(b\sqrt{-t}) \qquad 2.46$$

Successive terms in the multiple scattering series are then associated with two, three particle cuts etc.

The two particle cut is written:

$$F_{\lambda'\lambda}(s,t) = iq_s 4\pi\sqrt{s}\int_0^\infty bdb\,\chi^2(s,b^2)\, J_{\lambda'-\lambda}(b\sqrt{-t}) \qquad 2.47$$

The eikonal phase $\chi(s,b^2)$ is given by equation 2.46 and can be written in terms of the Regge pole parameters. APPENDIX A shows that this equation can be written as:

$$F^{cut}_{\lambda'\lambda}(s,t) = \frac{i}{32\pi\, q_s\sqrt{s}}\int_0^\infty dt_1\int_0^\infty dt_2\, R_{\lambda'\lambda}(s,t_1)\, R_{\lambda'\lambda}(s,t_2)\,\frac{\theta(\delta)}{\delta^{1/2}} \qquad 2.48$$

where the function $\theta(\delta)$ and δ are defined in APPENDIX A.

If the single pole amplitude is written:

$$R_{\lambda'\lambda}(s,t) = -\beta\, e^{bt}\, e^{-i\pi\alpha(t)} \left[\nu/\nu_o\right]^{\alpha(t)} \qquad 2.49$$

where $\alpha(t) = \alpha(0) + \alpha' t$

Then the 'n' particle cut for large s can be written

$$F^{cut}_{\lambda'\lambda}(s,t) = \frac{1}{\pi\, n!}\, \beta^n \left[16\pi\, \nu_o\, \alpha' \log\left[\frac{\nu}{\nu_o}\right]\right]^{-n+1} \left[\frac{\nu}{\nu_o}\right]^{\alpha_c{}^n(t)} e^{\frac{-i\pi}{2}\alpha_c{}^n(t)} \qquad 2.50$$

and the position of the cut $\alpha_c{}^n(t)$ is given by

$$\alpha_c{}^n(t) = n\,\alpha(0) + \frac{\alpha'}{n}\, t - n + 1 \qquad 2.51$$

The equation 2.50 is similar to the Feynman graph calculation equation 2.34, except that the absorptive and eikonal model calculations appear to violate t channel unitarity i.e. $\lambda = 0$ [26] in equation 2.50 for the two particle cut.

GENERAL PROPERTIES OF REGGE CUTS

The absorptive and eikonal models produce a Regge cut with the correct energy dependence and position as anticipated from Feynman graph calculations. However, their validity is not established, since it is equally possible that the Regge pole does not need to be corrected for absorption and, in the case of the eikonal model, the identification of the Regge pole with a relativistic Born term is dubious {Collins: Review Article [31]}. These models do however permit some general conclusions on the properties of cuts to be made.

a) Position

The position of the cut due to the exchange of n identical trajectories which are linear $\alpha = \alpha(0) + \alpha' t$ is

$$\alpha_c^n(t) = n\,\alpha(0) - n + 1 + \frac{\alpha'}{n}\,t \qquad 2.52$$

b) Signature and Phase

The signature of the cut is the product of the signature of the poles. For n identical poles [34]:

$$\text{Phase} = e^{i\pi\,\alpha_c^n(t)} \quad \text{for } \log_\Delta \frac{\nu}{\nu_o} \to \infty \qquad 2.53$$

c) Energy dependence

There is a logarithmic factor $\log\left[\nu/\nu_o\right]^{-n+1}$ associated with the n particle cut such that the contributions of the higher order cuts vanish relative to those of lower order by some power of $\log\left[\nu/\nu_o\right]$.

REGGE-MULTIPOLES

In the Sommerfeld-Watson transform equation 2.8, it was assumed that the only complex J-plane singularities were simple poles. If multipoles exist [35] such that their partial amplitudes can be represented by:

$$\tilde{f}^{\,q}_{++}(J,t) = \frac{B_{++}(t)\,(q-1)!}{\left[J-\alpha(t)\right]^q} \qquad 2.54$$

where q is a positive integer and indicates the order of the pole, then using the Cauchy integration formula on the contour round the poles.

$$\tilde{f}^{\,q}_{++}(t,s) = -\frac{\pi}{2}\,B_{++}(t)\left[\frac{d^{q-1}}{dJ^{q-1}}\,(2J+1)\left[\frac{1+\tau\,e^{-i\pi J}}{\sin \pi J}\right] P_J(-z_t)\right]_{J=\alpha(t)}$$

2.55

The simplest example is a dipole (q=2) and for a positive signature trajectory $\tau = +1$ Equation 2.55 is written:

$$\tilde{f}^{q}_{++}(t,s) = \pi B_{++}(t) \frac{(2\alpha+1)}{\sin^2 \pi\alpha/2} \left[\sin \frac{\pi\alpha}{2} e^{-i\pi\alpha/2} \left[\frac{d}{dJ} P_J(-z_t) \Big|_{J=\alpha} + \frac{P_\alpha(-z_t)}{\alpha+\frac{1}{2}} \right] - \frac{\pi}{2} P_\alpha(-z_t) \right] \qquad 2.56$$

The amplitudes are continued to the s-channel scattering region as in the simple Regge pole derivation. The asymptotic expansion of the Legendre function is:(Equation 2.11)

$$P_\alpha(-z_t) \underset{-z_t >> 1}{\rightarrow} \frac{\Gamma(\alpha+\frac{1}{2})}{\Gamma(\alpha+1)} \frac{(-2z_t)^\alpha}{\Gamma(\frac{1}{2})}$$

and equation 2.56 is written

$$\tilde{f}^{q}_{++}(t,s) = \frac{\Gamma(\alpha+\frac{3}{2})}{\Gamma(1+\alpha)} \frac{B_{++}}{\sin^2 \frac{\pi\alpha}{2}} \left[\sin \frac{\pi\alpha}{2} e^{\frac{-i\pi\alpha}{2}} \left[\log(-2z_t) + 2\beta(2\alpha+1) \right] - \frac{\pi}{2} \right] (-2z_t)^\alpha \qquad 2.57$$

where $2\beta(2\alpha+1) = \psi(1+\alpha) - \psi(\alpha+\frac{1}{2})$ and $\psi(\alpha) = \frac{d}{d\alpha} \ln \Gamma(\alpha)$.

A reduced residue is defined to cancel the unphysical poles arising from $\Gamma(\alpha+\frac{3}{2})$ and a scale factor ν' is defined such that:

$\cos\theta_t = z_t = -\frac{(s-u)}{4k_t p_t}$ (p_t, k_t etc. are defined in section A)

is given by $-2z_t = \frac{\nu}{\nu'}$; ν is the symmetric variable

defined in equation 1.48 and ν' is given by $\nu' = \frac{k_t p_t}{2M}$.

The dipole contribution to the Regge amplitude for the even signature trajectories is:

$$\tilde{f}_{++}(s,t) = \frac{B_{++}}{\Gamma(1+\alpha)} \frac{1}{\sin^2 \pi\alpha/2} \left[\sin \frac{\pi\alpha}{2} e^{-i\pi\alpha/2} \left[\log\left[\frac{\nu}{\nu'}\right] + 2\beta(2\alpha+1) \right] - \frac{\pi}{2} \right] \left[\frac{\nu}{\nu'} \right]^\alpha \qquad 2.58$$

which in the special case $\alpha = 1$ reduces to

$$\tilde{f}_{++}(s,t) = -i\, B_{++} \left[\log \frac{\nu}{\nu'} + 2\beta(2) - i\,\frac{\pi}{2} \right] \left[\frac{\nu}{\nu'} \right] \qquad 2.59$$

Similar expressions can be written for the odd signature trajectories.

CHAPTER 111

S E C T I O N A

INTRODUCTION

Scattering amplitudes are analytic functions of the energy variables and can be continued from the high energy region to the low energy region by some defined analytic continuation. There is usually a wealth of low energy data and a marked absence of high energy data on a particular scattering process. To maximise the information input of a high energy analysis the analytic properties of the scattering amplitudes must be exploited [36], [37].

Finite Energy Sum Rules represent the simples expression of these analytic constraints, and as such they are little different from ordinary dispersion relations. The sum rules are derived with reference to the asymptotic Regge model, they are not predictive of asymptotics and would be expected to be satisfied for any asymptotic model.

DERIVATION OF FINITE ENERGY SUM RULES [38], [39]

Suppose there exists an amplitude $f(\nu)$ which is a real analytic function of the variable ν (Equation 1.48), throughout the complex ν-plane, except for cuts from ν_0 to ∞, $-\nu_0$ to $-\infty$ and possible isolated poles along the real axis. FIG.17

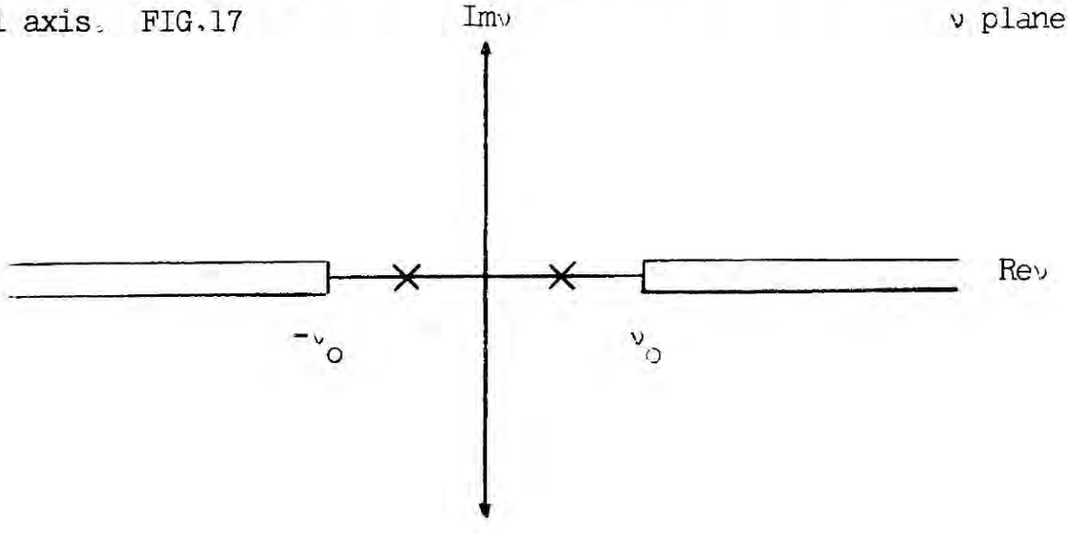

FIG.17

If $f(\nu)$ is an antisymmetric amplitude under $s \leftrightarrow u$ crossing which satisfies an unsubtracted, fixed t dispersion relation of the type:

$$f(\nu) = \frac{2\nu}{\pi} \int_0^\infty \frac{\mathrm{Im}\, f(\nu')\, d\nu'}{\nu'^2 - \nu^2} \qquad 3.1$$

and $f(\nu)$ has a Regge asymptotic expansion:

$$f^{\mathrm{Regge}}(\nu) = \sum_{\substack{\text{all} \\ \text{Regge Poles}}} \frac{\beta(t)}{\Gamma(1+\alpha)} \frac{1+\tau\, e^{-i\pi\alpha}}{\mathrm{Sin}\, \pi\alpha} \left[\frac{\nu}{\nu_0}\right]^\alpha \qquad 3.2$$

where α, β and τ are the trajectory, residue and signature of the Regge poles respectively.

Then if the leading Regge term has $\alpha < -1$, $f(\nu)$ will obey a superconvergence relation:

$$\int_0^\infty \mathrm{Im}\, f(\nu)\, d\nu = 0 \qquad 3.3$$

If the leading term has $\alpha > -1$ then it can be subtracted from $f(\nu)$ and the resulting amplitude will obey a superconvergence relation:

$$\int_0^\infty d\nu\, \mathrm{Im}\left[f(\nu) - f^{\mathrm{Regge}}_{\alpha>-1}(\nu)\right] = 0 \qquad 3.4$$

Further, if there is a pole at $\alpha = -1$ then its residue will appear on the right hand side of equation 3.4. To illustrate how different values of α contribute to the sum rules the poles whose α is below -1 are denoted by α_i, those at $\alpha = -1$ by α_j and the poles above $\alpha = -1$ by α_k.

$$\int_0^\infty d\nu \left[\mathrm{Im}\, f(\nu) - \sum_{\alpha_k} \frac{\beta_k}{\Gamma(1+\alpha_k)} \tau_k \left[\frac{\nu}{\nu_0}\right]^{\alpha_k}\right] = \beta_j\, \tau_j \qquad 3.5$$

Each term in the above equation diverges when evaluated separately. To write the equation in a practical convergent form, the integration is cut off at some $\left[\frac{\nu}{\nu_0}\right]_{\max} = N$ and the high energy behaviour is expressed by a sum of

Regge poles whose α is below -1.

$$\int_0^N \left[\text{Im } f(\nu) - \sum_{\alpha_k} \frac{\beta_k \tau_k}{\Gamma(1+\alpha_k)} \left[\frac{\nu}{\nu_0}\right]^{\alpha_k} \right] d\nu + \int_N^\infty \sum_{\alpha_i} \frac{\beta_i \tau_i}{\Gamma(1+\alpha_i)} \left[\frac{\nu}{\nu_0}\right]^{\alpha_i} d\nu = \beta_j \tau_j \qquad 3.6$$

The poles above below and at $\alpha = -1$ enter the 'finite energy sum rules' in differing ways but the integrals are all now convergent. In the final form of the sum rules the Regge terms appear the same regardless of their α.

$$S(N) = \int_0^N \text{Im } f(\nu)\, d\nu = \sum_{\text{all } \alpha} \frac{\beta N^{\alpha+1} \tau}{\Gamma(\alpha+2)} \qquad 3.7$$

GENERALISATION OF THE F.E.S.R.

An alternative derivation of the F.E.S.R. on a fixed contour [40] generalises trivially to the 'non-integer moment sum rules' and 'the continuous moment sum rules'.

Suppose an amplitude $f(\nu)$ is a real analytic function of the variable ν throughout the complex ν plane except for cuts from ν_0 to ∞ and $-\nu_0$ to $-\infty$ plus perhaps isolated poles along the real axis. FIG.14.

If there exists a value N such that for all $|\nu/\nu_0| > N$ the asymptotic form (equation 3.2) is already a good approximation to the amplitude then Cauchy's theorem can be applied round the closed contour C fig.18

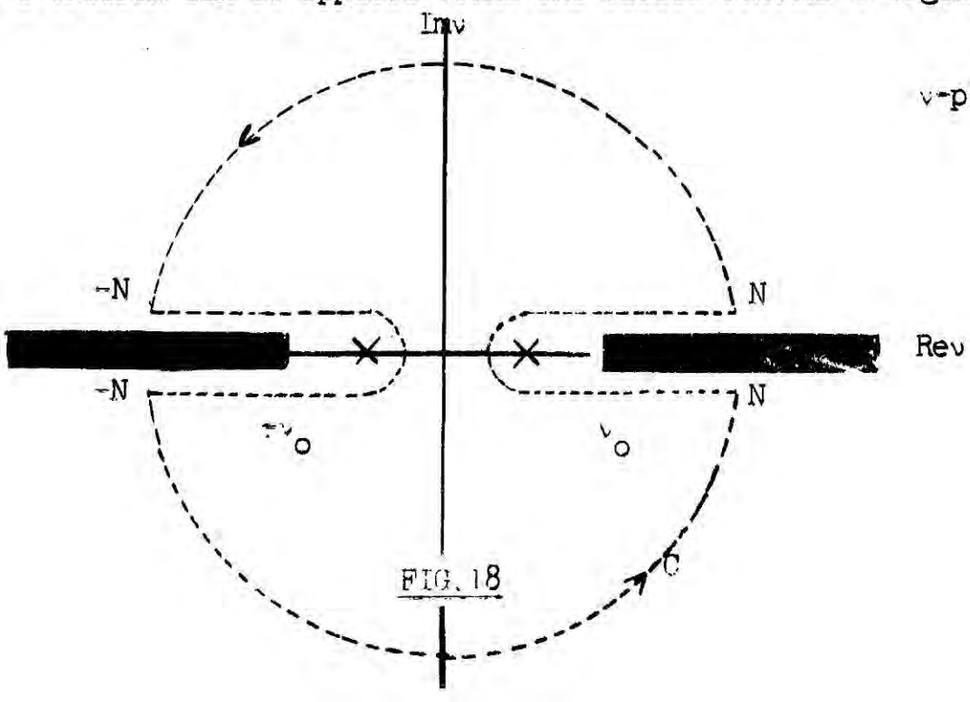

FIG. 18

Since the contour C encloses no singularities, then by Cauchy's theorem

$$\int_C f(\nu)\, d\nu = 0$$

The contributions from the upper and lower semi-circles are separated out of the integral,

$$\int_{\nu_o}^{N} f(\nu-i\varepsilon)\, d\nu + \int_{-N}^{-\nu_o} f(\nu+i\varepsilon)\, d\nu + \int_{-\nu_o}^{-N} f(\nu-i\varepsilon)\, d\nu + \int_{N}^{\nu_o} f(\nu-i\varepsilon)\, d\nu +$$

$$+ \int_{\frown} f(\nu)\, d\nu + \int_{\smile} f(\nu)\, d\nu = 0 \qquad 3.8$$

where $\nu + i\varepsilon$, $\nu - i\varepsilon$ indicates the function is to be evaluated above and below the real axis respectively and $\smile$ $\frown$ represent the upper and lower semi-circle contours.

The Regge asymptotic expansion gives $f(\nu)$ on the upper and lower semi-circle contours and equation 3.8 is written

$$\int_{-N}^{-\nu_o} \mathrm{Im}\, f(\nu)\, d\nu + \int_{\nu_o}^{N} \mathrm{Im}\, f(\nu)\, d\nu + \sum_k \frac{\beta_k}{\Gamma(1+\alpha_k)} \frac{N^{\alpha_k+1}}{\alpha_{k+1}} \{\tau_k - 1\} = 0 \qquad 3.9$$

The isolated poles are assumed to be included in the continium integrals and k labels the Regge poles in the asymptotic expansion.

INTEGRAL MOMENT F.E.S.R.

The function $\nu^m f(\nu)$ for integral $m > 0$ has the same anlytic properties as $f(\nu)$. Hence from equation 3.9 'the integral moment sum rules' are:

$$\int_{-N}^{-\nu_o} \mathrm{Im}\, f(\nu)\, \nu^m\, d\nu + \int_{\nu_o}^{N} \mathrm{Im}\, f(\nu)\, \nu^m\, d\nu + \sum_k \frac{\beta_k}{\Gamma(1+\alpha_k)} \frac{N^{\alpha_k+m+1}}{\alpha_k+m+1} \left[\tau_k - (-1)^m\right] = 0 \qquad 3.10$$

The integer moment F.E.S.R. can be simplified when $f(\nu)$ is exactly symmetric or antisymmetric.

a) $f(\nu)$ is antisymmetric $\qquad f_A(\nu) = -f_A(-\nu)$

$$\int_{\nu_o}^{N} \mathrm{Im}\, f_A(\nu)\, \nu^m\, d\nu = \sum_k \frac{\beta_k}{\Gamma(1+\alpha_k)} \frac{N^{\alpha_k+m+1}}{\alpha_k+m+1} \qquad m = 0,2,4 \qquad 3.11$$

The antisymmetric combination involves odd signature exchanges only.

b) $f(\nu)$ is symmetric $\qquad f_S(\nu) = f_S(-\nu)$

$$\int_{\nu_o}^{N} \mathrm{Im}\, f_s(\nu)\, \nu^m\, d\nu = -\sum_k \frac{\beta_k}{\Gamma(1+\alpha_k)} \frac{N^{\alpha_k+m+1}}{\alpha_k+m+1} \qquad m = 1,3,5 \qquad 3.12$$

The symmetric amplitude $f_s(\nu)$ involves even signature exchanges only.

The F.E.S.R. integrals involve the imaginary part of the amplitude only. If the real part is used instead, then these new sum rules are derived using the amplitude $-iq\, f(\nu)$ where q is given by equation 3.13

$$q^2 = \nu^2 - \nu_o^2 \qquad 3.13$$

This amplitude is still an analytic function with the same cut structure as above and the sum rule for the antisymmetric combination analgous to a) is

$$\int_{\nu_o}^{N} \mathrm{Re}\, f(\nu)\, q\, \nu^m = \sum_k \frac{\beta_k}{\Gamma(1+\alpha_k)} \frac{N^{\alpha_k+m+2}}{\alpha_k+m+2} \tan\frac{\pi}{2}\alpha_k \qquad 3.14$$

omitting terms of order ν_o^2/N^2 on the right.

CONTINUOUS MOMENT SUM RULES

To combine the sum rules for the real and imaginary parts of the amplitude [41] a sum rule is written for the amplitude $(-iq)^{-\varepsilon-1} f(\nu)$ where ε is a continuous real parameter ($\varepsilon \lesssim 1$) and q is given by equation 3.13. The cuts of the function $q^{-(\varepsilon+1)}$ are chosen to run from ν_o to ∞ and $-\nu_o$ to $-\infty$

and $q^{-(\varepsilon+1)}$ is normalised such that it assumes a real number on the right hand cut in the upper half-complex plane. The sum rule is then written, omitting terms of order ν_o^2/N^2:

$$\int_{\nu_o}^{N} \left[\text{Cos}\,\frac{\pi}{2}(\varepsilon+1)\ \text{Im}\,f(\nu) + \text{Sin}\,\frac{\pi}{2}(\varepsilon+1)\ \text{Re}\,f(\nu)\right] q^{-\varepsilon-1}\,d\nu =$$

$$= \sum_k \frac{\beta_k}{\Gamma(1+\alpha_k)} \frac{N^{\alpha_k-\varepsilon}}{\alpha_k-\varepsilon} \frac{\text{Cos}\,\pi/2(\alpha_k-\varepsilon-1)}{\text{Cos}\,\pi/2\ \alpha_k} \qquad 3.15$$

Such a sum rule is termed a 'continuous moment sum rule' and, although it contains no more information than the individual F.E.S.R., it represents the information in a convenient form.

S E C T I O N B

BOOTSTRAPS

The Regge pole parameters on the right of equation 3.15 are related to bound states and resonance properties in the t-channel whereas the left hand side low energy integrals are dominated by s-channel bound states and resonances. The sum rules resemble self-consistency relations between s and t channel exchanges i.e. bootstrap equations.

There are several ways in which the sum rules can be applied to a phenomenological analysis and they are divided into three types differing only in emphasis.

a) Resolving ambiguities in the low energy region by means of the high energy data [42].

b) Using low energy data to predict high energy parameters [39].

c) Making simultaneous fits to high and low energy data in a manner consistent with analyticity [44] [45] [46].

Since in general high energy data is less accurate than that at low energies type b) and c) analyses outweigh type a) in importance. An advantage of the sum rules is that they relate directly to amplitudes rather than quadratic

functions of amplitudes as with scattering data. They exploit the unscrambling of quadratics that has already been done in the low energy analyses.

The usefulness and accuracy of 'finite energy sum rules' depends mainly on the available data. A particularly favourable case is the sum rule at $t = 0$ [47], [48] where by means of the optical theorem the imaginary part of the amplitude is simply related to the total cross sections. With the accurate measurements of total cross-sections available, accurate predictions of Regge parameters can be made at $t = 0$.

Away from the forward direction $t \neq 0$, the imaginary part of the amplitude is no longer given directly in terms of measured cross-sections and it is then necessary to utilise a phase shift analyses which for pion nucleon scattering are quite reliable.

The finite energy sum rules for the real part of the amplitude are, in general difficult to construct, since only in a few cases are the real parts of the amplitudes known directly (e.g. Coulomb interference). If the real parts are determined from dispersion relations then they do not give independent information about the high energy behaviour and the sum rules are trivially satisfied.

To construct the continuous moment [44] sum rules, it is necessary to rely totally on phase shift analyses, since they involve combinations of the real and imaginary parts. In principle, there is an infinite sequence of these continuous moment sum rules suggesting that all the high energy parameters are determined by this infinite set of consistency equations. However the Regge series on the right hand side of the C.M.S.R. must be truncated after a few terms since the finer details are lost in experimental errors and the relevant importance of different Regge terms on the right hand side of the C.M.S.R. is only the same as in the Regge expansion itself

evaluated at the sum rule cut off N.

PION-NUCLEON : CONTINUOUS MOMENT SUM RULES

The sum rules are constructed for the arising odd pion nucleon signatured amplitudes $\nu A'^{(+)}$, $A'^{(-)}$, $B^{(+)}$, $\nu B^{(-)}$ where the asymptotic forms are given by equations [49] 2.19.

The sum rules are:

$$\int_{\nu_o}^{\nu_1} d\nu\ \nu\ \mathrm{Im}\left[(\nu_o^2-\nu^2)^{-\frac{[\varepsilon+1]}{2}} A'^{(+)}\right] = -\sum_{PP'} \gamma^{+}(\alpha(t),t)\ \frac{\mathrm{Sin}\pi/2(\alpha-\varepsilon-1)}{\mathrm{Sin}\pi/2\ \alpha}\ \frac{(\nu_1^2-\nu_o^2)^{\frac{\alpha-\varepsilon+1}{2}}}{\alpha-\varepsilon+1}$$

$$\int_{\nu_o}^{\nu_1} d\nu\ \mathrm{Im}\left[(\nu_o^2-\nu^2)^{-\frac{[\varepsilon+1]}{2}} B^{(+)}\right] = -\sum_{PP'} \beta^{+}(\alpha(t),t)\ \frac{\mathrm{Sin}\pi/2(\alpha-\varepsilon-1)}{\mathrm{Sin}\pi/2\ \alpha}\ \frac{(\nu_1^2-\nu_o^2)^{\frac{\alpha-\varepsilon-1}{2}}}{\alpha-\varepsilon-1}$$

$$\int_{\nu_o}^{\nu_1} d\nu\ \mathrm{Im}\left[(\nu_o^2-\nu^2)^{-\frac{[\varepsilon+1]}{2}} A'^{(-)}\right] = -\sum_{\rho} \gamma^{-}(\alpha(t),t)\ \frac{\mathrm{Cos}\pi/2(\alpha-\varepsilon-1)}{\mathrm{Cos}\pi/2\ \alpha}\ \frac{(\nu_1^2-\nu_o^2)^{\frac{\alpha-\varepsilon}{2}}}{\alpha-\varepsilon}$$

$$\int_{\nu_o}^{\nu_1} d\nu\ \nu\ \mathrm{Im}\left[(\nu_o^2-\nu^2)^{-\frac{[\varepsilon+1]}{2}} B^{(-)}\right] = -\sum_{\rho} \beta^{-}(\alpha(t),t)\ \frac{\mathrm{Cos}\pi/2(\alpha-\varepsilon-1)}{\mathrm{Cos}\pi/2\ \alpha}\ \frac{(\nu_1^2-\nu_o^2)^{\frac{\alpha-\varepsilon}{2}}}{\alpha-\varepsilon}$$

3.16

where the nucleon pole term situated at $\nu = \nu_B$ is assumed to be included on the left hand side of the equations. The pole term for each sum rule is given in table I.

TABLE I

$\nu A'^{(+)}$	$-G^2 \frac{\pi}{2M} \frac{\nu_B^2}{1-t/4M^2} (\nu_o^2-\nu_B^2)^{-\frac{[\varepsilon+1]}{2}}$
$B^{(+)}$	$-G^2 \frac{\pi}{2M} (\nu_o^2-\nu_B^2)^{-\frac{(\varepsilon+1)}{2}}$
$A'^{(-)}$	$-G^2 \frac{\pi}{2M} \frac{\nu_B}{1-t/4M^2} (\nu_o^2-\nu_B^2)^{-\frac{(\varepsilon+1)}{2}}$
$\nu B^{(-)}$	$-G^2 \frac{\pi}{2M} \nu_B (\nu_o^2-\nu_B^2)^{-\frac{(\varepsilon+1)}{2}}$

The evaluation of the continuous moment sum rules is dependent on three parameters. ν_1 the cut off, t the momentum transfer and ε the continuous moment parameter [50]. The judicious choice of values for these parameters is of paramount importance in the useful application of the sum rules.

MOMENTUM TRANSFER t

a) C.M.S.R. at fixed negative t involve integrations over an unphysical region at low energies.

$$\text{Cos } \theta_s < -1 \quad \text{for } \nu = \frac{(4M^2-t)^{1/2} (4\mu^2-t)^{1/2}}{4M}$$

The extrapolation beyond $z_s = -1$ is done by using the partial wave expansion which will diverge at the nearest u-channel singularity. Such extrapolations are dubious since they differ greatly from one phase shift solution to another.

b) By definition of the variable ν the 's' and 'u' cuts are symmetric about the origin in the complex ν plane. At the point $\nu_o = 0 \rightarrow t = -4M_\mu$

the 's' and 'u' cuts overlap so that the low energy part of the integral is more dubious.

CONTINUOUS MOMENT PARAMETER ε

The sum rules emphasise high energy or low energy parts of the integral depending on the moment. This is a property of the incomplete Mellin transform [51] which is the class of functions of the type:

$$g(a) = \int_0^a f(x)\, x^{s-1}\, dx$$

a) For very high moments the low energy integral comes overwhelmingly from near the upper limit $\nu = \nu_1$ and the sum rules reduce to the Regge expression evaluated at $\nu = \nu_1$. The high moment sum rules are unreliable, since non-Regge fluctuations may still be present at the upper limit whereas in the low moment sum rules these fluctuations have a chance of averaging out.

b) Very low moment sum rules emphasise the low energy region where the partial wave extrapolation is unknown and as such do not yield useful information.

c) The derivation of the F.E.S.R. was for even (odd) integers 'n' for the antisymmetric (symmetric) part of the physical amplitude $f(\nu)$ and these are termed 'right signature sum rules'. The finite energy sum rules for the other integer values of 'n' [52] are obtained by writing down the sum rules for the amplitudes of definite signature in the t channel e.g:

$$A'(\nu,t) = \tfrac{1}{2}\left[A'^{(+)}(\nu,t) + A'^{(+)}(-\nu,t) + A'^{(-)}(\nu,t) - A'^{(-)}(-\nu,t)\right]$$

The amplitudes might contain such terms as ν^{2m-1}, ν^{2m} respectively which

cancel when constructing the physical amplitude. In Regge formalism $2m - 1, 2m$ correspond to the wrong signature values of J for the amplitudes $A'^{(+)}$, $A'^{(-)}$ respectively and the sum rules for these amplitudes, or their products with the variable ν which retain the initial crossing symmetry, may contain contributions from fixed poles at these points [23].

CUT OFF ν_1

The right hand side of the sum rules are constructed from the leading Regge trajectories which are, in practice, identified by fitting high energy experiments. The experimental errors are large enough so that the analyses warrant only a few Regge poles, and this expression is used at the low values of s {cut offs of ν_1 = 2 GeV have been used}.

The sum of crossed channel Regge poles is an asymptotic representation of the amplitude and although it may be expedient to retain only the leading terms, it is certainly not obvious that the right hand sides of equations 3.16 are well approximated by the leading Regge trajectories for low s. For example a Regge pole lying one unit below the leading poles introduces a correction of order $\left(\frac{1}{\cos\theta_t}\right)$, which for a low cut off $\nu_1 \sim 2$ GeV is of the order one. Thus it is not obvious, a priori that the prescription of extrapolating only the experimentally established traejctories to low s does not introduce a large error into the sum rule [53].

S E C T I O N C

Finite Energy sum rules are based on two theoretical concepts, analyticity and asymptotic behaviour. Being so general they have few predictions unless they are supplemented by assumptions (A) and (B) below.

(A) The scattering amplitudes are well approximated by the exchange of

a few Regge poles down to low energies (2 GeV/c).

(B) The imaginary part of the amplitude is dominated entirely by direct channel resonances.

(Both statements being subject to an important exception 'The Pomeron' - which is referred to later).

GLOBAL DUALITY

This implies the equivalence of resonance and Regge integrals in finite energy sum rules. This relation between direct channel resonances and Regge poles [54] then constitutes a 'bootstrap equation' since the Regge poles are themselves related to the resonances in the exchanged channel.

SEMI-LOCAL DUALITY

The duality [55] or equivalence between the direct channel resonances and Regge pole exchange should not be taken too literally, at least in the low energy region where the resonance amplitude shows large fluctuations as a function of the energy. Assumption (A) is supposed to hold only in an average sense when the resonance amplitude is integrated over a small (1 GeV) interval. It is this 'semi-local average' over the resonance contribution which is equated to the Regge amplitude.

LOCAL DUALITY

There cannot be local duality between fluctuating resonance terms and smooth Regge terms but Schmid [56] observed that the direct channel partial wave amplitudes resulting from Regge pole exchange trace out loops in the Argand diagrams as the energy increases. These loops are very similar to those obtained from phase shift analyses as evidence for nucleon

resonances [57] and Schmid suggested that the Regge induced loops do approximate the true resonance loops. This is 'local duality' and is an extreme form of the original duality concept. Suffice it to say that local duality is the subject of much controversy [58].

POMERANCHUK TRAJECTORY

As discussed in Chapter 2 the Pomeranchuk trajectory has the quantum numbers of the vacuum and it has a much smaller slope than other known trajectories to avoid giving rise to particle recurrencies in the exchanged channel physical region. Chiu and Kotanski [59] [60] demonstrated that Regge Argand loops are essentially generated by the exponential term $e^{-i\pi\alpha(t)}$ in the signature factor, and for a flat trajectory this term does not generate loops to be associated with resonances. Further since the Pomeron carries the quantum number of the vacuum, its exchange has the same contributions in all isospin states in the direct channel. If the Pomeron is dual to resonances then one expectsresonances in all isospin states which are more or less degenerate. This is certainly contradictory to everything that is observed experimentally. Freund and Harari [61] [62] conjectured that the Pomeron plays a separate role in duality, being dual to the non-resonant background term and this is the exception to be made to assumptions (A) and (B).

INTERFERENCE MODEL AND DOUBLE COUNTING

At low energies phase shift analyses indicate that the scattering amplitude is dominated by a large number of resonances, whereas at high energies the amplitude is dominated by the exchange of a few Regge poles. To interpolate between the two regions, a natural assumption is just to add the

resonance contribution to the Regge amplitude:

$$A = A(\text{resonance}) + A(\text{Regge})$$

At low energies A (resonance) dominates and A (Regge) is small while at higher energies A (resonance) will diminish and A (Regge) will take over. In the intermediate region (2-6 GeV) A (resonance) and A (Regge) are comparable and will interfere, this is the so-called Interference Model [63] [64].

The finite energy sum rules coupled with assumptions (A) and (B) gave a prescription for continuing the amplitudes from the high energy regions where A (resonance) and A (Regge) both represent one and the same thing and cannot possibly interfere. This has led to the term 'double counting' to describe the interference model since from a duality argument the resonances are already included in the Regge terms.

The criticism, based on the F.E.S.R., against the interference model is only valid if the sum rules are well satisfied and in certain cases (e.g. the B^+ amplitude in pion nucleon scattering) the sum rules are strongly violated. Also the absolute magnitudes of the resonance and Regge contributions are not determined. It is not difficult to modify the Regge energy dependence at low energies, with threshold factors etc. whilst retaining the necessary asymptotic behaviour.

CHAPTER lV

LOW ENERGY PHASE SHIFT - ANALYSES

The partial wave structure of pion-nucleon scattering has been studied at low energies by phase shift solutions of the scattering data [65]. This procedure has been carried out up to momenta of about 2.5 GeV/c and discloses a structure in which many partial waves can be represented as a combination of Breit-Wigner resonances with a relatively smoothly varying background [66].

In a 'conventional phase shift analyses' [67], complete sets of data ($\pi^{\pm}p$ total, differential and polarisation cross-sections, charge exchange differential and polarisation cross-sections) are assembled at individual energies in the energy range of the analyses. A series of random searches are carried out at each energy to determine the possible phase shift parameters and elasticities. At each energy there are many solutions and a solution must be selected at each energy in such a way that they form a continuous family over the whole range. The construction of a continous solution over a range of several GeV is not simple, since for each value of the angular momentum there are four phases and four elasticities, and when there can be upwards of ten solutions for each energy the task is somewhat tedious. Several computerised techniques have been developed to ensure the continuity of the solution (minimal path, minimal angle, minimal surface) but even then the phase shifts have a lot of wobbles. The continuous solution can be further smoothed by making independent fits to the different partial waves using dispersion theoretic parameterisations. Some of these dispersion fits are very good but the total amplitudes constructed from the dispersion smoothed solution do not reconstruct the data within the acceptable statistical errors.

ENERGY DEPENDENT MODEL PHASE SHIFT ANALYSES

At momenta in excess of 2 GeV/c, the phase shift analysis of the con-

ventional type becomes increasingly difficult, partly because of the relative paucity of experimental data but also because of the increasing number of angular momentum states that are of importance.

An alternative approach is to construct an energy dependent model which does not necessitate complete experiments at individual energies, since the model provides an interpolation over the whole energy range. The partial wave phase shift and elasticity parameters are then obtained from the partial wave projection of the model total amplitudes.

Roychoudhury et al. analysed pion-nucleon scattering in the momentum range 2-5 GeV/c by such an energy dependent model [68] [69]. The s-channel scattering amplitude is represented as a sum of two terms

$$F(s,\theta) = F_R(s,\theta) + F_p(s,\theta)$$

where $F_R(s,\theta)$ represents the amplitude for Regge pole exchanges determined to fit the high energy scattering data (> 6 GeV) in the forward and backward directions and $F_p(s,\theta)$ is a parameterised algebraic function of the variable s and θ (c m.s. scattering angle). The parameters in $F_p(s,\theta)$ are then varied so as to reproduce a good fit to all the extant data in the energy range specified and the partial wave phase-shifts are derived from the partial wave projection of the total amplitude $F(s,\theta)$.

The amplitude $F_p(s,\theta)$ is not to be associated with any particular model. Whether $F_p(s,\theta)$ represents an interference model resonance contribution or the difference between the resonance contribution and the averaged resonance contribution as in a dual type prescription is unimportant. The success of the decomposition depends on whether an economic parameterisation of $F_p(s,\theta)$ can be found which fits the data. In the form adopted both $F_p(s,\theta)$ and $F_R(s,\theta)$ contribute to the lower order phase shifts ($\ell \leq 8$) while only the Regge pole exchange amplitude $F_R(s,\theta)$ contributes to the higher

order phase shifts ($\ell > 8$). A good overall fit to the data was found but in common with most energy dependent parameterisations over a wide range of energy, the 'goodness of fit' obtained was not equal to that given by the single energy 'conventional' phase shift analyses.

NEW PHASE SHIFT SOLUTIONS [70]

In the following analysis we had the objective of constructing a new phase shift solution in the intermediate energy region (2 → 4.0 GeV)*† by combining the energy dependent results of Roychoudhury et al. and the conventional phase shift analysis techniques. We investigated whether statistically satisfactory fits that lie close to the Roychoudhury solution can be obtained at individual energies. The statistical criterion required that the normalised χ^2 should correspond to those given by Donnachie [71] [72] and more recently by Ayed et al. [73] for their single energy analyses. If such solutions do exist, they have the advantage of having the smoothness and continuity properties built in from the initial energy dependent fits, avoiding the difficulties encountered in dispersion theoretic fits by Donnachie et al.

The method employed is to start from the phase shift parameters given by Roychoudhury et al. and search for solutions by varying the parameters in a limited field chosen to be within ± 20% of the starting values. From both our own work and from that of Ayed et al. [73] it is clear that phase shifts for $\ell \geq 5$ cannot be determined meaningfully from the data. However it is clear by inspecting the results given by the model of Roychoudhury et

---

*† The analysis has been completed over the whole range 2-5 GeV but the results for the single energy phase shift analysis are not quoted in the range 4-5 GeV because minimisation was only possible at the two extremities of the range. However there are several pieces of data at other intermediate energies and satisfactory fits can be obtained by interpolating the phase shift data at those points without minimisation. The phase for these energies would artificially enhance the partial waves and as such are not quoted.

al. that the phase shifts in the interval $5 \lesssim \ell < 9$, although small, are collectively of considerable importance and make a significant contribution to the amplitude. As higher order phase shifts are connected with the peripheral part of the interaction it is reasonable to suppose that the Roychoudhury model being based on Regge pole exchanges, will provide these phases with sufficient accuracy. Accordingly the phase shifts for $\ell > 5$ were taken from the work of ref. [69] and held fixed to these values throughout the minimisation.

COULOMB SCATTERING

The phase shift analysis is complicated by the presence of the Coulomb interaction, the effect of which is important at small angles ($\sin\theta \sim \theta$). To account for the electromagnetic effects in $\pi^{\pm}p \to \pi^{\pm}p$ scattering we used the formalism of Roper et al. [74] and constructed electromagnetic amplitudes, correct relativistically to first order in α and non-relativistically to all orders in α. In terms of the partiy conserving helicity amplitude $f_1(\pi^{\pm}p)$ and $f_2(\pi^{\pm}p)$, (see Equations 1.41), we write

$$f_1^{em}(\pi^{\pm}p) = f_1^{rem}(\pi^{\pm}p) + f_1^{coul}(\pi^{\pm}p) - f_1^{coul\ \alpha}(\pi^{\pm}p)$$
$$f_2^{em}(\pi^{\pm}p) = f_2^{rem}(\pi^{\pm}p) + f_2^{coul}(\pi^{\pm}p) - f_2^{coul\ \alpha}(\pi^{\pm}p) \qquad 4.1$$

where $f_1^{rem}(\pi^{\pm}p)$, $f_2^{rem}(\pi^{\pm}p)$ are the relativistic amplitudes correct to first order in α, $f_1^{coul}(\pi^{\pm}p)$, $f_2^{coul}(\pi^{\pm}p)$ are the non relativistic electromagnetic (Coulomb) amplitudes correct to all orders in α and $f_1^{coul\ \alpha}(\pi^{\pm}p)$, $f_2^{coul\ \alpha}(\pi^{\pm}p)$ are the non-relativistic limits of $f_1^{rem}(\pi^{\pm}p)$, $f_2^{rem}(\pi^{\pm}p)$ correct to first order in α.

The total amplitudes for $\pi^{\pm}p \to \pi^{\pm}p$ scattering are then

$$f_1(\pi^{\pm}p) = f_1^{N}(\pi^{\pm}p) + f_1^{em}(\pi^{\pm}p)$$
$$f_2(\pi^{\pm}p) = f_2^{N}(\pi^{\pm}p) + f_2^{em}(\pi^{\pm}p) \qquad 4.2$$

where $f_1^{N}(\pi^{\pm}p)$ and $f_2^{N}(\pi^{\pm}p)$ are the pion nucleon amplitudes constructed from the phase shifts and free from Coulomb scattering effects. The forms of the electromagnetic amplitudes as taken from Roper et al. are given in Appendix B.

DATA AND MINIMISATION PROCEDURE

As emphasised by Ayed et al. [73] complete sets of experiments (differential cross-sections and polarisation measurements) do not exist at any energy in the interval under consideration. However, the results of experiments whose momenta lie close together within the momentum resolution of the beam can be grouped together, and in this way nearly complete sets of measurements can be assembled. The data employed amounts to 1,104 experimental points taken from the data references [DATA 1]. At momenta between those used in the analysis the small number of experimental results available does not constrain the behaviour of the partial waves because it is possible to find a solution which interpolates solutions at adjacent momenta. If we were to include the solutions at these momenta amongst the results they would artificially enhance the behaviour of the partial wave amplitudes.

We made no preliminary selection of the data and all the available data at the quoted energies has been used. If there were many experiments at each energy one could perhaps in theory isolate the likely discrepancies but in practical work one rarely finds such a clear cut judgement is possible. In many cases the different sets of data are inconsistent particularly in normalisation and account of this inconsistency was made in the 'fitting'.

At each energy for which the data was assembled the quantity F defined below [75] was minimised. The normalisation parameters enter as a direct contribution to F. Alternative expressions for F [76], involving different weights for the normalisation parameters were used but the expression below was used in the actual fits.

$$F = \sum_n \left[\frac{\alpha_i(n)\, G_n(\text{exp}) - G_n(\text{calc})}{\Delta\, G_n(\text{exp})}\right]^2 + \sum_i \left[\frac{\alpha_i - 1}{\Delta\, \alpha_i}\right]^2 \qquad 4.3$$

In this expression $G_n(\text{exp})$ are the measured quantities, differential cross-sections, polarisations etc. and $G_n(\text{calc})$ are the same quantities calculated in terms of the phase shift parameters. The normalisation of different sets of angular distribution measurements, as noted previously, can be inconsistent. To allow for a common normalisation error on a set of measurements the parameters $\alpha_i(n)$ are introduced, these being varied during the minimisation. The normalisation error $\Delta\, \alpha_i$ has been taken from the experimental papers or, where this is not given a possible error of 5%-10% depending on the nature of the measurements, has been assumed.

No attempt was made to determine all solutions at each energy, rather we sought an acceptable solution such that the phase-shift parameters for $\ell < 5$ were within ± 20% of those given by the Roychoudhury model while keeping the phase shifts for $\ell > 5$ fixed to those given by that model.

RESULTS

At each energy for which the data could be assembled a satisfactory solution was found of the type specified. The phase shift parameters are illustrated in Figs.1-18 where they are compared with those given by the Roychoudhury model. The existence of the solutions corresponding to a normalised χ^2 in the range 1 to 1.8 confirms that the fit provided by the smoothed energy dependent model is meaningful and represents a possible

solution to the problem.

In most partial waves the energy dependent model provides phases which are the average of those phases given by the single energy fits. The rapid and erratic variation of the single-energy phase shift parameters as a function of energy within a limit about the smoothed phase shifts is certainly, in the main, due to inconsistencies in the data. A careful check eliminated the possibility that the variations seen were due to the existence of two or more different smooth solutions in that part of parameter space considered. It is impossible to assign errors to the individual phase parameters because of the inconsistencies in the data, but it is clear that these errors cannot be less than 10-15%. The errors are largest in the lowest partial waves and the S wave, in particular, is possibly not well determined [77]

In the energy-dependent model the partial waves exhibited structure which can be interpreted in terms of the resonances listed in table V. The resonances given in table V can also be identified in the single energy solutions with the exception of those in the D_{33}, S_{11} partial waves. In these particular partial waves identification is not possible because of the erratic behaviour of the phase parameters

$T = 3/2$ RESONANCES

POSITION (W in GeV)	PARTIAL WAVE
2.1	S_{31}
2.2	D_{33}
2.2	D_{35}
2.4	F_{35}
2.4	H_{311}
2.6	P_{33}

T = ½ RESONANCES

POSITION (W in GeV)	PARTIAL WAVE
2.16	G_{17}
2.10	G_{19}
2.59	H_{19}
2.20	P_{11}
2.16	F_{15}
2.52	S_{11}

TABLE V

CONCLUSION

Comparison with the results of Ayed et al. and Donnachie are difficult, especially due to the increasing number of partial waves used in each solution but substantial differences do exist between the phase shifts given by these two analyses and between those given here. The major difficulties arising in the single energy analyses are those of ensuring that out of the great multiplicity of solutions, the proposed solution is the physical solution and at the same time of ensuring that phase shifts of sufficiently high order are included. Because of these difficulties and in particular because only a limited number of phase shifts have been employed ($\ell \leq 5$), none of the existing single energy phase shift analyses can be considered completely satisfactory above 1.5 GeV.

Partial wave decomposition of particle reactions remains an interesting analytical tool at high energies because resonances continue to appear in individual partial waves as the energy of the reaction is raised. It is one of the central questions of particle physics whether resonances exist at any arbitrarily high energy or not and since high energy resonances are often

partly inelastic and are buried within many other angular momentum state contributions, they are not apparent without detailed angular momentum decomposition of the experimental observables.

'Conventional' phase shift analyses become increasingly difficult at intermediate and high energies because of the large number of parameters needed. The energy dependent model analysis represents a useful alternative involving fewer parameters. Even then the analysis suffers from a lack of the 'right' data. We strongly encourage experimentalists to complete measurements of reactions at all angles, not just the extremities and to complete sets of measurements at individual energies in the intermediate energy region.

FIGURE CAPTIONS - CHAPTER 4

FIGS. 1-18 Phase shift parameters for elastic pion nucleon scattering. The continuous line represents the solution of Roychoudhury et al. [ref.68,69] and the individual points are the results from the present work.

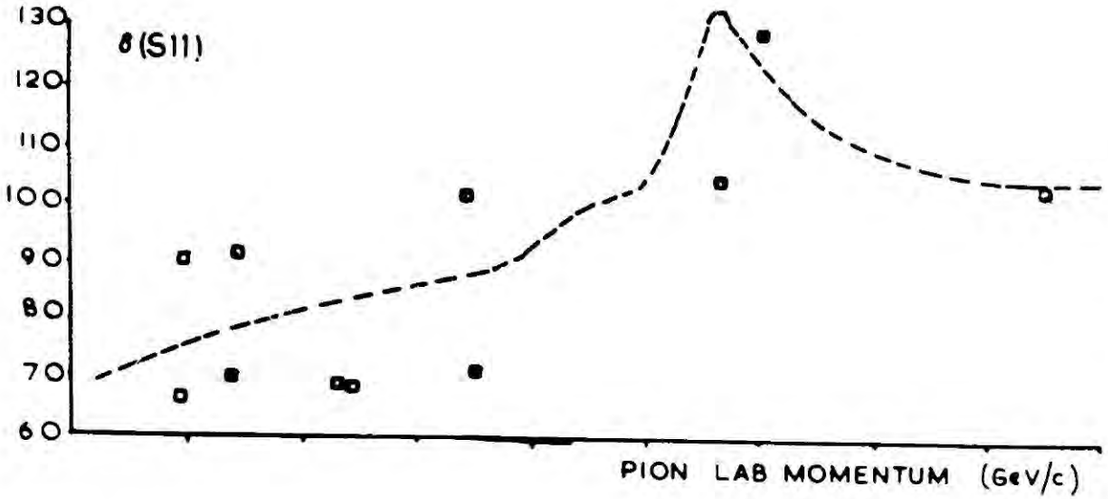
δ(S11)
130
120
110
100
90
80
70
60
PION LAB MOMENTUM (GeV/c)

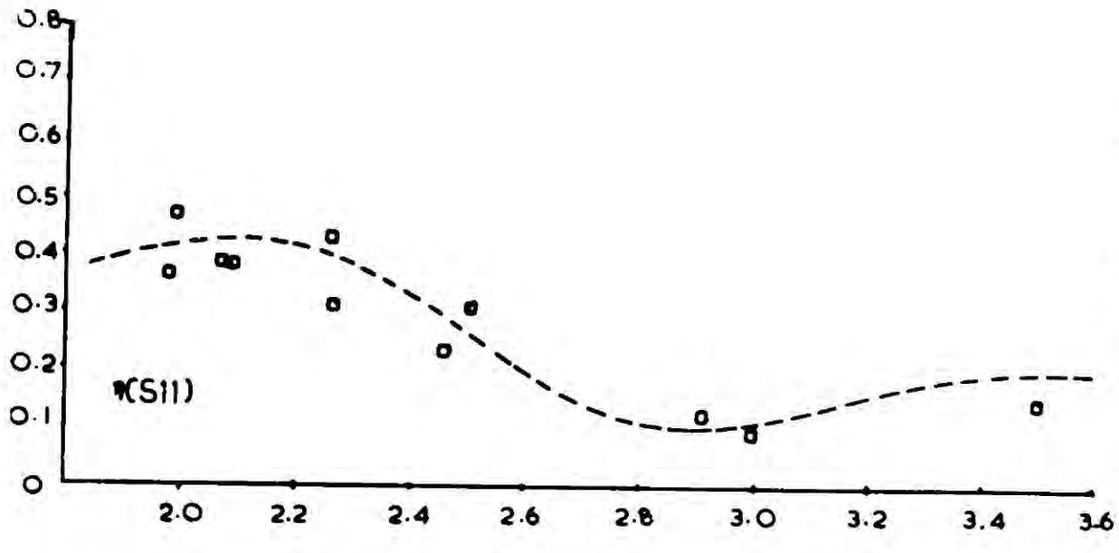
η(S11)
0.8
0.7
0.6
0.5
0.4
0.3
0.2
0.1
0
2.0
2.2
2.4
2.6
2.8
3.0
3.2
3.4
3.6

Fig. 1.

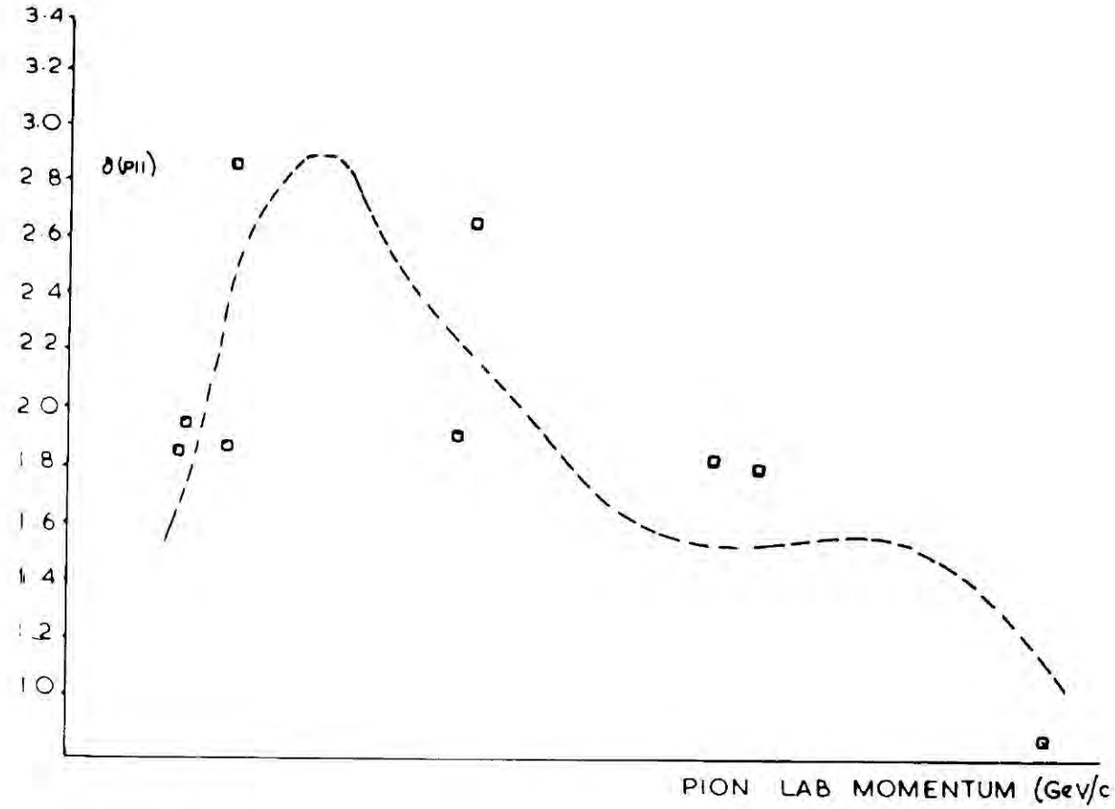
δ(P11)
3.4
3.2
3.0
2.8
2.6
2.4
2.2
2.0
1.8
1.6
1.4
1.2
1.0
PION LAB MOMENTUM (GeV/c

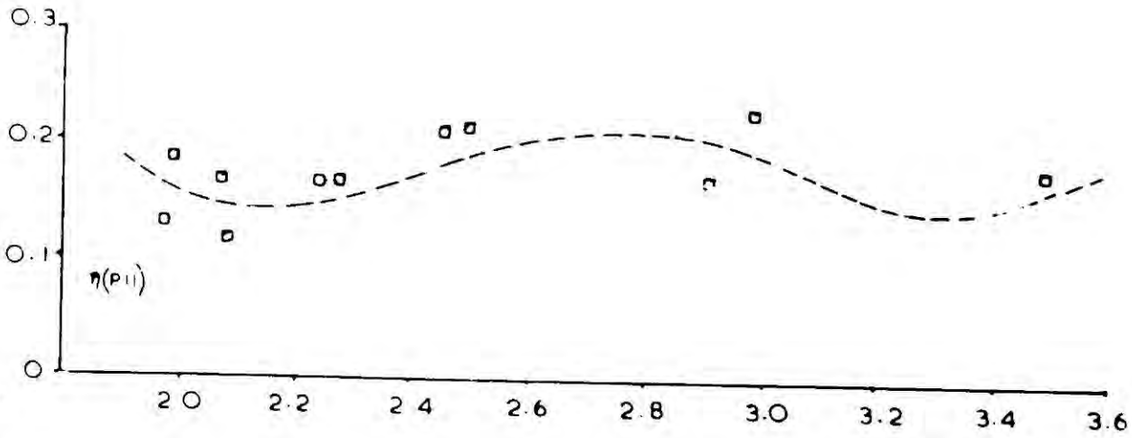
η(P11)
0.3
0.2
0.1
0
2.0
2.2
2.4
2.6
2.8
3.0
3.2
3.4
3.6

Fig. 2

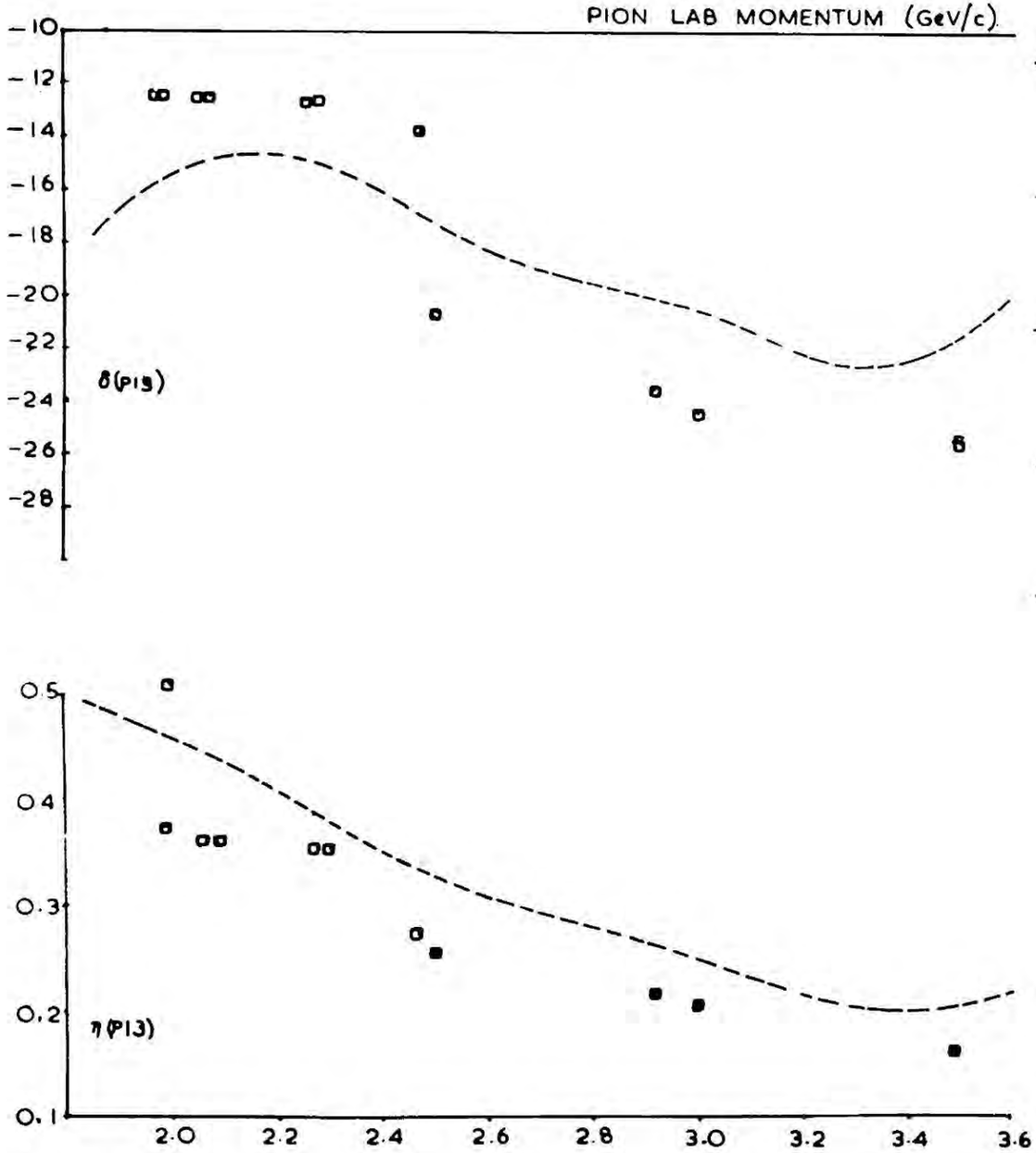
PION LAB MOMENTUM (GeV/c)
-10
-12
-14
-16
-18
-20
-22
-24
-26
-28
δ(P13)
0.5
0.4
0.3
0.2
0.1
η(P13)
2.0
2.2
2.4
2.6
2.8
3.0
3.2
3.4
3.6

Fig. 3.

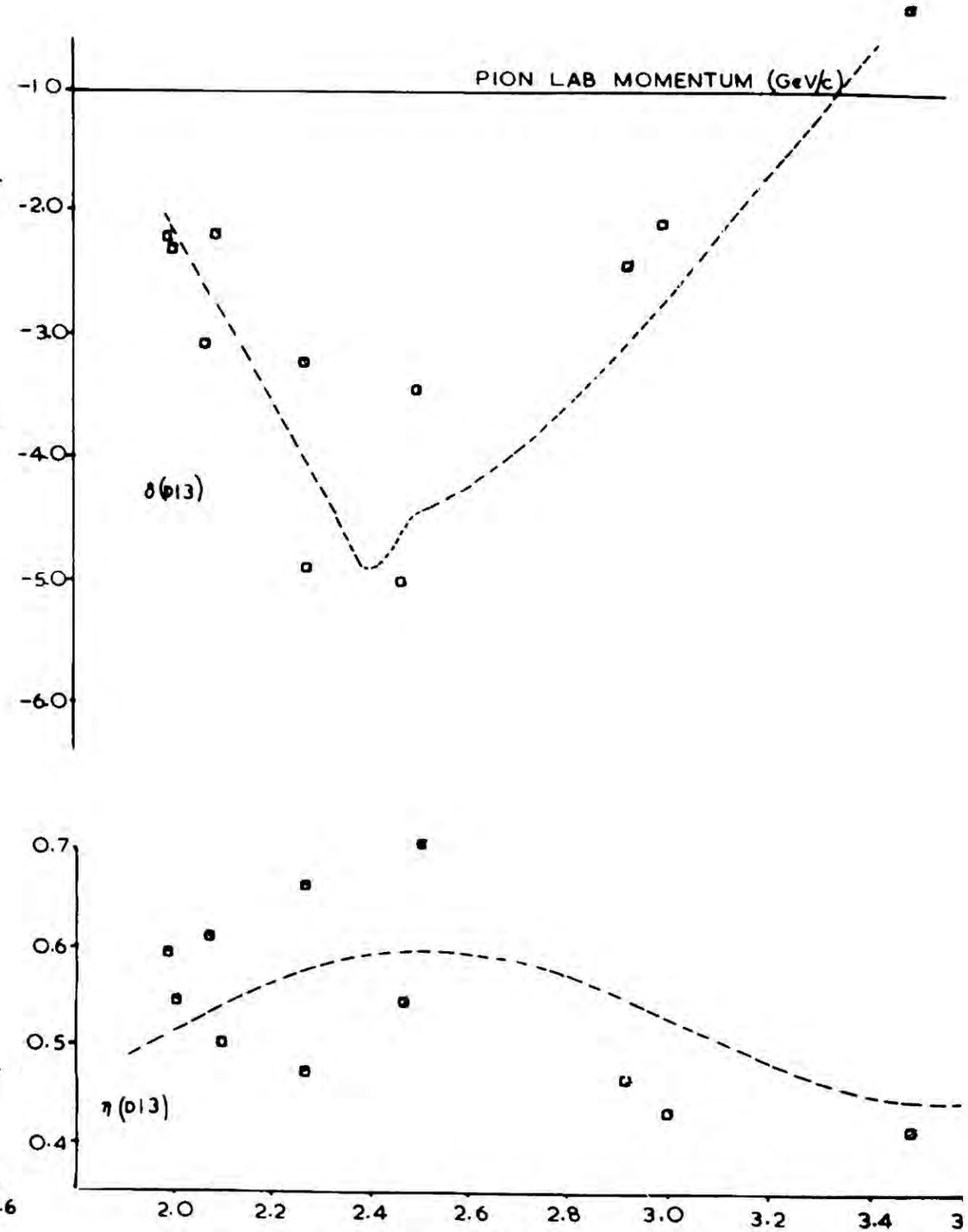
PION LAB MOMENTUM (GeV/c)
-1.0
-2.0
-3.0
-4.0
-5.0
-6.0
δ(P13)
0.7
0.6
0.5
0.4
η(D13)
2.0
2.2
2.4
2.6
2.8
3.0
3.2
3.4

Fig. 4.

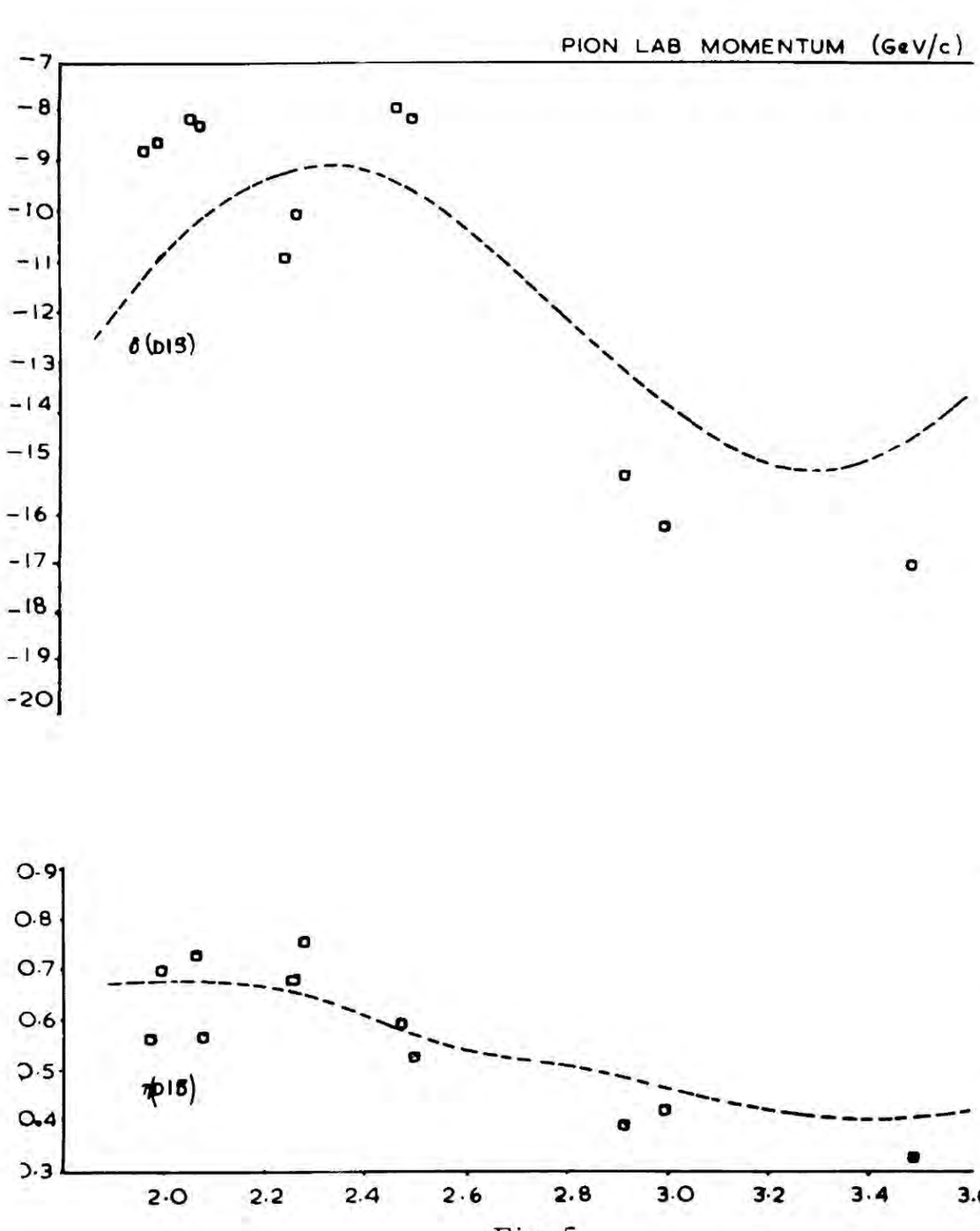
PION LAB MOMENTUM (GeV/c)
δ(DIS)
-7
-8
-9
-10
-11
-12
-13
-14
-15
-16
-17
-18
-19
-20
η(DIS)
0·9
0·8
0·7
0·6
0·5
0·4
0·3
2·0
2·2
2·4
2·6
2·8
3·0
3·2
3·4
3·6

Fig. 5.

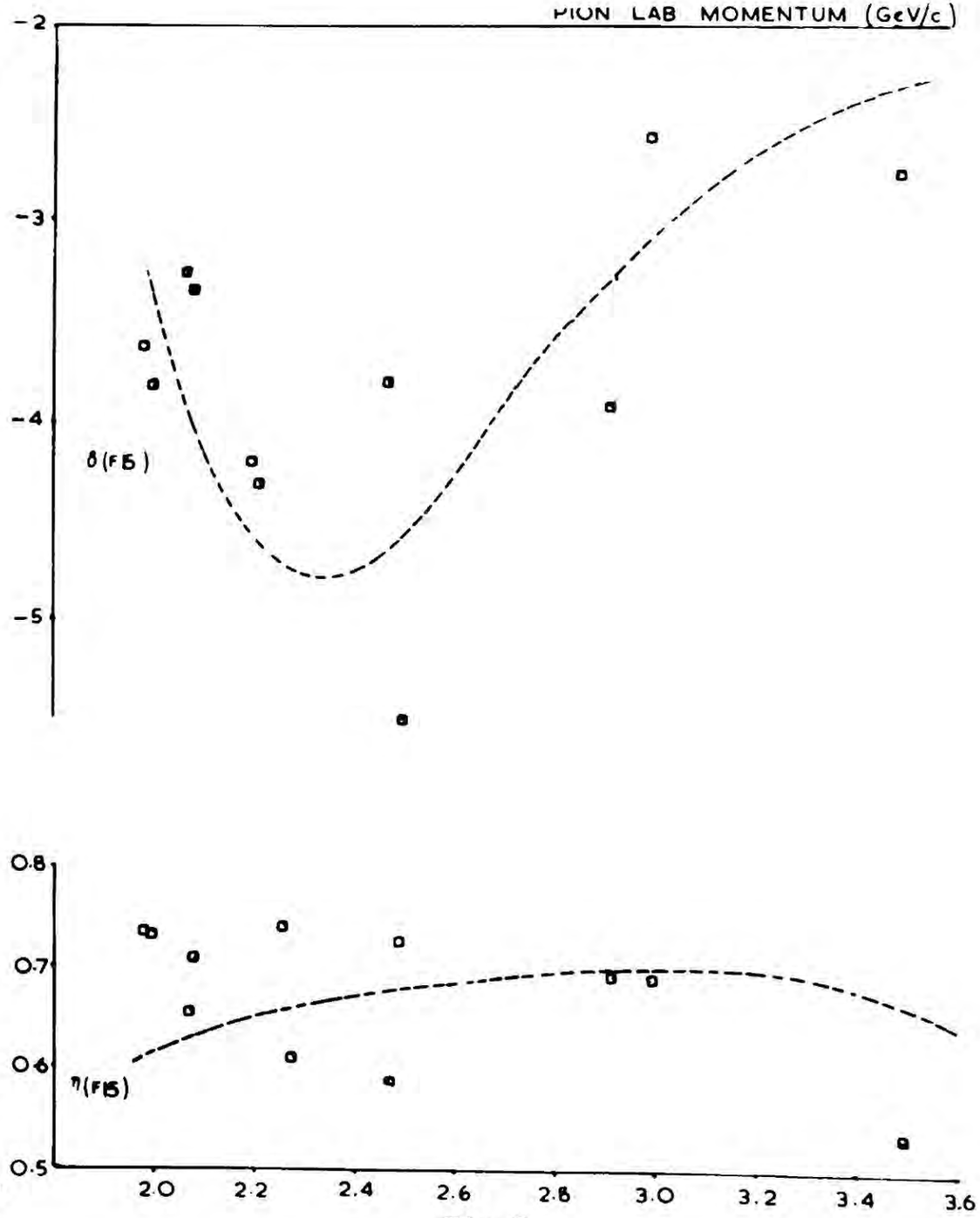
PION LAB MOMENTUM (GeV/c)
δ(FIS)
-2
-3
-4
-5
η(FIS)
0·8
0·7
0·6
0·5
2·0
2·2
2·4
2·6
2·8
3·0
3·2
3·4
3·6

Fig. 6.

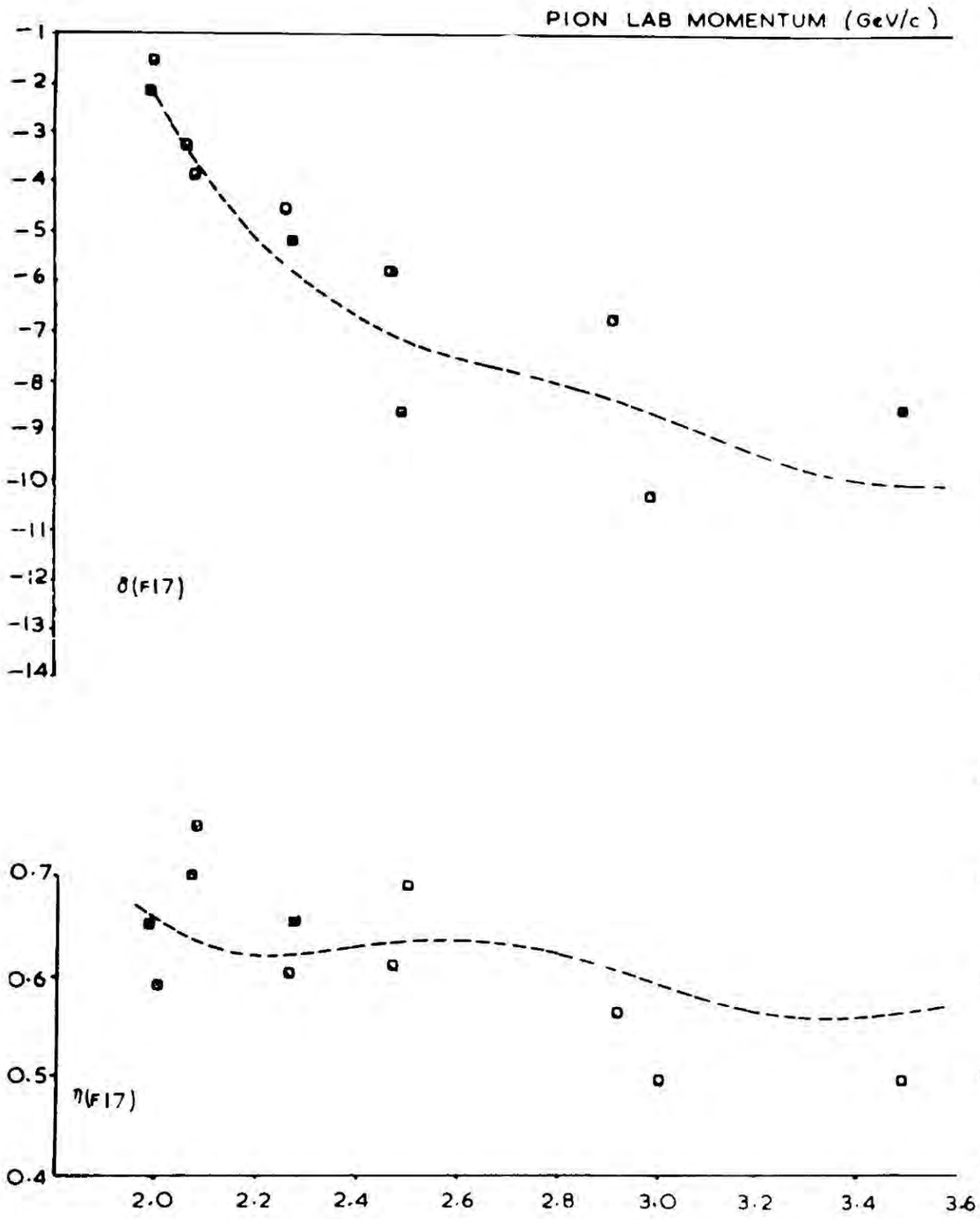
PION LAB MOMENTUM (GeV/c)
δ(F17)
η(F17)

Fig. 7.

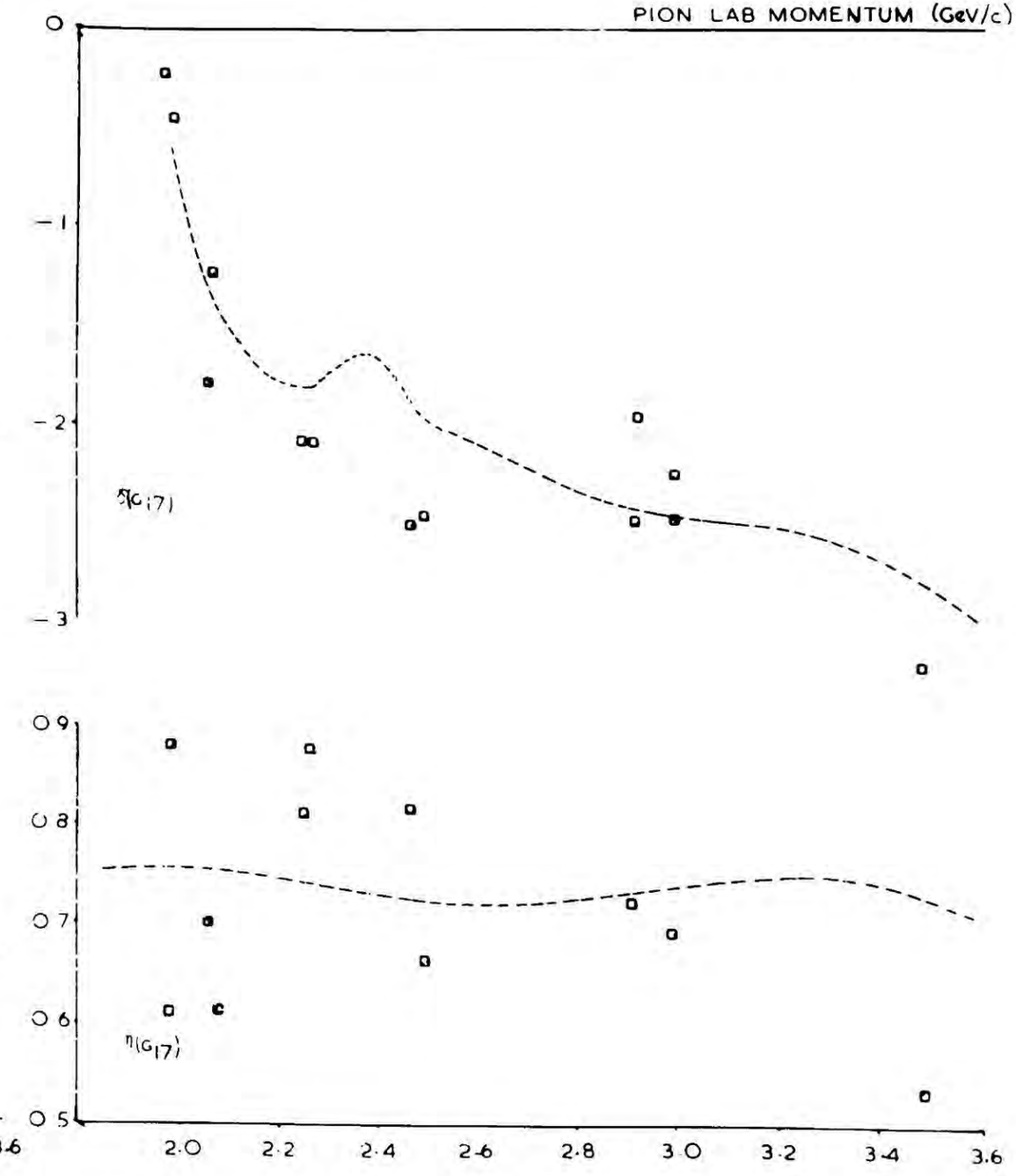
PION LAB MOMENTUM (GeV/c)
δ(G17)
η(G17)

Fig. 8.

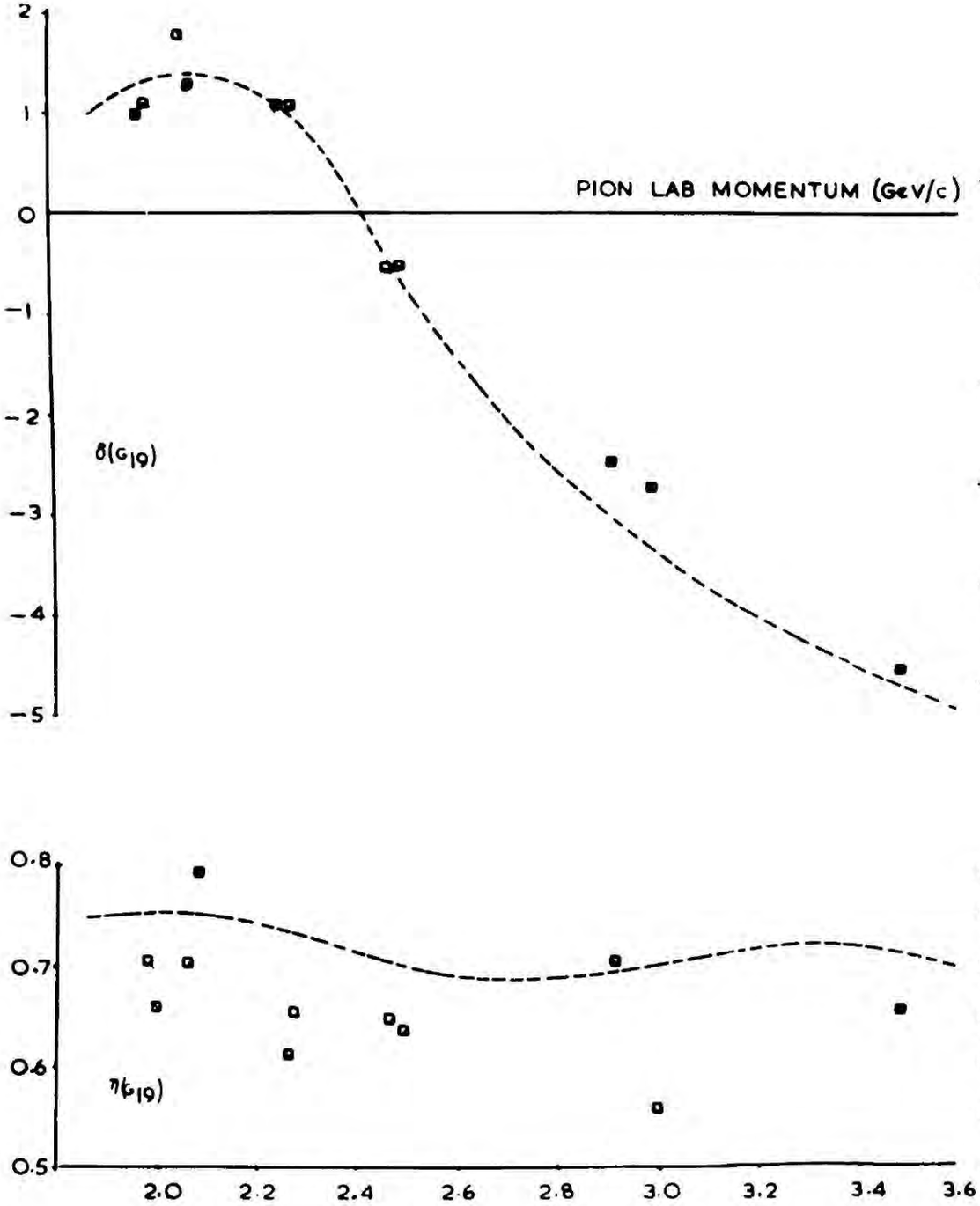
PION LAB MOMENTUM (GeV/c)
δ(G19)
η(G19)

Fig. 9.

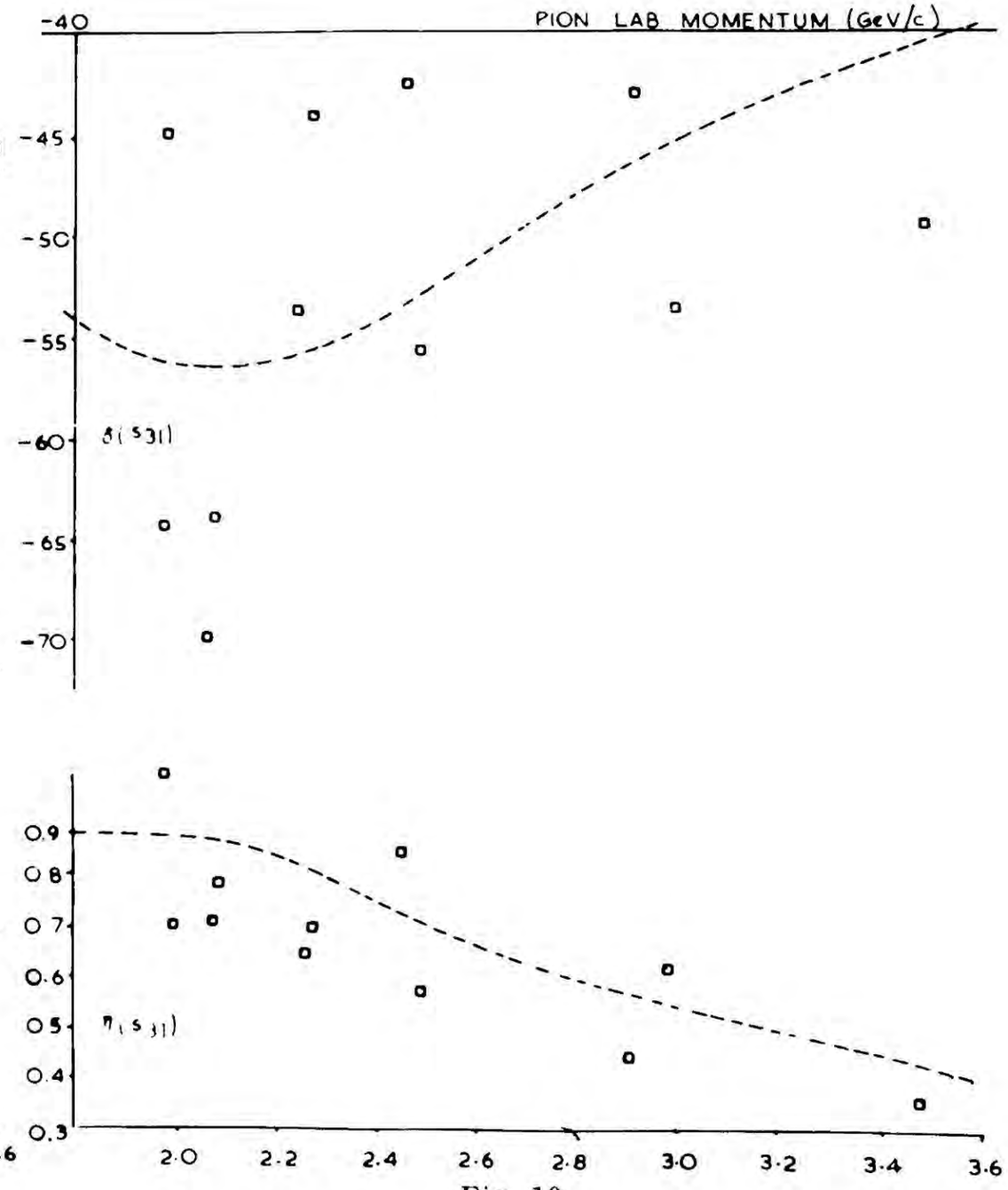
PION LAB MOMENTUM (GeV/c)
δ(S31)
η(S31)

Fig. 10.

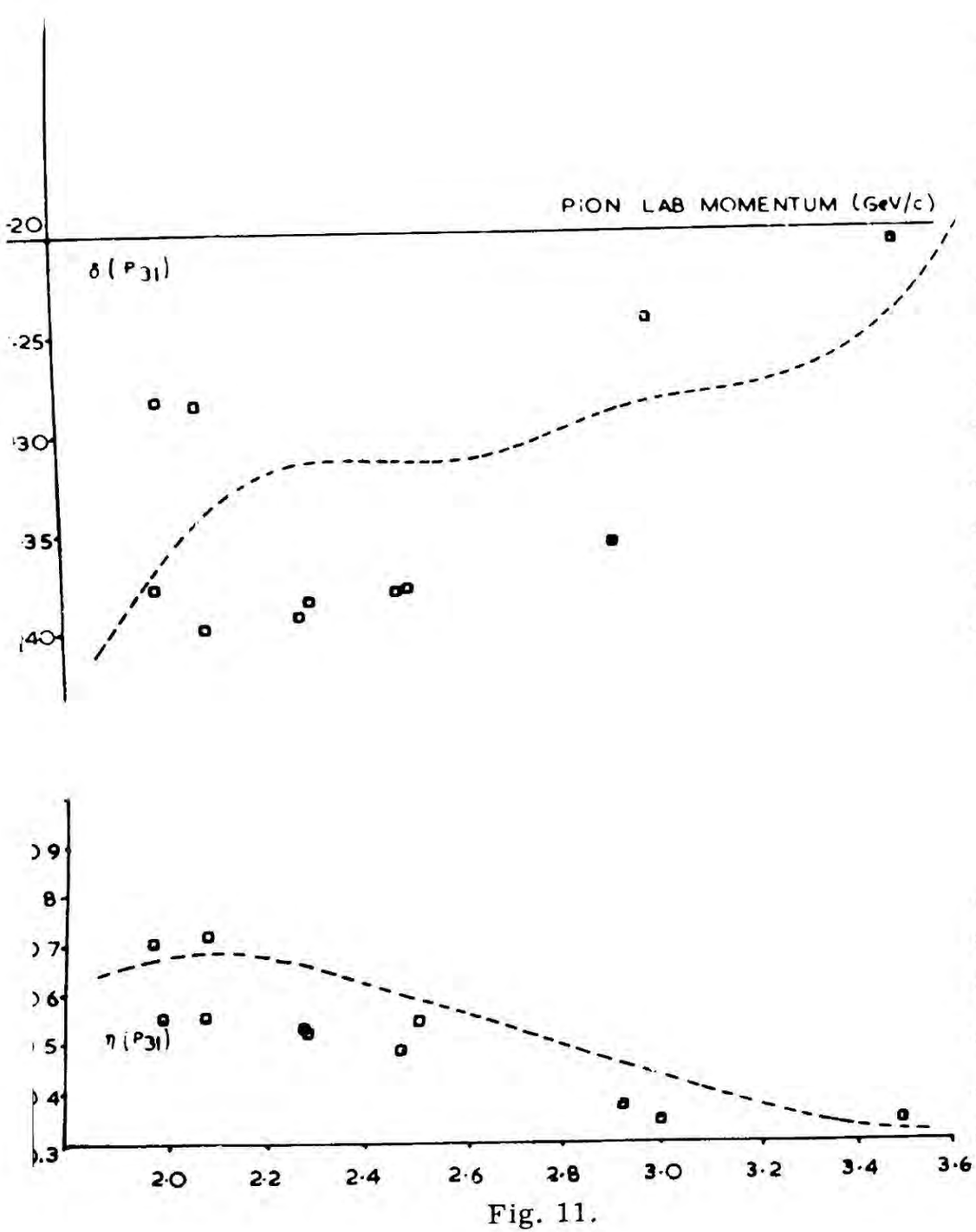
PION LAB MOMENTUM (GeV/c)
δ(P31)
-20
-25
-30
-35
-40
η(P31)
0.9
0.8
0.7
0.6
0.5
0.4
0.3
2.0
2.2
2.4
2.6
2.8
3.0
3.2
3.4
3.6

Fig. 11.

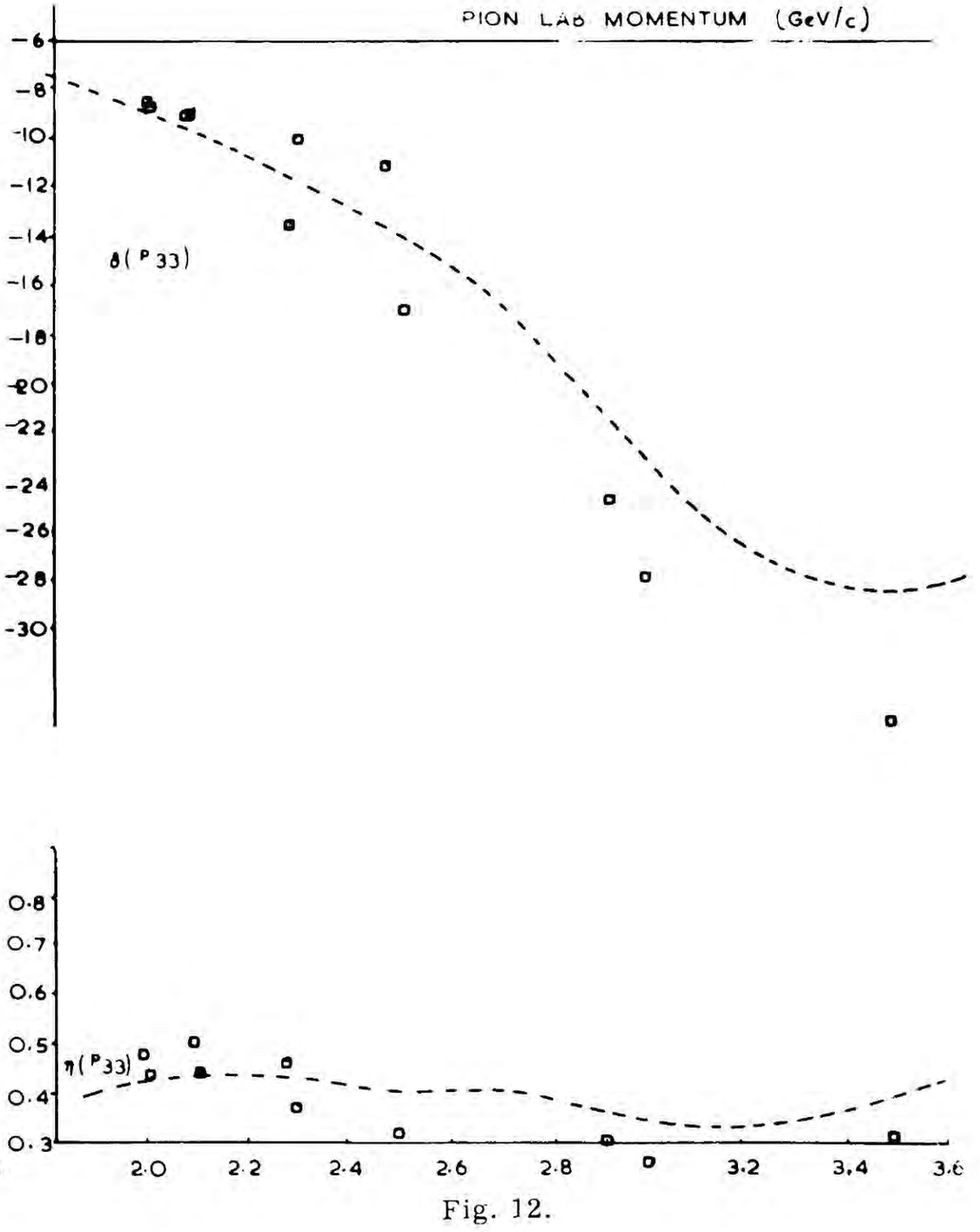
PION LAB MOMENTUM (GeV/c)
δ(P33)
-6
-8
-10
-12
-14
-16
-18
-20
-22
-24
-26
-28
-30
η(P33)
0.8
0.7
0.6
0.5
0.4
0.3
2.0
2.2
2.4
2.6
2.8
3.2
3.4
3.6

Fig. 12.

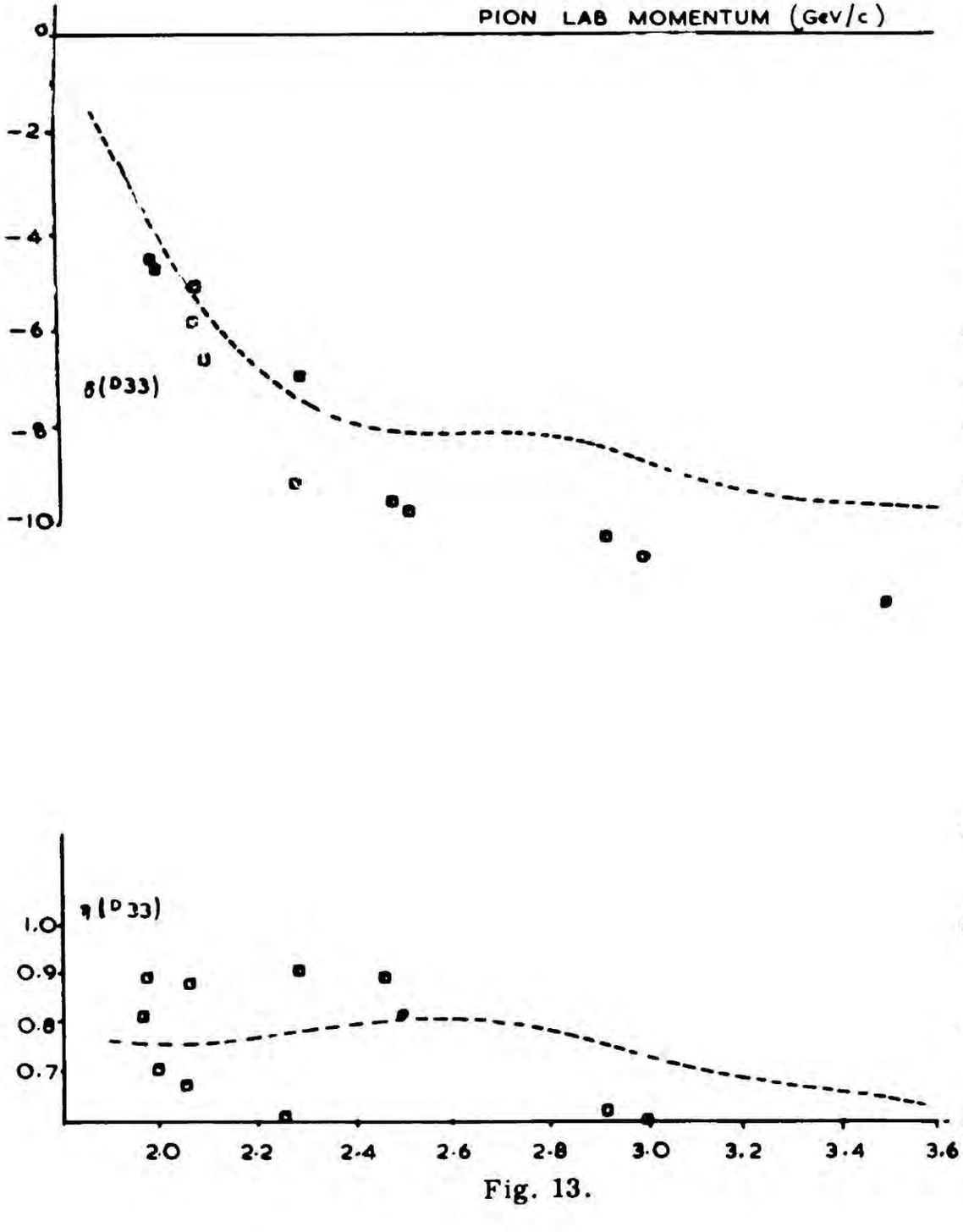
PION LAB MOMENTUM (GeV/c)
0
-2
-4
-6
-8
-10
δ(D33)
η(D33)
1.0
0.9
0.8
0.7
2.0
2.2
2.4
2.6
2.8
3.0
3.2
3.4
3.6

Fig. 13.

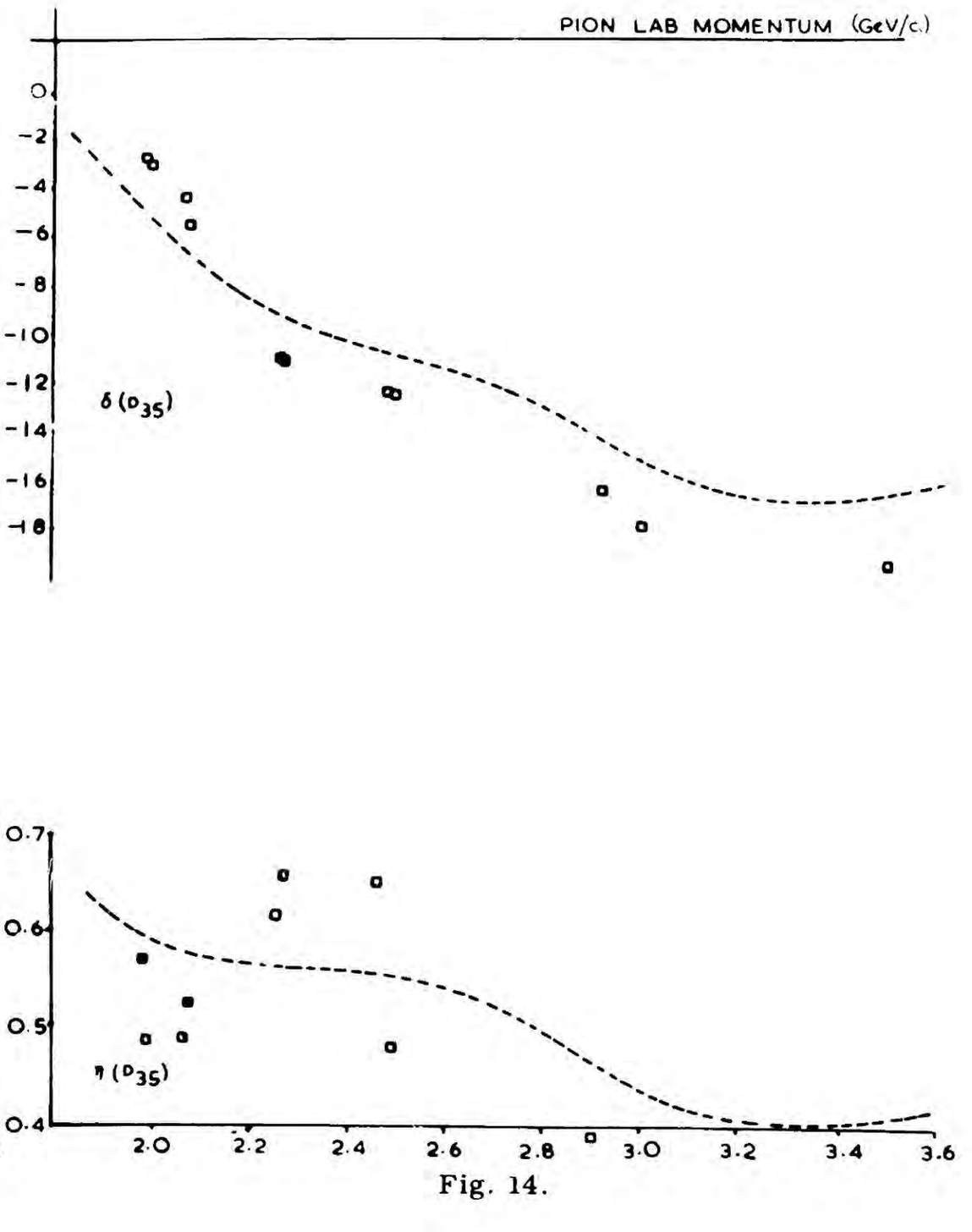
PION LAB MOMENTUM (GeV/c)
0
-2
-4
-6
-8
-10
-12
-14
-16
-18
δ(D35)
η(D35)
0.7
0.6
0.5
0.4
2.0
2.2
2.4
2.6
2.8
3.0
3.2
3.4
3.6

Fig. 14.

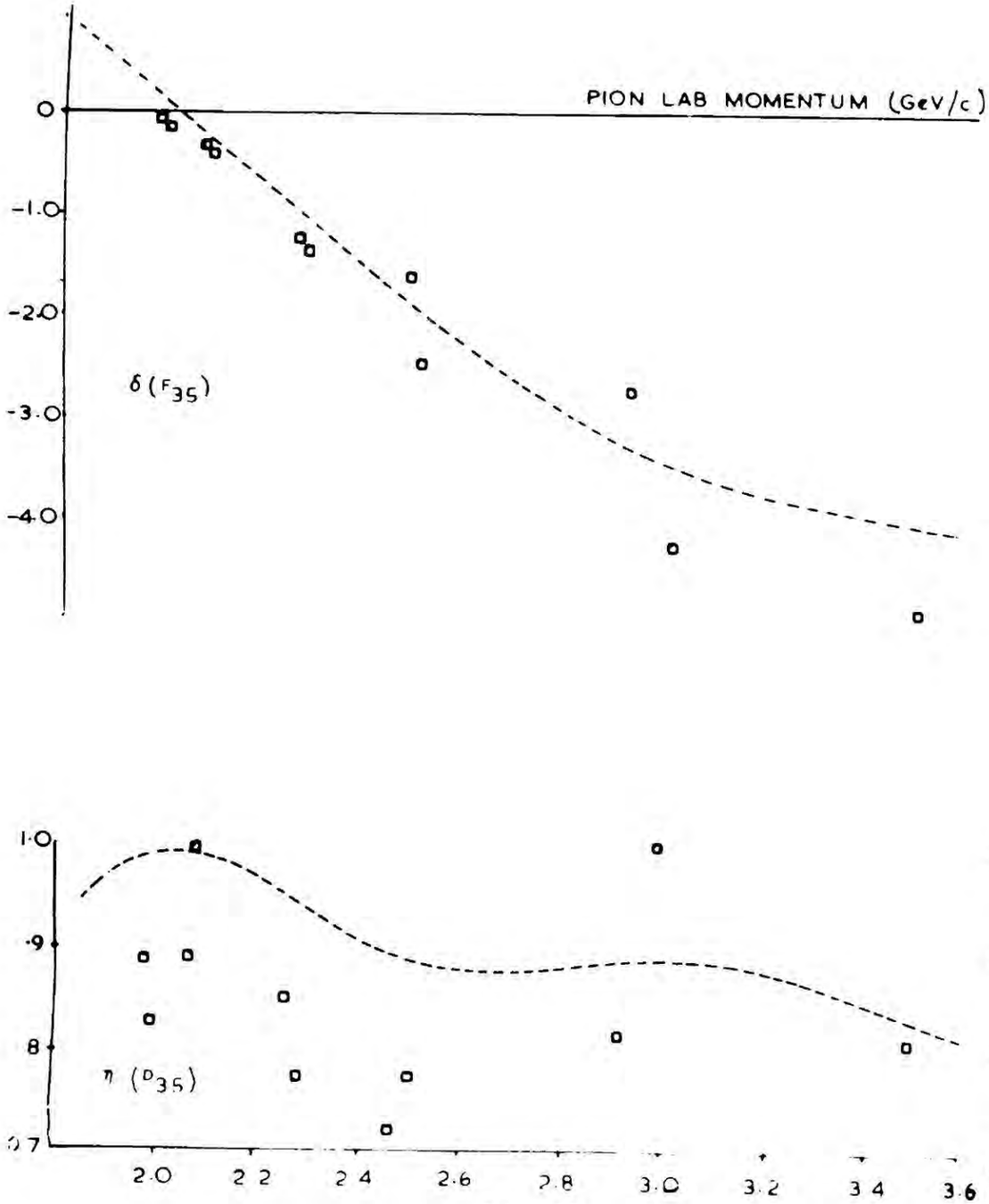
PION LAB MOMENTUM (GeV/c)
0
-1.0
-2.0
-3.0
-4.0
δ (F35)
1.0
·9
·8
·7
η (D35)
2.0
2.2
2.4
2.6
2.8
3.0
3.2
3.4
3.6

Fig. 15.

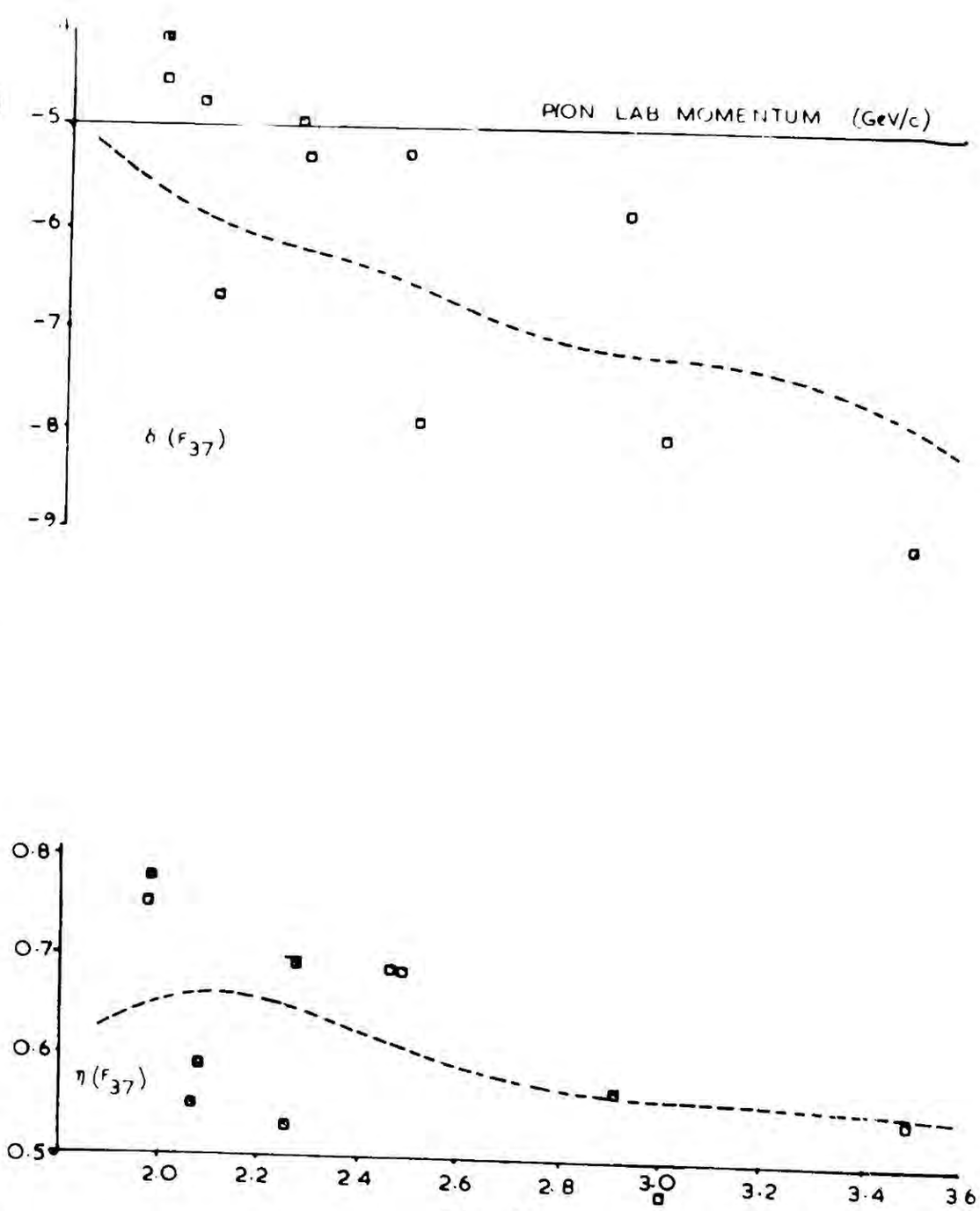
PION LAB MOMENTUM (GeV/c)
-5
-6
-7
-8
-9
δ (F37)
0.8
0.7
0.6
0.5
η (F37)
2.0
2.2
2.4
2.6
2.8
3.0
3.2
3.4
3.6

Fig. 16.

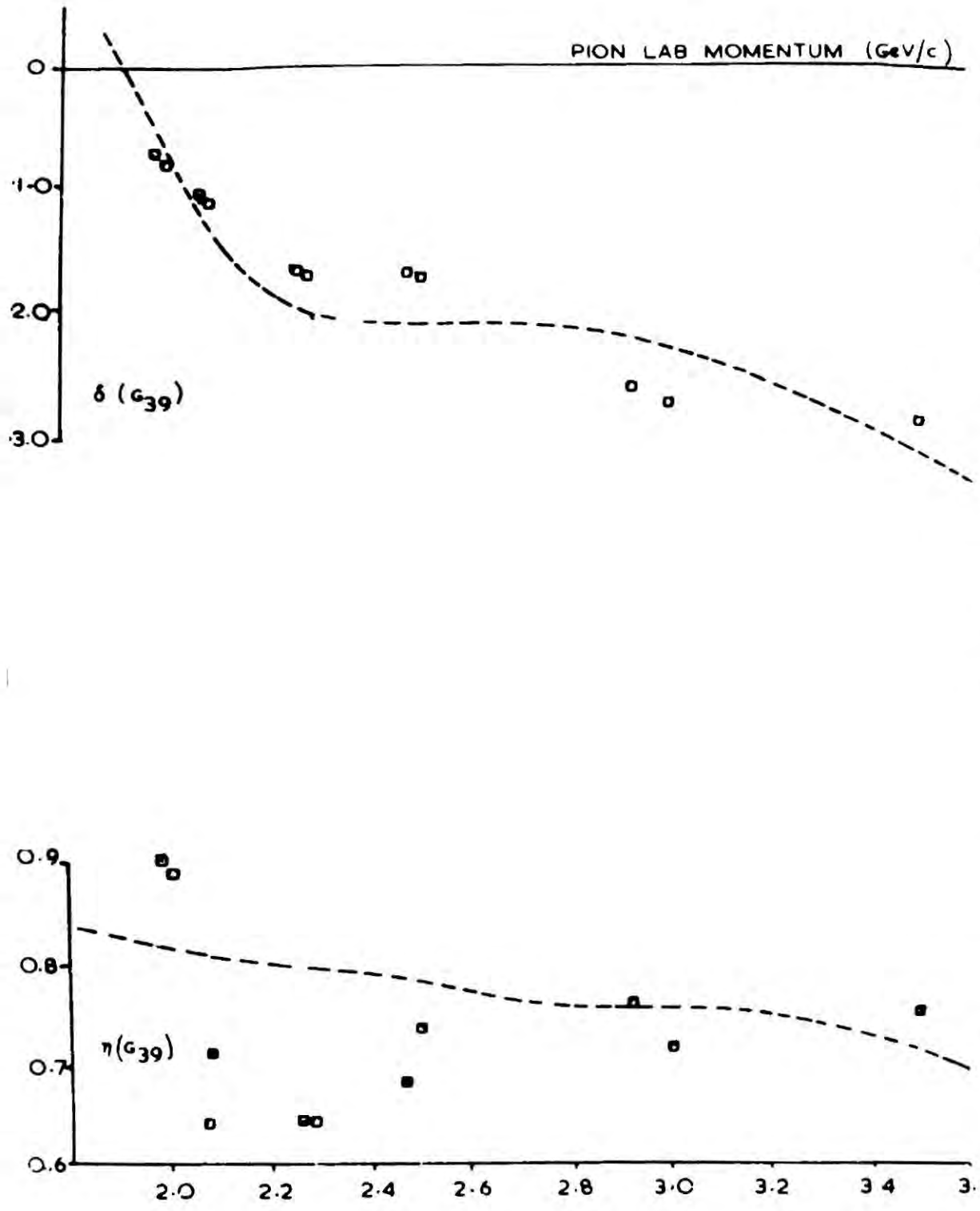

Fig. 17.

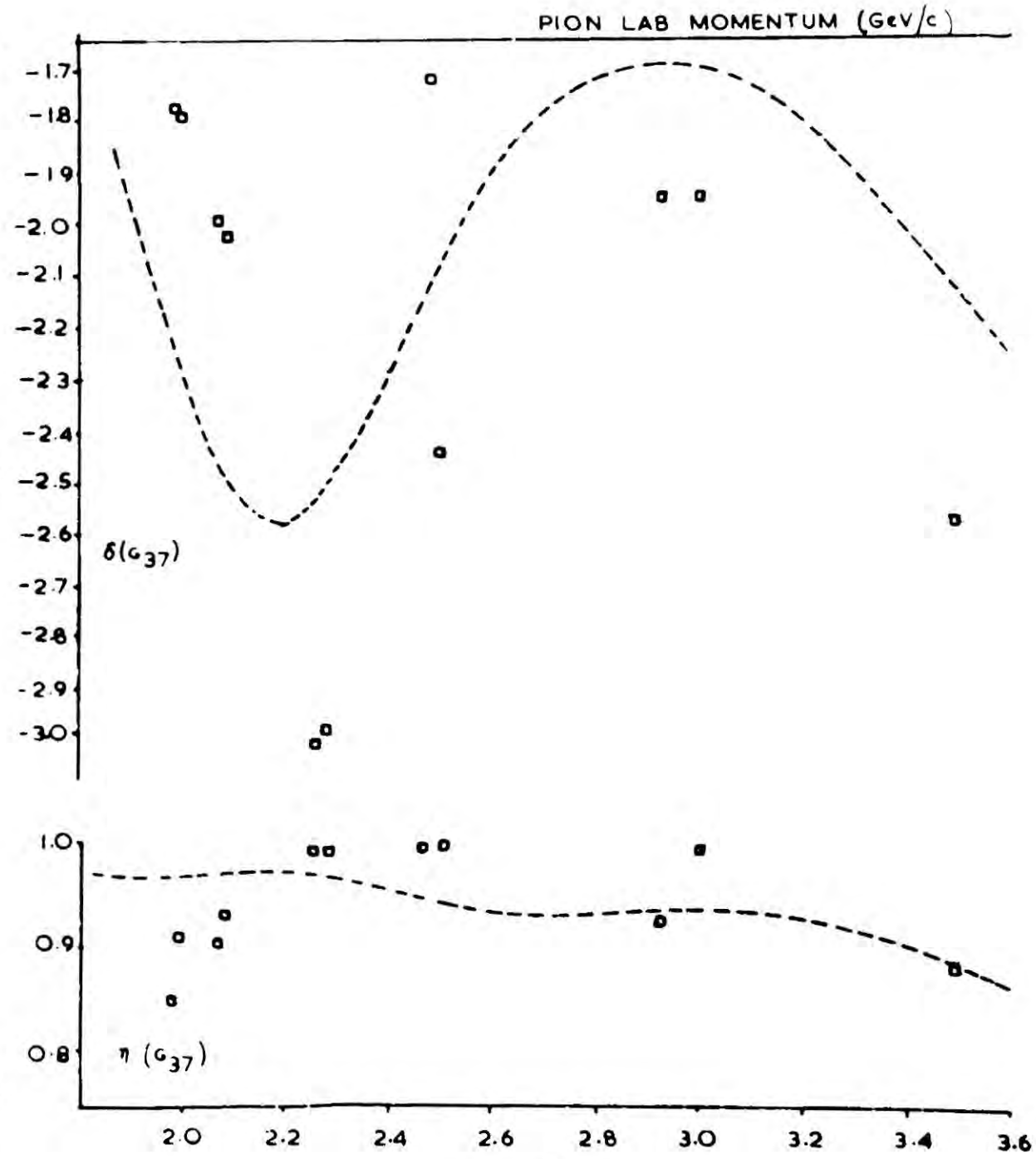

Fig. 18.

Figs. 1 - 18. Phase-shift parameters for elastic pion-nucleon scattering. The continuous line represents the solution of Roychoudhury et al. [1, 2], and the individual points result from the present work.

CHAPTER V

Pion nucleon elastic and charge exchange scattering are particularly suitable processes for investigation via the finite energy sum rules since reliable phase shift data is available at low energies from which to construct the low energy 'left hand side' amplitudes. Phase shift data exists up to 2 GeV for pion-nucleon elastic scattering and extensive analyses using [78] [79] [80] the sum rules for the isospin one and zero exchanges have been performed at this particular cut off. Their results indicate that only the trajectories identified from the scattering data in the Regge region (> 5 GeV) are necessary to satisfy the continous moment sum rules evaluated at the low cut off of 2 GeV and that these few Regge poles give the mean behaviour of the physical amplitude in the intermediate energy range.

In the present analysis we have the objective of comparing the results from a simultaneous analysis of the scattering data and the continuous moment sum rules evaluated at the low energy cut off of 2 GeV with those from a similar analysis at a 5 GeV cut off. Since it is not obvious that the leading trajectories, sufficient to fit the high energy data should be the only important ones at energies well below the Regge region, we wish to identify the contributory Regge terms for each particular cut off and determine whether the leading trajectories are sufficient to construct the amplitudes via the C.M.S.R. at 2 GeV without further contributions.

From the analysis we are able to make several general observations of the use of the C.M.S.R. to supplement high energy scattering data and under what circumstances the sum rules alone are useful in determining high energy parameters.

It is apparent from the high energy pion-nucleon scattering data that the spin flip amplitude νB^- parameterised by a single ρ Regge pole and the non-spin flip amplitude $\nu A'^+$ parameterised by a sum of Pomeron and P' Regge

poles are the dominant amplitudes and that the details of these amplitudes account for the general features of the scattering data.

The C.M.S.R. at 5 GeV for these amplitudes are in excellent agreement with the scattering data. This is not surprising, since we know from the scattering data that we have given the amplitudes the correct asymptotic forms. Even down to low energies the scattering data exhibits the dominance of the ρ spin flip amplitude and the P,P' non spin flip amplitude such that contributions from other lying trajectories still appear relatively unimportant in these amplitudes and the C.M.S.R. are well satisfied at low cut-offs by the above few Regge poles.

The amplitudes A'^{-}, B^{+} are not resolved by the scattering data very well and the sum rules offer a chance of unscrambling the details of the individual amplitudes which are not overt in the scattering data. The high energy cut off sum rules for A'^{-}, B^{+} although giving reasonable agreement with the scattering data are not satisfied as well as the equivalent $\nu A'^{+}$, νB^{-} sum rules. The divergencies are even greater in the low energy cut off C.M.S.R. for the amplitudes A'^{-}, B^{+} and there is strong evidence that contributions from trajectories other than those identified in the scattering region are present in these amplitudes at the low cut-off.

The results for these amplitudes emphasise the non predictive nature of the C.M.S.R. The sum rules will only yield physically meaningful solutions if they are given all the contributing terms at the cut off at which they are evaluated and what is more important, the sum rules evaluated at cut-offs below the Regge region (> 5 GeV/c) are only useful if we have information on the extrapolation properties of the various contributions which can only be supplied by the data.

RESULTS

The Regge pole contributions to the amplitudes $\nu A'^{+} A'^{-}$, B^{+}, νB^{-} as identified from the simultaneous analysis of the scattering data and C.M.S.R. are summarised below:

1) The C.M.S.R. and the scattering data are complementary in determining the Regge contributions to the amplitudes $\nu A'^{+}$, νB^{-}. Analysis of the sum rules alone or the scattering data indicate that these amplitudes are given by the P,P',ρ Regge poles where

$$\alpha_P = 1.0 + 0.25t$$
$$\alpha_{P'} = 0.57 + 0.9t$$
$$\alpha_\rho = 0.55 + 0.9t$$

2) The Pomeron and P' effectively decouple from the B^{+} amplitude in the Regge region and we show that the P,P',P'' fits to this amplitude from the low energy cut-off sum rules and the scattering data represent a non physical solution. The B^{+} amplitude, determined from a simultaneous analysis of the scattering data and C.M.S.R. evaluated at 5 GeV, is characterised by a single new vacuum trajectory:

$$\alpha_\eta = -0.46 + 0.8t$$

3) Two trajectories ρρ' are necessary to construct the A'^{-} C.M.S.R. and reproduce the charge exchange polarisation data:

a) The analysis at 5 GeV indicates that the ρ' contribution to this amplitude is large for $t \neq 0$ and that the ρ' is given by

$$\alpha_{\rho'} = 0.0 + 0.8t$$

b) The A'^- C.M.S.R. evaluated at 2 GeV indicate a ρ' trajectory given by

$$\alpha_{\rho'} = 0.3 + 0.8t$$

which is not suggested by the energy dependence of the charge exchange polarisation and indicates that contributions other than those identified from the high energy scattering data are important in this amplitude at low energies.

THE ANALYSIS

The analysis divides into two distinct parts. In the first part the isospin 1 exchanges are determined from the charge exchange scattering data and the C.M.S.R. for the amplitudes A'^-, νB^- (simply related by isospin invariance to the charge exchange amplitudes, equation 2.18). In the second part the isospin 1 exchanges are fixed from the preceding analysis and the isospin 0 exchanges determined from a further analysis of the elastic scattering data together with the $\nu A'^+$ and B^+ sum rules.

The Regge asymptotic forms for the pion-nucleon amplitudes are taken from equations 2.19

$$A'^+_{(\nu,t)} = \sum_{\substack{\text{all isospin} \\ 0 \text{ exchanges}}} -\gamma^+(\alpha(t),t)\, \xi^+(t)\, (\nu^2-\nu_o^2)^{\alpha/2}$$

$$B^+_{(\nu,t)} = \sum_{\substack{\text{all isospin} \\ 0 \text{ exchanges}}} -\beta^+(\alpha(t),t)\, \xi^+(t)\, \nu(\nu^2-\nu_o^2)^{\frac{\alpha-2}{2}}$$

5.1

$$A'^-_{(\nu,t)} = \sum_{\substack{\text{all isospin} \\ 1 \text{ exchanges}}} \gamma^-(\alpha(t),t)\, \xi^-(t)\, \nu(\nu^2-\nu_o^2)^{\frac{\alpha-1}{2}}$$

$$B^-_{(\nu,t)} = \sum_{\substack{\text{all isospin} \\ 1 \text{ exchanges}}} \beta^-(\alpha(t),t)\, \xi^-(t)\, (\nu^2-\nu_o^2)^{\frac{\alpha-1}{2}}$$

where $\alpha(t)$ denotes the trajectories, γ^-, β^-, γ^+ and β^+ are the residue factors and the signature factor $\xi^{\pm}(t)$ is given by:

$$\xi^{\pm}(t) = \frac{1 \pm e^{-i\pi\alpha}}{\sin\pi\alpha}$$

The C.M.S.R. derived for these amplitudes are given in equations 3.16 where the nucleon pole term contributions given in table IV are understood to be added to the left hand side integrals. The left hand sides of the sum rules were evaluated from the Donnachie phase shifts, the upper limit being $\nu_1 = 2.075 + t/4M$ and from the phase shift given in Chapter 4, extending the upper limit to $\nu_1 = 5.0 + t/4M$. The left hand sides are illustrated in Figs.1 and 8 for the two cut-offs at several moments and the continuous lines represent various fits, the details of which are discussed later.

In a simultaneous analysis of the scattering data and sum rules the assignment of errors to the sum rules is an important factor. In a process such as pion-nucleon elastic scattering where we have a wealth of scattering data, the significance of the sum rules is greatly reduced since their overall weighting in the analysis is small compared to the scattering data. Conversely in the charge exchange analysis the sum rules play a more important role because of the paucity of experimental data. We assumed a common percentage error of 20% for the $\nu A'^+$, A'^-, B^+, νB^- sum rules which gives about equal weight to the C.E.X. data and the sum rules in the charge exchange analysis and proportionally less in the analysis of the elastic scattering data.

The charge exchange data set comprised 129 points in the range $t = 0.0 \sim -1.8$ $(GeV/c)^2$ 95 differential cross-sections and 34 polarisation measurements taken from the references DATA2

$\frac{d\sigma}{dt}$ $(\pi^- p \to \pi^0 n)$ 5.9,6.0,9.8,10.0,13.3,18.2 GeV/c

P $(\pi^- p \to \pi^0 n)$ 5.0,5.9,11.2,8.0 GeV/c

The elastic scattering data comprised 508 points in the range $t = 0.0 \sim -2.0$ (GeV/c)^2 320 differential cross-sections, 51 total cross-sections and 137 polarisation measurements taken from reference DATA3.

$\frac{d\sigma}{dt}$ $(\pi^{\pm}p \to \pi^{\pm}p)$ 5.0, 6.8, 7.0, 8.5, 8.9, 10.0, 10.8, 12.4, 12.8, 13.0, 14.8, 15.0, 16.7, 17.0, 18.9 GeV/c

P $(\pi^{\pm}p \to \pi^{\pm}p)$ 6.0, 8.0, 10.0, 12.0, 14.0 GeV/c

ISOSPIN 1 EXCHANGES

We considered two ranges of the momentum transfer t given below to gauge the effects of the large momentum transfer sum rules which may be unreliable due to extrapolations of the partial wave series outside the physical region

$$\left.\begin{array}{l} t = 0.0 \sim -0.6 \text{ (GeV/c)}^2 \\ t = 0.0 \sim -1.0 \text{ (GeV/c)}^2 \end{array}\right\} \text{ in steps of } 0.1 \text{ (GeV/c)}^2$$

and we analysed the sum rules over three ranges of the continuous moment parameter ε

$$\left.\begin{array}{l} \varepsilon = 0.0 \sim -3.0 \\ \varepsilon = -1.0 \sim -4.0 \\ \varepsilon = -1.0 \sim -5.0 \end{array}\right\} \text{ in steps of } 0.5$$

The residues were parameterised by the following functions:

$$\gamma_{\rho}^{-}(\alpha(t),t) = C_o(1-C_2t)\, e^{C_1 t} \qquad \beta_{\rho}^{-}(\alpha(t),t) = D_o\, e^{D_1 t}\, \alpha_{\rho} \qquad 5.2$$

$$\gamma_{\rho}^{-\prime}(\alpha(t),t) = t\, C_o(1-C_2t)\, e^{C_1 t} \qquad \beta_{\rho}^{-\prime}(\alpha(t),t) = D_o\, t\, e^{D_1 t}$$

The factor t in the ρ' residue ensures that the contributions of the ρ and ρ' are of opposite sign for $t < 0$ and if the ρ' is a Regge pole then we can regard this as a nonsense mechanism or a conspiring pole. If the ρ' is an effective cut, we do not expect such factors to be present and if we give the ρ' an arbitrary negative sign w.r.t. to the ρ then there is little evidence in the high energy analysis of such a t-factor.

We fitted all the charge exchange data and the sum rules over the given ranges at the high and low cut offs and the results are summarised below.

a) The low cut off sum rules were compatible over both ranges of 't' but they were susceptible to the choice of the continuous moment parameter; the higher moments, $|\mathfrak{L}| > 3$ causing a dramatic change in the solution. The best fit to the sum rules and data indicated a ρ' with an intercept $\alpha_{\rho'}(0) = 0.3$ (Fig.1) but this was attributable to the fitting of the $A^{\prime}_{-}$ sum rule. We relaxed the errors on this sum rule, effectively weighting them out of the analysis and improved the fit to the data considerably, solution 1 table VI. The fits to the polarisation data and the sum rules are illustrated in figs.2 and 3 and the discrepancies in the $A^{\prime}_{-}$ sum rules are apparent.

It was evident from our analysis that to construct the solutions of similar analyses [80] at 2 GeV we had to assign large errors ~ 80% to the sum rules and their usefulness in constraining the analysis is then questionable.

b) The analysis of the C.M.S.R. at 5 GeV and the scattering data was very satisfactory. The sum rules and the data were fitted well over all the ranges of ϵ and t. The best fit solution is given in table VI solution 2 and the fits to the data are illustrated in figs.4,5,6.

There is some evidence from the parameters of the fit for a factor α_{ρ} in the $A^{\prime}_{\rho}$ amplitude equivalent to a nonsense mechanism for the [illegible]. The cross-

over zero then arises from a cancellation between the ρ and ρ' residues in the range $t = -0.1 \sim -0.2$ $(GeV/c)^2$.

d) An important feature of the ν A^- sum rules is the second zero in Im A^- at $t = -0.9 \sim -1.0$ $(GeV/c)^2$ (see fig.1a,b). Although the C.M.S.R. are somewhat unreliable at these large t values, the zero is apparent in the C.M.S.R. evaluated at both cut offs. In the ρ,ρ' parameterisation we have used, it is difficult to reconcile the positions of both zeros without introducing further $(1+\alpha_{\rho'})$ factors which we do not expect to be present if the ρ' is an effective cut parameterisation.

Discussion

The parameterisation of the charge exchange amplitudes in terms of the ρ,ρ' Regge poles gives a good description of the scattering data, especially the recent polarisation measurements at large t-values. If the ρ' is a bona-fide Regge pole, then a straight line extrapolation would place a $J^P = 1^-$ particle in the $1 \sim 1.5$ GeV mass region. No such meson has been observed and it is expedient to regard the ρ' as an effective cut contribution.

Regge absorptive cuts [32] are commonly added to the ρ Regge pole to generate the different phases of the spin flip and non spin flip amplitudes so as to obtain a non zero polarisation. However such a prescription is unable to account for the recent large 't' polarisation measurements and calculations of α_{eff} show no evidence of absorption in pion-nucleon charge exchange.

With reference to the summary of the 'general properties of cuts' Chapter 2, section C a ρ P' cut would have the same asymptotic phase, energy dependence and signature as the ρ' and further it would have the right sign contribut-

ion w.r.t. the ρ pole which is arbitrarily introduced by the factor t in the ρ' (the factor t also ensures that the ρ' contribution is small at t = 0 which is not compatible with a cut contribution but we were able to show that the ρ' contribution did not need to be small at t = 0 when we gave its residue function an arbitrary negative sign w.r.t. the ρ pole). However the low energy phase of an eikonal cut is very different from the asymptotic phase The excellent description of the spin flip amplitude B^- by a single ρ pole with a single α factor in the residue suggests that the ρ pole must have the nonsense wrong signature zeros. Hence the ρ P' cut calculated in a Regge absorptive-eikonal prescription will be necessarily small because of the large cancellations in the cut convolutions due to the sign change of the Regge amplitudes at the nonsense zeros.

This necessitates the introduction of unknown multiplicative factors to vary the strength of the cut, in particular to enhance the cut contribution to the A'^- amplitude to account for the large ρ' contribution. This is a very unsatisfactory situation and in the absence of any other prescription for calculating Regge cuts we are forced to conclude that the ρ', parameterised as a Regge pole is about the best description we have of the A'^- amplitude's contribution to the charge exchange polarisation.

ISOSPIN 0 EXCHANGES

Pion-nucleon elastic scattering involves both isospin 1 and 0 exchanges. The isospin 1 exchanges are fixed from the previous analysis of the charge exchange data and the isospin 0 exchanges are to be determined from the analysis.

This part of the work falls into two sections, a fit to the elastic scattering data alone and a simultaneous fit to the $\nu A'^+$, B^+ C.M.S.R. and the scattering data.

All our fits are highly constrained by the total cross-section measure-

ments which we fitted within the quoted experimental errors. The χ^2 contribution from these points is necessarily large and they have not been included in the quoted χ^2. However it will be observed from the fits to the total cross-sections that our fits give an excellent description of this data up to 20 GeV.

a) Fits to the data

We first analyse the data in terms of the P,P' model outlined in Chapter II. The best fits to the data indicated the following residue parameterisations

$$\gamma_P^+(\alpha(t),t) = C_o e^{C_1 t} \alpha_P \qquad \beta_{P'}^+(\alpha(t),t) = D_o e^{D_1 t} \alpha_{P'}^2 (1+\alpha_{P'})^2$$

$$\gamma_{P'}^+(\alpha(t),t) = C_o e^{C_1 t} \alpha_{P'}^2 (1+\alpha_{P'})^2 \qquad \beta_{P'}^+(\alpha(t),t) = D_o e^{D_1 t} \alpha_{P'}^2 (1+\alpha_{P'})^2 \qquad 5.3$$

The 'no compensation mechanism' was preferred to the 'Chew mechanism' for the P' residue in all our fits.

Two solutions A and B are constructed which differ is that solution A is constrained to have residues of the same sign in the spin flip and non spin flip amplitude and solution B has opposite signs.

The parameters and χ^2 for these fits are given in table VII and it is seen that solution B yields the best fit and that there is a large increase in χ^2 for solution A, the predominant part arising from a bad fit to the polarisation data. Unfortunately C.M.S.R., as will be demonstrated resolve the sign of the B^+ amplitude and do not allow solutionsof type B.

This necessitates the addition of a further trajectory designated by the P" to improve the fit to the polarisation data in solution A. The essential feature of such a trajectory, is that for $t < 0$, $\alpha < 0$ it contributes with opposite sign to that of a trajectory $\alpha > 0$ in the imaginary

part of the amplitude because of the signature factor $e^{-i\pi\alpha/2}$. Thus a P" allows us to construct solution B in effect without introducing opposite sign residues.

We fitted the data alone, including this additional vacuum trajectory and the P,P' residues are parameterised according to Equation 5.3 with the P" residue given by

$$\gamma^{+}_{P''}(\alpha(t),t) = C_o e^{C_1 t} \alpha_{P''} \qquad \beta^{+}_{P''}(\alpha(t),t) = D_o e^{D_1 t} \alpha_{P''} \qquad 5.4$$

An immediate result is that the contribution of this trajectory to the non-spin flip amplitude is negligible. This is not surprising since the Pomeron and P' contributions are large and well determined by the total cross-sections. Its contribution to the B^+ amplitude in comparison is large. A typical solution is given in table VIII. Solution C and all the fits indicate that β_P, $\beta_{P'}$ are small, compatible with zero and we used this constraint in a re-analysis

$$\gamma_{P''} = \beta_P = \beta_{P'} = 0$$

This parameterisation gave an excellent description of the data. The best χ^2 was 950 on 457 differential and polarisation cross-sections. If all single points for which $\chi^2 > 10$ are removed, which can be described as bad data points, the χ^2 is improved to 580 on 428 points. The parameters of the fit are given in Table VIII solution D but it must be observed that the scattering data is insensitive to the details of the $\alpha_{P''}$ trajectory and equally good fits are obtained for the following range of slope and intercept

$$-0.3 < \alpha_{p''}(0) < -0.5$$

$$0.7 < \alpha'_{p''} < 0.9$$

A Simultaneous Analysis of the elastic scattering data and the sum rules

The polarisation, which is constructed predominantly from the interference between the P.P' non-spin flip amplitudes and the ρ spin flip amplitudes together with the total cross-section data determine the non-spin flip contributions of the P,P' very well but from the preceding analysis the spin flip contributions are not well determined in detail. It would be hoped in a simultaneous analysis of the C.M.S.R. and the scattering data that the sum rules will resolve the contributions to the B^+ amplitude better.

We performed two analyses, one at each cut off for the sum rules, determined from the low energy phase shifts. The C.M.S.R. were fitted over two ranges of t

$$\left.\begin{array}{l} 0 < t < -0.5 \quad (\mathrm{GeV/c})^2 \\ 0 < t < -0.9 \quad (\mathrm{GeV/c})^2 \end{array}\right\} \text{ in steps of } 0.1 \quad (\mathrm{GeV/c})^2$$

and one range of ε

$$-1.0 < \varepsilon < -5.0 \qquad \text{in steps of } 0.5$$

The results of the analyses at the high and low energy cut offs differ especially in the contributions to the B^+ amplitude and for clarity we report the details of the fits separately.

a) C.M.S.R. evaluated at 2 GeV

Three trajectories P,P',P" are necessary to give an adequate description of the sum rules, evaluated at a 2 GeV cut off, and the high energy scattering data. The Regge residues are parameterised by the forms given in equations 5.3 and 5.4.

The best fit indicated a χ^2 of 980 on 417 differential and polarisat-

ion cross-section measurements {this is the reduced χ^2 in which points $\chi^2 > 10$ are not included}. The parameters of the fit are given in table IX solution E and the fits to the C.M.S.R. illustrated in fig.7.

The two poles P and P' give an excellent description of the $\nu A'^{+}$ sum rules as illustrated in Fig.7. Comparison of the data only solution C with the above solution E indicates the $\nu A'^{+}$ sum rules are in agreement to such an extent that an analysis of these sum rules alone would yield the same high energy contributions.

The C.M.S.R. for the amplitude B^{+} are not fitted very well even by three trajectories and any attempt to force the solution to fit the B^{+} C.M.S.R. destroys the fit to the polarisation data completely.

This suggests that the B^{+} C.M.S.R. evaluated at 2 GeV and the scattering data are incompatible and that the P,P',P" solution to this amplitude is spurious.

We considered the B^{+} C.M.S.R. independent of the scattering data to determine the leading contribution in a one pole model of this amplitude. From a simple consideration of the function $\mathrm{Sin}\pi/2\ (\alpha-\varepsilon-1)\ /\ \alpha-\varepsilon-1$ appearing in the r.h.s. of the B^{+} C.M.S.R. and the left hand side plots at several integer moments fig.8 a. it is apparent that the B^{+} C.M.S.R. are constructed from an effective single pole term with $\alpha > 0$ and positive residue.

A one pole fit to the B^{+} sum rule, illustrated by the continuous line in fig.8(a) gives a good description of the data over the whole t range with

$$\alpha_B = 0.5 + 0.9t$$

This solution is certainly incompatible with the scattering data {see solution A,B table VII} which indicated that the leading contribution to the B^{+} amplitude was characterised by a single trajectory $\alpha < 0$.

The P,P',P" solution is a 'compromise solution' between the requirements

of the scattering data and the requirements of the C.M.S.R. The large contributions of the P,P' trajectories ($\alpha>0$) required to construct the sum rules must be cancelled by equally large contributions from a trajectory $\alpha < 0$ to preserve the fit to the polarisation data.

The P,P',P" solution involving such large cancellations between several Regge terms must be regarded with suspicion and we suggest that it represents a non-physical solution to the B^+ amplitude in the high energy scattering region.

C.M.S.R. evaluated at 5 GeV and scattering data

The left hand sides of the B^+ C.M.S.R. evaluated at 5 GeV are given by the opposite sign, for the odd integer moments, to those at 2 GeV (Fig.8(a), (b)). This qualitative change in behaviour indicates that the sum rules are given an effective single pole model by a trajectory $\alpha < 0$. Such a contribution is compatible with the high energy scattering data and the parameters of this trajectory are determined from a fit to the C.M.S.R. and the scattering data.

The Regge residues were parameterised according to equations 5.3, 5.4 subject to the constraint:

$$\beta_P = \beta_{P'} = \gamma_{P''} = 0$$

This solution, which is very economic in parameters, gives an excellent description of both the C.M.S.R. {fig.12} and the scattering data {figs.9, 10,11}. The best fits gave a χ^2 of 630 on 430 scattering data points and the parameters of the fit are given in table IX solution F.

The A^+ C.M.S.R. are satisfied well within very small errors, they do not constrain the solution and could have been predicted from the scattering data solution alone.

The B^+ C.M.S.R. are fitted well over the whole t range 0.0 ~ -1.0 $(GeV/c)^2$ and for moments $|\varepsilon| > 1.5$. (The low moments are not fitted as well because they emphasise the low energy part of the sum rules which we have already shown gives misleading results).

The scattering data and B^+ C.M.S.R. evaluated at the 5 GeV cut off indicate a single new vacuum trajectory

$$\alpha_\eta = -0.46 + 0.8t$$

is sufficient to construct this amplitude. Because of the quantum numbers in the t channel of elastic scattering this trajectory must have $I^G = 0^+$ $J^P = J^+(J=0,2\ldots)$, C = + . The first particle recurrence, assuming a straight line extrapolation, should be a spin zero particle, in the mass range 700 ~ 800 MeV. A likely candidate is the spin one resonance η_{0+} (700) ~ width 400 MeV.

It is interesting to note that Ordorico et al. [81] predicted the existence of such a trajectory with $\alpha(0)$ ~ -0.5 ~ -1.0 but were unable to resolve the intercept and slope accurately. Further evidence for such a trajectory is provided by Olsson [82] who made a three pole fit to the π-N forward scattering amplitude. Calculating the real part by means of dispersion relations, he got in addition to the contributions of P and P' a third pole $\alpha(0) = -0.5$. Chavda [83] obtained a similar result with a sum rule whose weight function was constructed in order to gain a good Pomeron intercept.

TABLE VI

		C_o	C_1	C_2	D_o	D_1	$\alpha(0)$	α'
SOLUTION 1	ρ	6.5	1.9	0.6	136.0	1.6	0.55	0.9
	ρ'	87.0	4.7	0.6	257.0	4.9	0.0	0.9
SOLUTION 2	ρ	6.8	1.4	1.9	124.0	1.5	0.55	0.9
	ρ'	46.0	3.7	0.0	132.0	5.2	0.0	0.9

TABLE VII

		C_o	C_1	D_o	D_1	$\alpha(0)$	α'
SOLUTION A	P	50.0	2.3	5.0	4.0	1.0	0.2
	P'	50.0	0.4	12.6	0.2	0.57	1.00
SOLUTION B	P	50.0	2.3	- 7.5	0.8	1.0	0.25
	P'	50.0	0.7	-21.5	0.0	0 57	0.80

TABLE VIII

		C_o	C_1	D_o	D_1	$\alpha(0)$	α'
	P	50.0	2.5	1.9	4.0	1.01	0.25
SOLUTION C	P'	50.0	0.1	0.1	0.2	0.57	0.90
	P"			45.0	0.1	-0.38	0.80
	P	50.0	2.4			1.0	0.26
SOLUTION D	P'	52.0	0.1			0.57	0.90
	P"			40.0	0.0	-0.40	0.80

TABLE IX

		C_o	C_1	D_o	D_1	$\alpha(0)$	α'
	P	50.0	3.8	12.0	1.7	1.0	0.2
SOLUTION E	P'	51.0	0.0	24.0	0.1	0.57	0.9
	P"			32.0	2.1	0.0	0.8
	P	50.0	2.5			1.00	0.26
SOLUTION F	P'	50.0	0.2			0.57	0.90
	P"			40.0	0.0	-0.46	0.80

FIGURE CAPTIONS - CHAPTER 5

FIG.1(a) Continuous sum rules (C.M.S.R.) for the A'^{-}, νB^{-} amplitudes. The solid dots represent the C.M.S.R. low energy integrals constructed from the phases (ref. [71]). The solid curves illustrate the best fit with the ρ,ρ' Regge poles to the C.M.S.R. only.

FIG.1(b) Continuous moment sum rules (C.M.S.R.) for the A'^{-}, νB^{-} amplitudes. The solid dots represent the C.M.S.R. high cut off integrals constructed from the phases of ref. [70]. The solid curves illustrate the best fit with the ρ,ρ' Regge poles to the C.M.S.R. only.

FIG.2 ρ,ρ' fits to the charge exchange polarisation data from a simultaneous analysis of the scattering data and C.M.S.R. evaluated at 2 GeV.

FIG.3 C.M.S.R. (evaluated at 2 GeV) for amplitudes A'^{-}, νB^{-} and ρ,ρ' Regge fits from a simultaneous analysis of the scattering data and C.M.S.R. [cf ref.Fig.1(a)].

FIG.4 ρ,ρ' fit to the charge exchange differential cross-section data from the simultaneous analyses of the scattering data and C.M.S.R. evaluated at 5 GeV.

FIG.5 ρ,ρ' fit to the charge exchange polarisation data from a simultaneous analysis of the scattering data and C.M.S.R. evaluated at 5 GeV.

FIG.6 C.M.S.R. (evaluated at 5 GeV) for amplitudes A^{-}, νB^{-} and ρ,ρ' Regge fit from simultaneous analysis above [cf ref.Fig.1(b)].

FIG.7 C.M.S.R. (evaluated at 2 GeV) for the amplitudes $\nu A'^{+}$, B^{+} and the P,P',P'' Regge fits [cf ref.Fig.1(a)].

FIG.8(a) (b) Comparison of C.M.S.R. for the amplitude B^{+} evaluated at 2 GeV and 5 GeV.

FIG.9 P,P',P'' fit to $(\pi^{\pm}p)$ total cross-sections from simultaneous analysis of scattering data and the C.M.S.R. evaluated at 5 GeV.

FIG.10 P,P',P" fit to the ($\pi^{\pm}$p) elastic differential cross-sections for the simultaneous analysis of the scattering data and C.M.S.R. evaluated at 5 GeV.

FIG.11 P,P',P" fit to the ($\pi^{\pm}$p) polarisation measurements from the simultaneous analysis of the scattering data and C.M.S.R. evaluated at 5 GeV.

FIG.12 P,P',P" fit to the C.M.S.R. for the amplitude ν A'^{+}, B^{+} evaluated at a 5 GeV cut off [cf. ref.Fig.1(b)].

$\int_{\nu_0} d\nu\ \mathrm{Im}\left\{(\nu_0^2-\nu^2)^{-E-1/2}\, A^-(\nu,t)\right\}$ $\int_{\nu_0} d\nu\ \mathrm{Im}\left\{(\nu_0^2-\nu^2)^{-E-1/2}\, B^-(\nu,t)\right\}$

$\nu_1 = 2{\cdot}075 + t/4M$

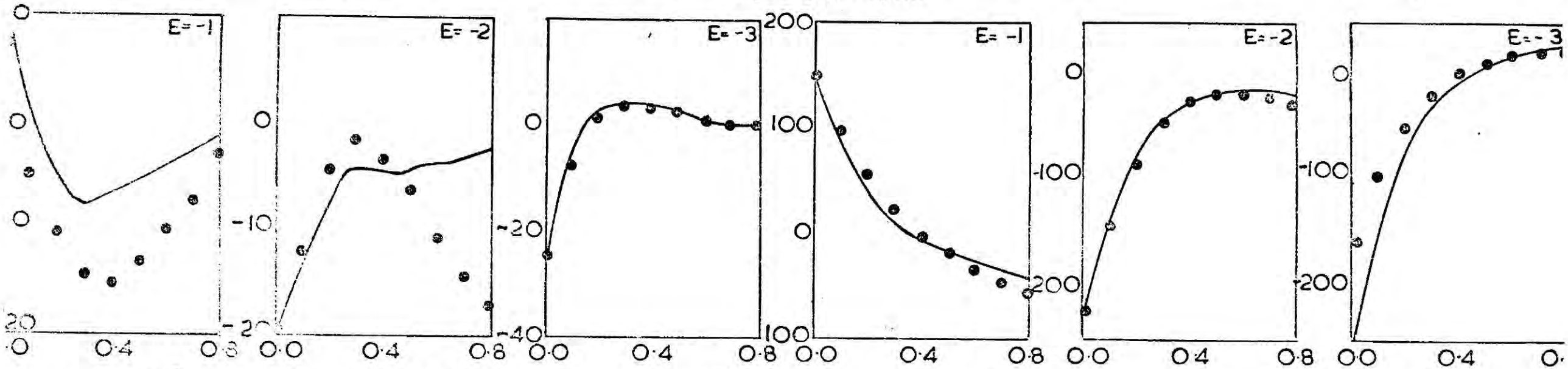

$\nu_1 = 5{\cdot}0 + t/4M$

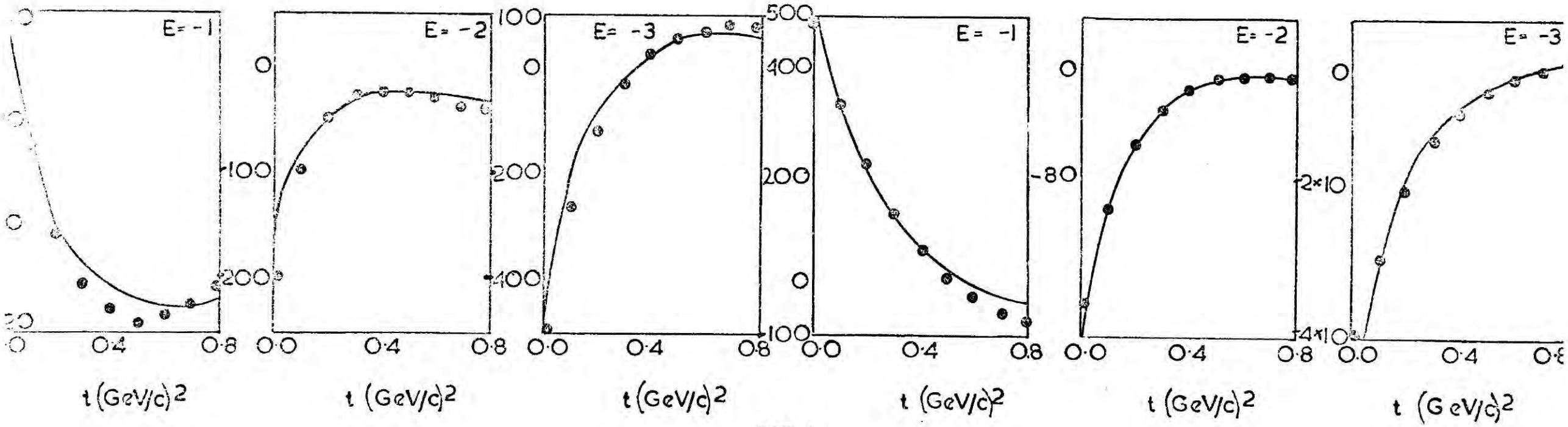

FIG. 1.

CHARGE EXCHANGE POLARISATION

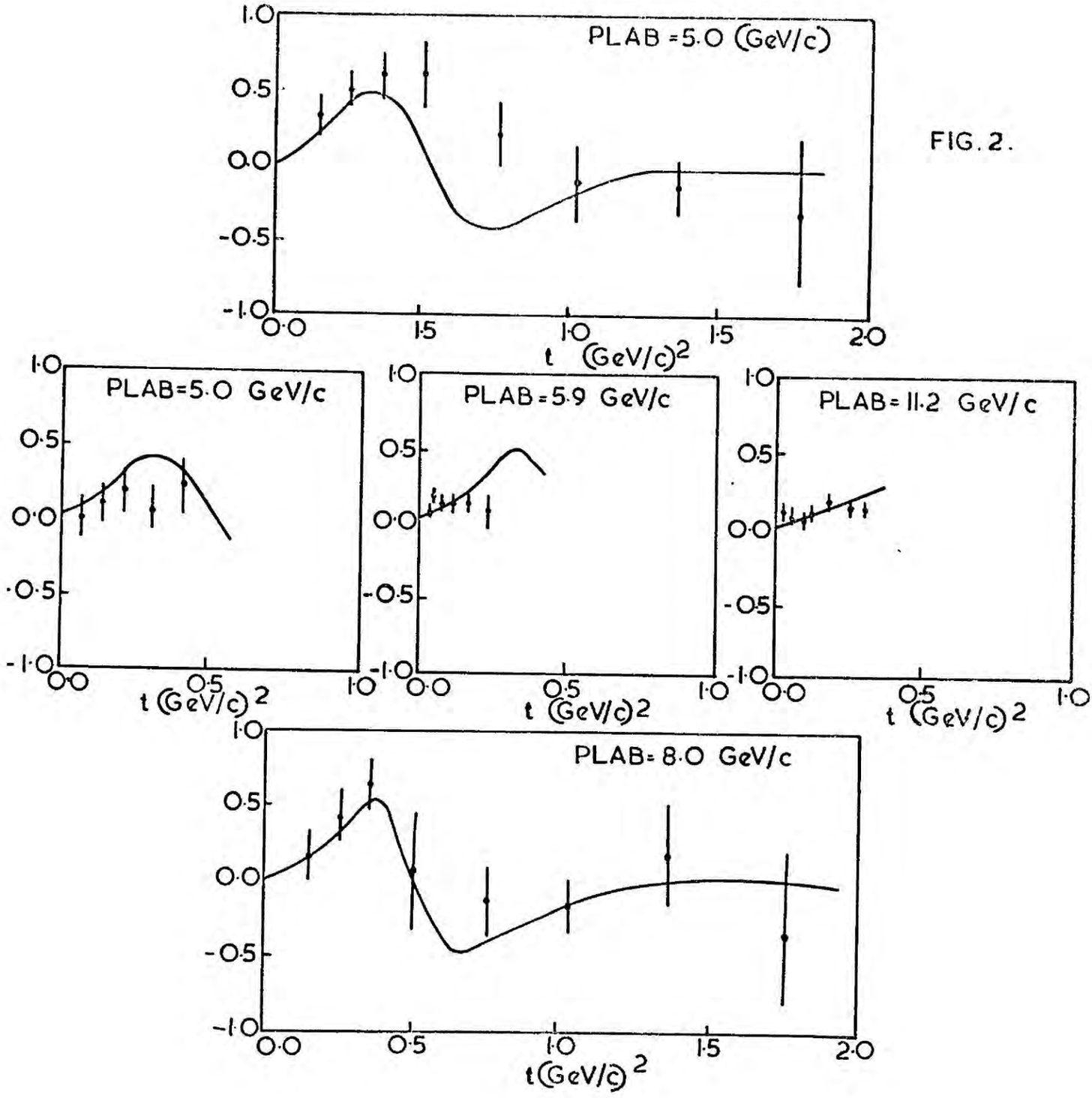

FIG. 2.

$$\int_{\nu_0}^{\nu_1} d\nu \; \mathrm{Im}\left\{(\nu_0^2-\nu^2)^{-(E+1)/2}\, A^{1-}(\nu,t)\right\} \qquad \nu_1 = 2.075 + t/4M \qquad \int_{\nu_0}^{\nu_2} d\nu \; \mathrm{Im}\left\{(\nu_0^2-\nu^2)^{-(E+1)/2}\, \nu\, B^{-}(\nu,t)\right\}$$

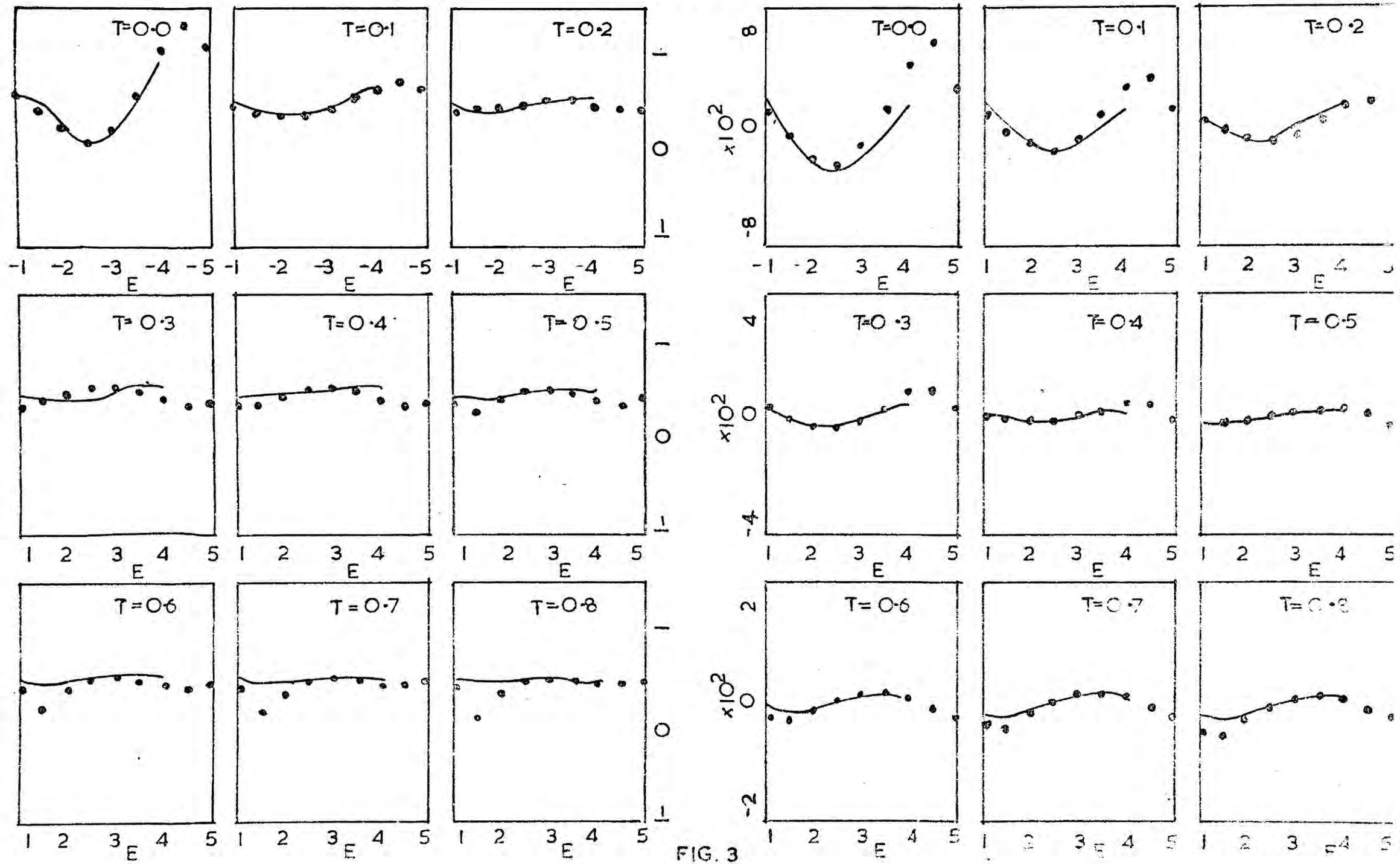

FIG. 3

FIG. 4.

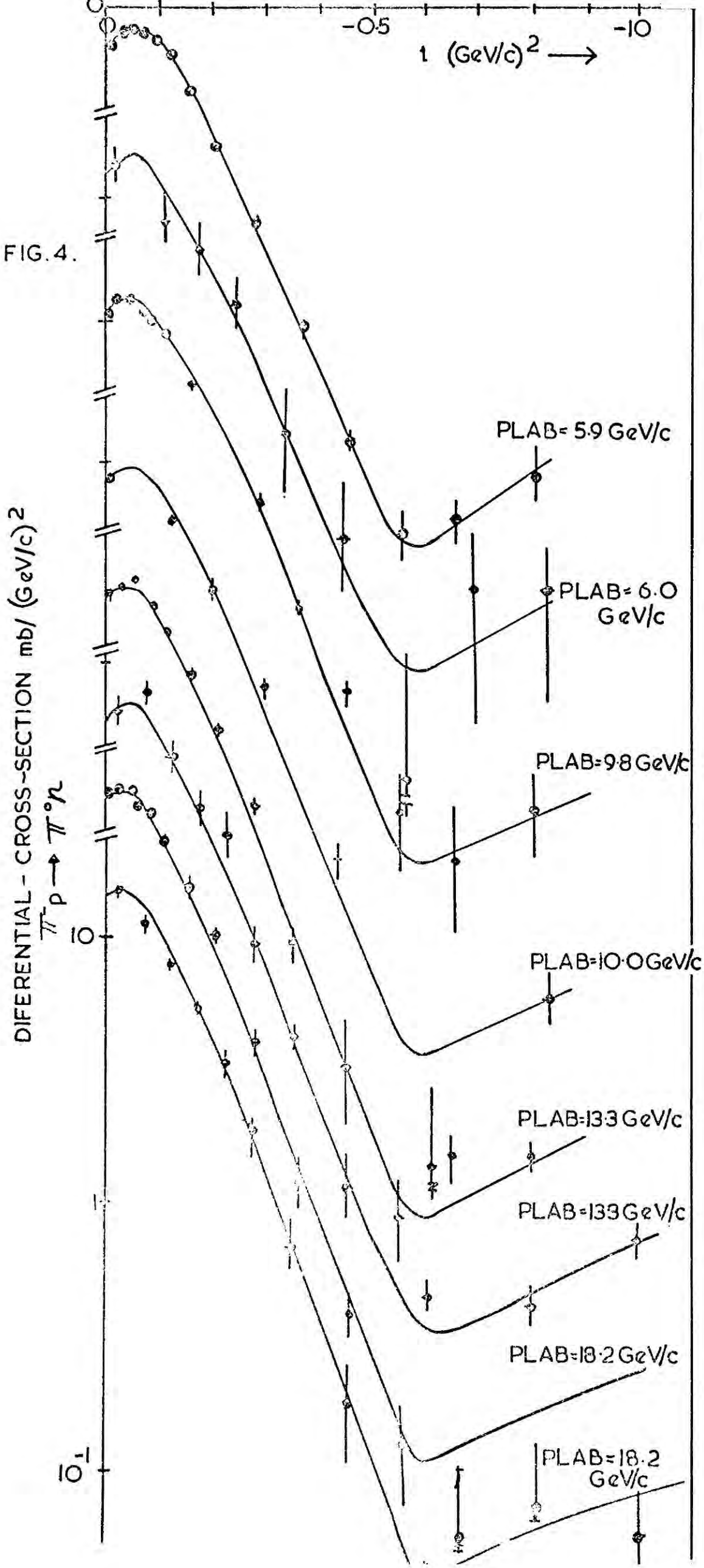
0
-0.5
-1.0
t (GeV/c)^2 ⟶
DIFERENTIAL - CROSS-SECTION mb/ (GeV/c)^2
$\pi^- p \rightarrow \pi^0 n$
10
1
10^{-1}
PLAB= 5.9 GeV/c
PLAB= 6.0 GeV/c
PLAB= 9.8 GeV/c
PLAB=10.0 GeV/c
PLAB=13.3 GeV/c
PLAB=13.3 GeV/c
PLAB=18.2 GeV/c
PLAB=18.2 GeV/c

CHARGE EXCHANGE POLARISATION MEASUREMENTS

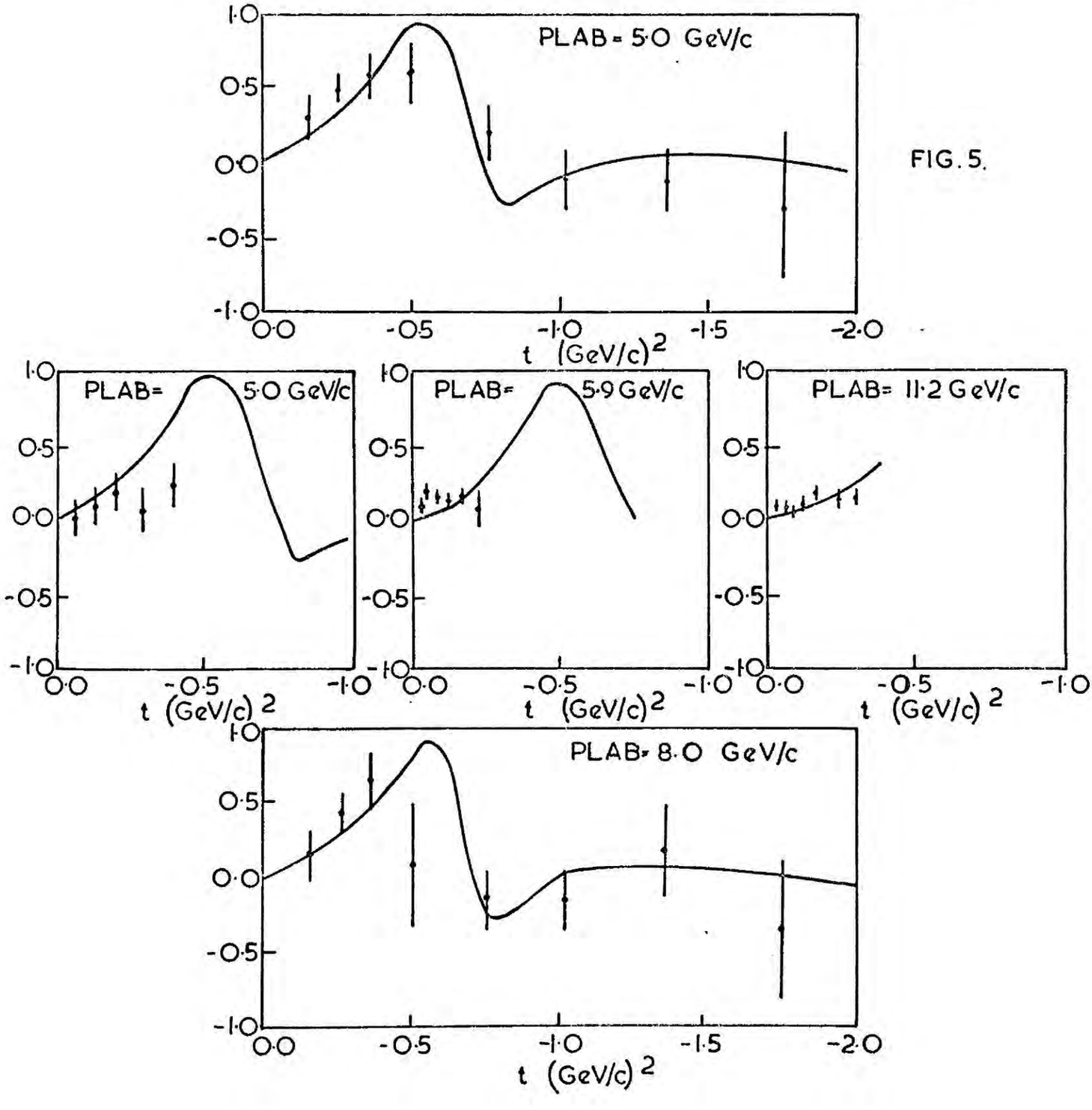

FIG. 5.

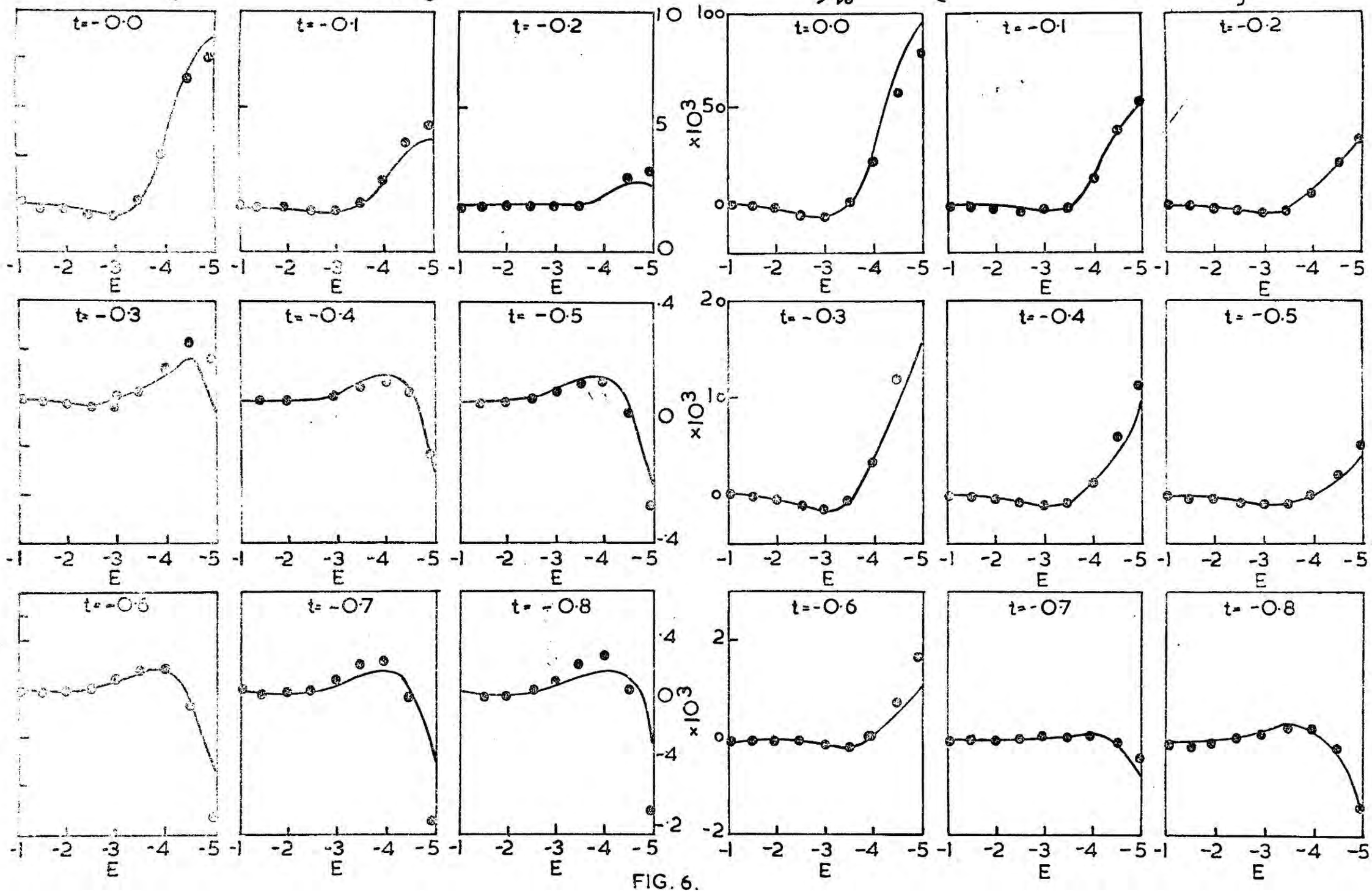
$\int_{\nu_0}^{d\nu} Im\{(\nu_0^2-\nu^2)^{-(\ell+1)/2} A^-(\nu,t)\}$
$V_1 = 5.0 + 1/4M$
$\int_{\nu_0}^{d\nu} Im\{(\nu_0^2-\nu^2)^{-(\ell+1)/2} \nu B^-(\nu,t)\}$
t = -0.0
t = -0.1
t = -0.2
t = -0.3
t = -0.4
t = -0.5
t = -0.6
t = -0.7
t = -0.8
E
$\times 10^3$

FIG. 6.

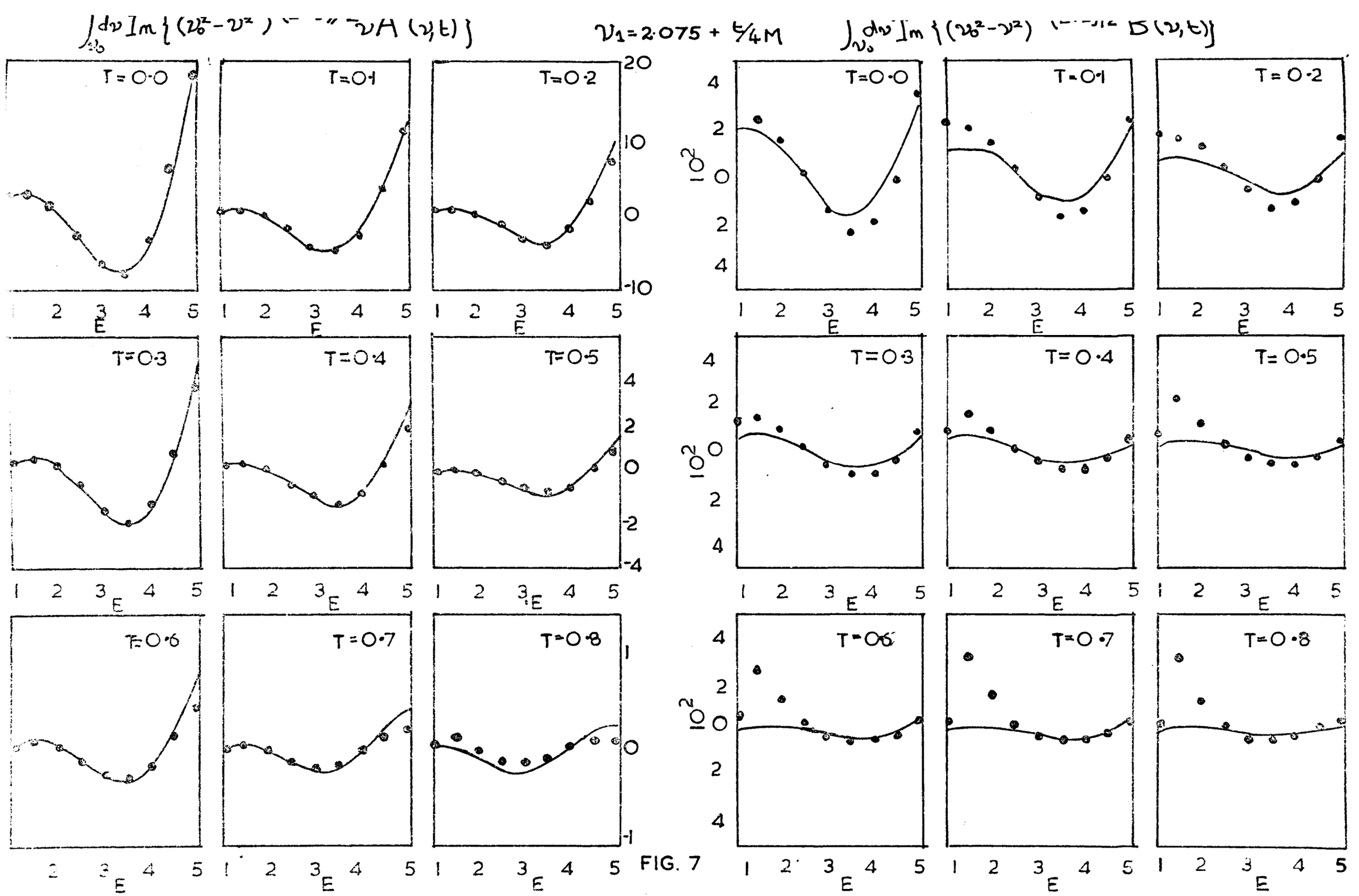
$\int_{\nu_0} d\nu\, \mathrm{Im}\{(\nu_0^2-\nu^2)^{-1-\alpha_0} \nu A(\nu,t)\}$
$\nu_1 = 2.075 + t/4M$
$\int_{\nu_0} d\nu\, \mathrm{Im}\{(\nu_0^2-\nu^2)^{-1-\alpha_0} B(\nu,t)\}$
T=0·0
T=0·1
T=0·2
T=0·3
T=0·4
T=0·5
T=0·6
T=0·7
T=0·8
E
10^2

FIG. 7

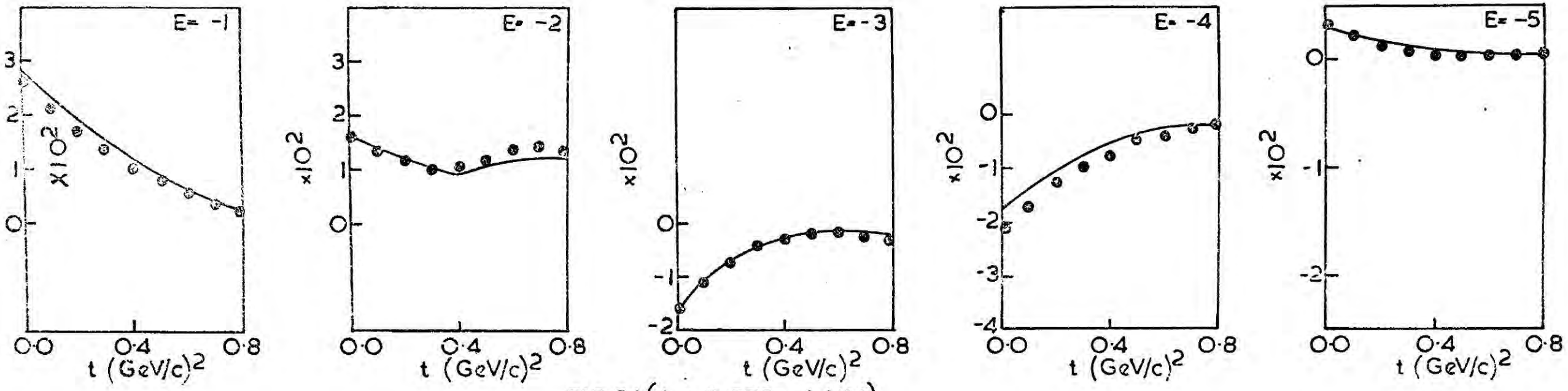

FIG. 8A ($\gamma_1 = 2{\cdot}075 + t/4M$)

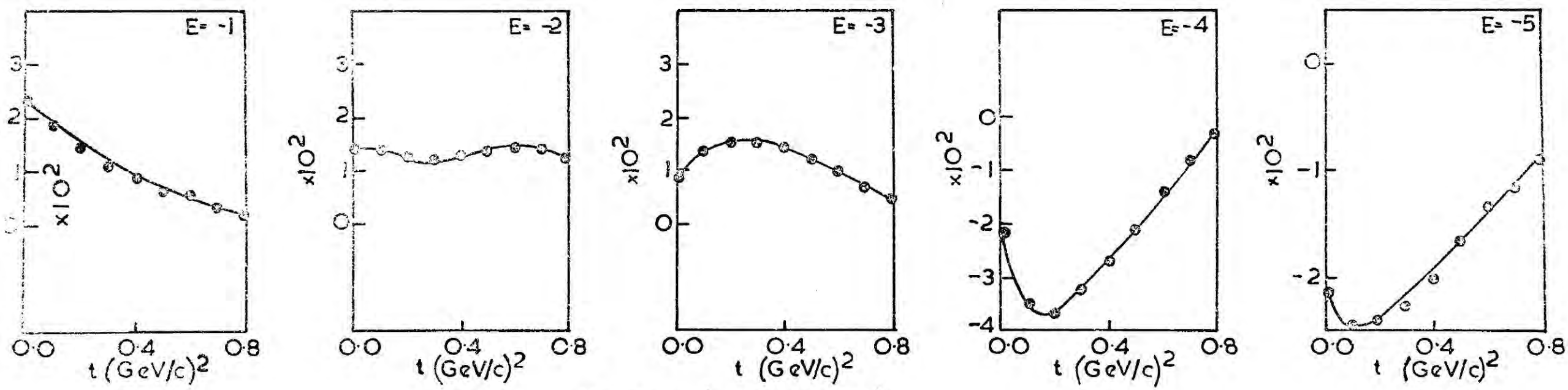

FIG. 8B ($\gamma_1 = 5{\cdot}0 + t/4M$)

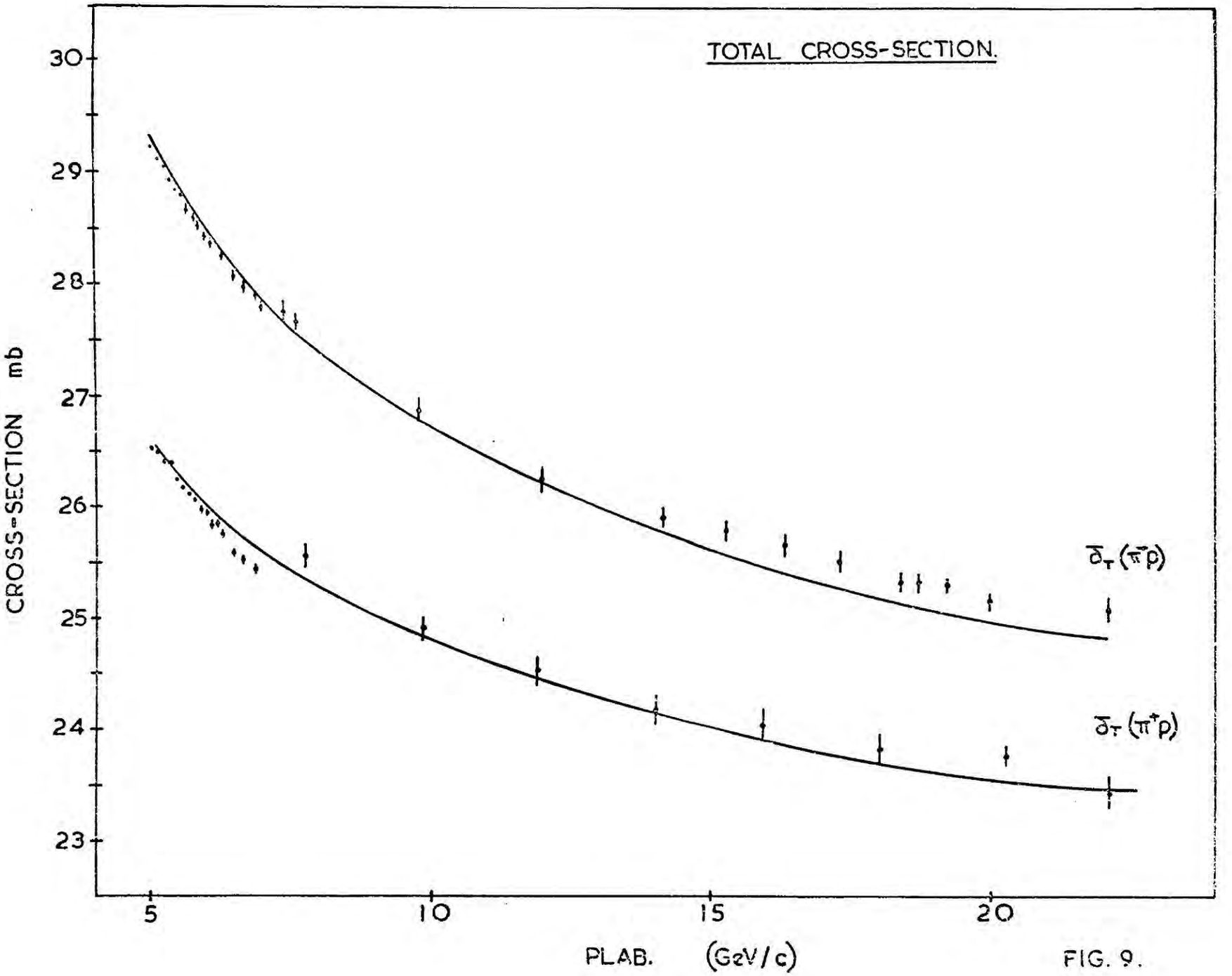
TOTAL CROSS-SECTION.
CROSS-SECTION mb
30
29
28
27
26
25
24
23
5
10
15
20
PLAB. (GeV/c)
$\bar{\sigma}_T(\pi^- p)$
$\bar{\sigma}_T(\pi^+ p)$

FIG. 9.

FIG. 10.

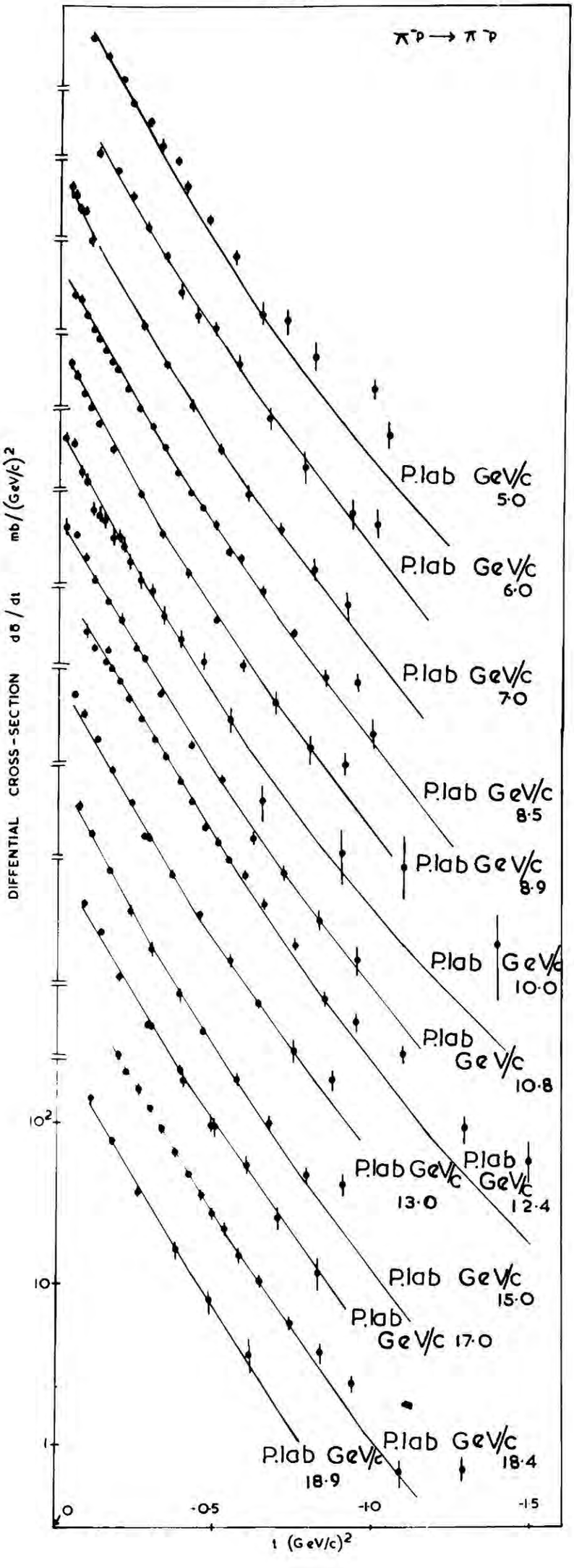
$\pi^- p \rightarrow \pi^- p$
DIFFENTIAL CROSS-SECTION $d\sigma/dt$ mb/(GeV/c)^2
P.lab GeV/c 5·0
P.lab GeV/c 6·0
P.lab GeV/c 7·0
P.lab GeV/c 8·5
P.lab GeV/c 8·9
P.lab GeV/c 10·0
P.lab GeV/c 10·8
P.lab GeV/c 12·4
P.lab GeV/c 13·0
P.lab GeV/c 15·0
P.lab GeV/c 17·0
P.lab GeV/c 18·4
P.lab GeV/c 18·9
10^2
10
1
0
-0·5
-1·0
-1·5
t (GeV/c)^2

FIG. 10.

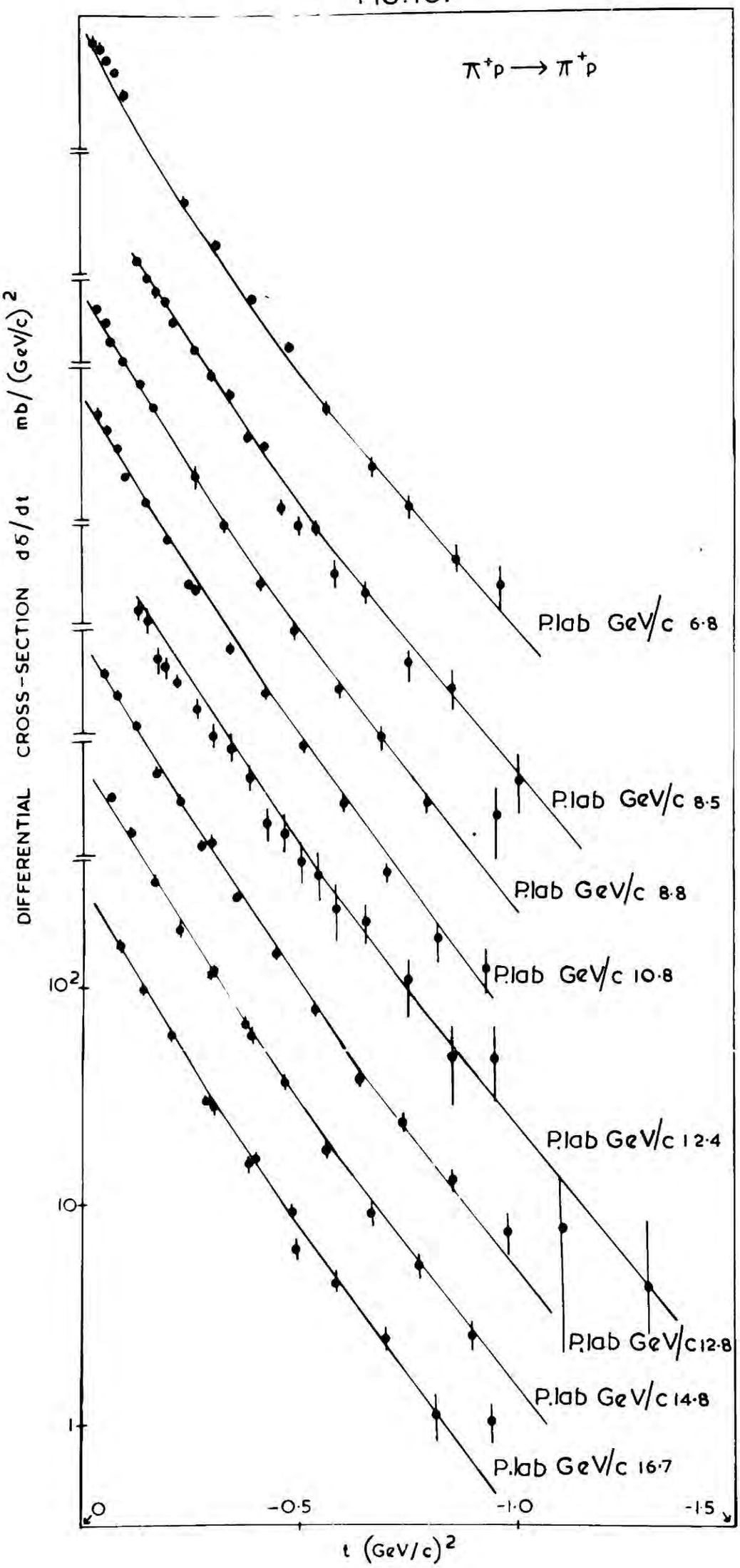
$\pi^+ p \longrightarrow \pi^+ p$
DIFFERENTIAL CROSS-SECTION $d\sigma/dt$ mb/(GeV/c)^2
P.lab GeV/c 6·8
P.lab GeV/c 8·5
P.lab GeV/c 8·8
P.lab GeV/c 10·8
P.lab GeV/c 12·4
P.lab GeV/c 12·8
P.lab GeV/c 14·8
P.lab GeV/c 16·7
10^2
10
1
0
-0·5
-1·0
-1·5
t (GeV/c)^2

FIG. 11.

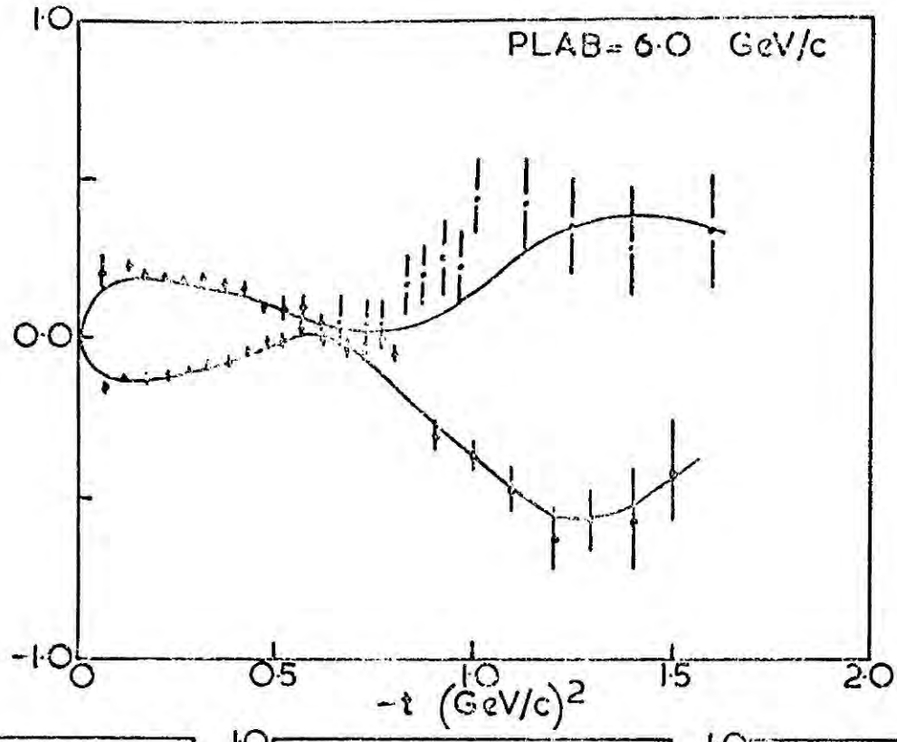
PLAB= 6·0 GeV/c
1·0
0·0
-1·0
0
0·5
1·0
1·5
2·0
-t (GeV/c)²

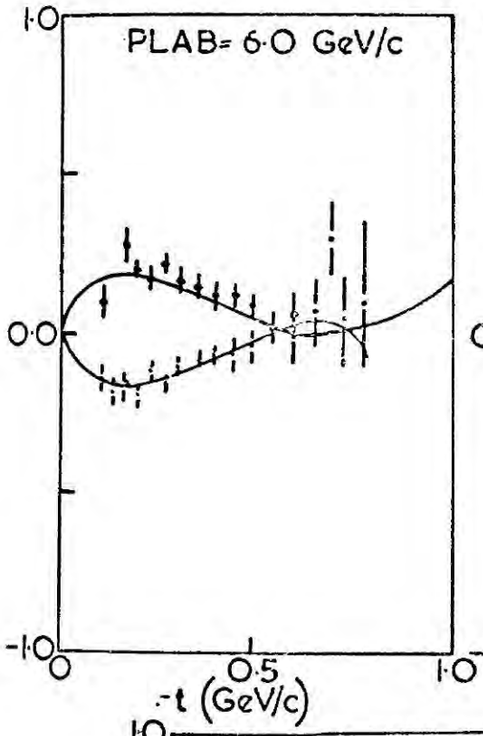
PLAB= 6·0 GeV/c
1·0
0·0
-1·0
0
0·5
1·0
-t (GeV/c)

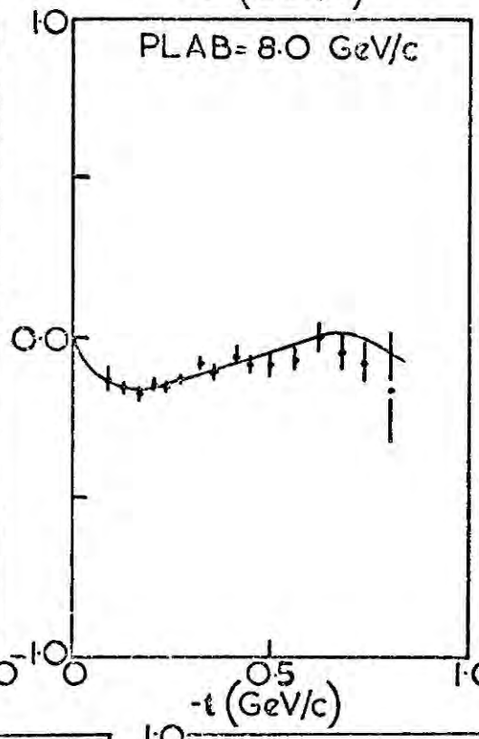
PLAB= 8·0 GeV/c
1·0
0·0
-1·0
0
0·5
1·0
-t (GeV/c)

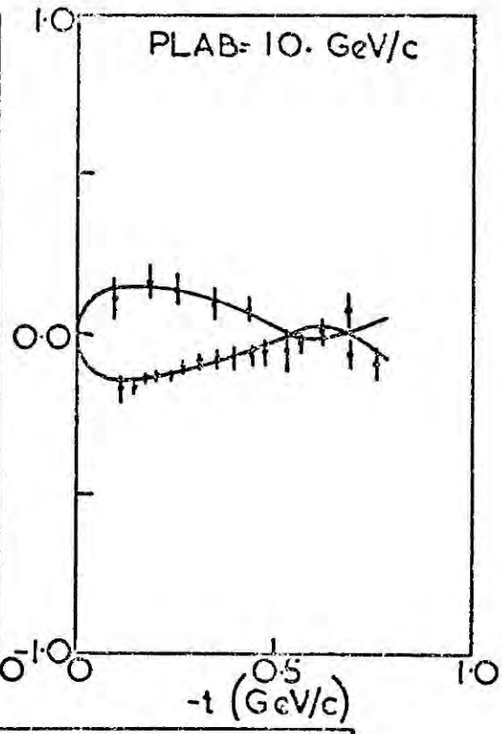
PLAB= 10. GeV/c
1·0
0·0
-1·0
0
0·5
1·0
-t (GeV/c)

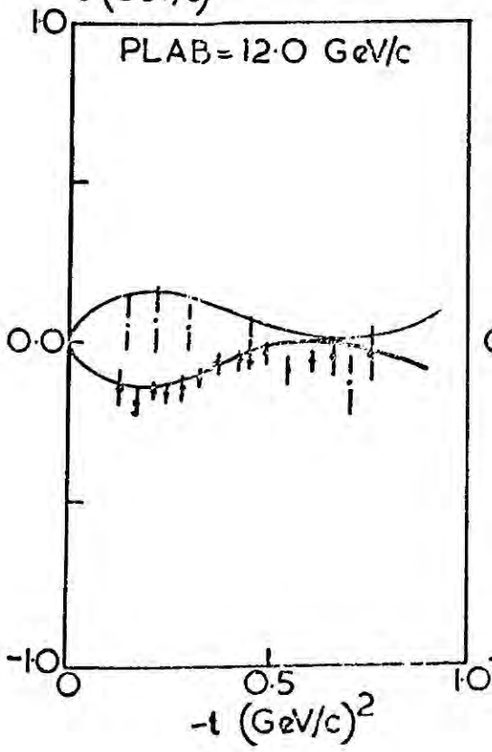
PLAB= 12·0 GeV/c
1·0
0·0
-1·0
0
0·5
1·0
-t (GeV/c)²

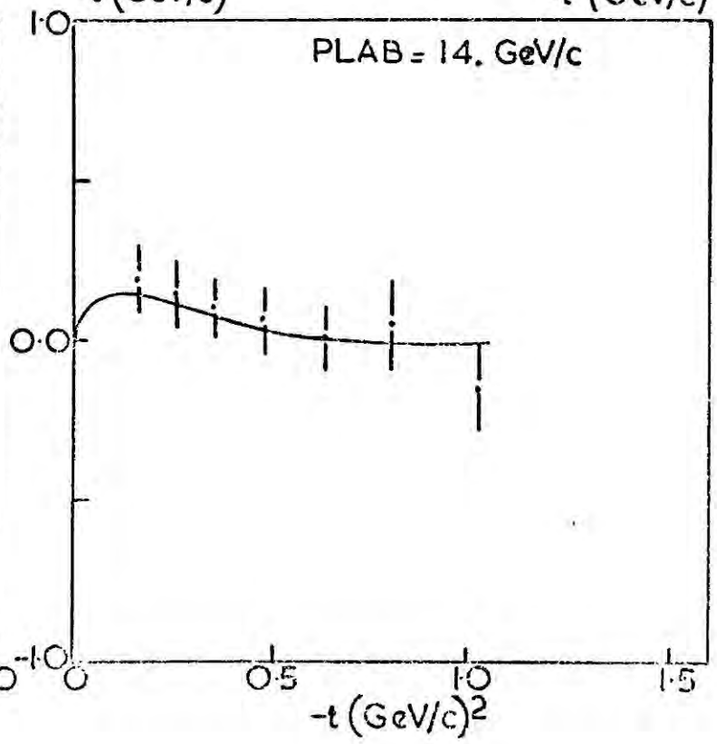
PLAB = 14. GeV/c
1·0
0·0
-1·0
0
0·5
1·0
1·5
-t (GeV/c)²

$\int_{\nu_0}^{\infty} d\nu\ \mathrm{Im}\left\{(\nu_0^2-\nu^2)^{-(E+1)/2}\ \nu A^{1+}(\nu,t)\right\}$ $\nu_1 = 5.0 + t/4M$ $\int_{\nu_0}^{\infty} d\nu\ \mathrm{Im}\left\{(\nu_0^2-\nu^2)^{-(E+1)/2}\ B^{+}(\nu,t)\right\}$

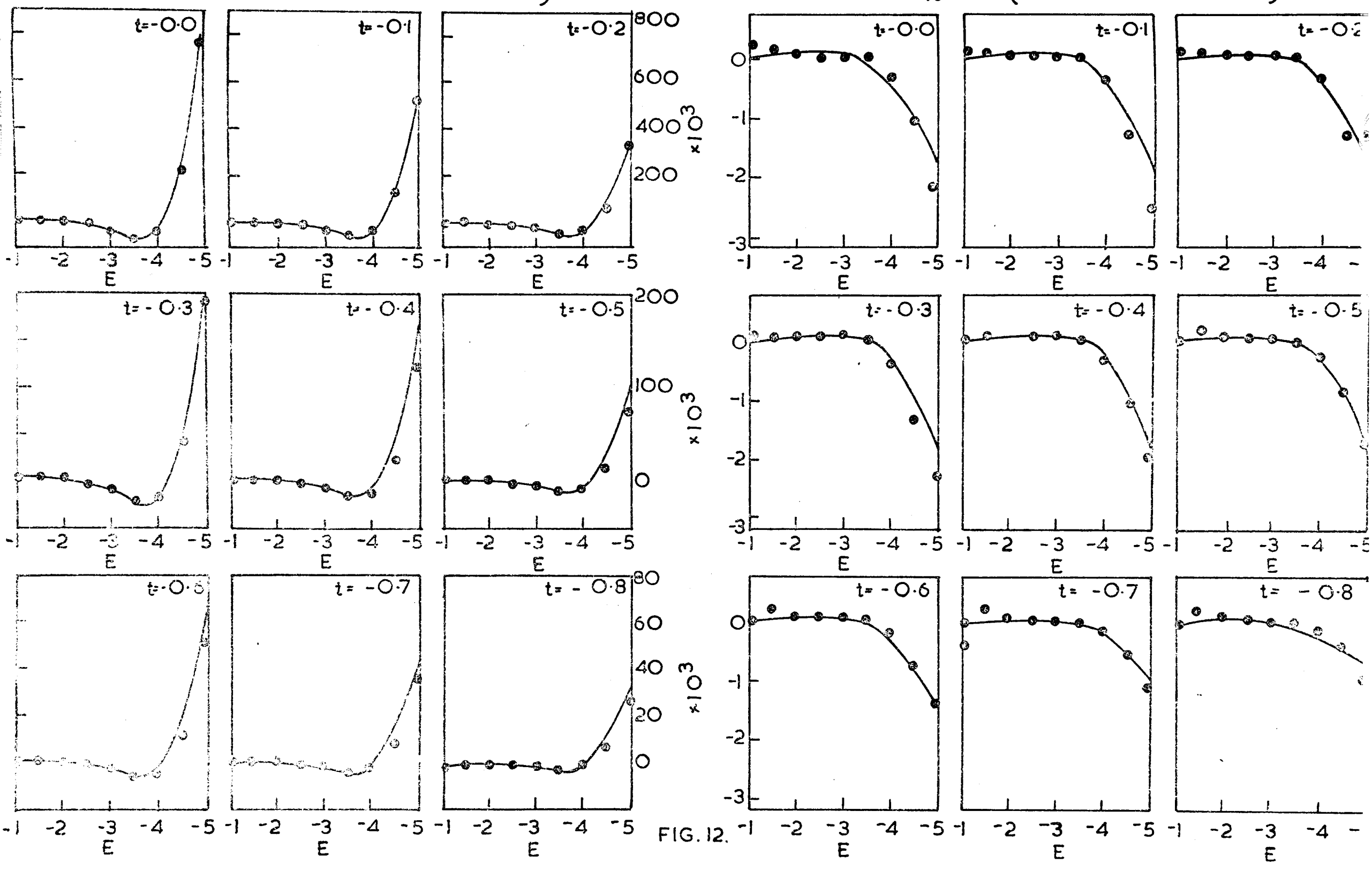

FIG. 12.

CHAPTER VI

ABSTRACT

There have been several attempts to explain the features of the Serpukhov pion-nucleon total cross-section data within the framework of the Regge model by the addition of further pole contributions or multi-Pomeron cuts[84] to the conventional P,P' and ρ Regge poles and by the inclusion of other Regge singularities such as Regge dipoles[85], which represent the simplest violation of conventional asymptotics at t = 0.

All these models give a reasonable description of the data which is not surprising because of the increased freedom in the fit from the addition of further parameters.

In this work we use the additional information of the F.E.S.R. to improve our knowledge of the scattering amplitude at high energies and the sum rules are applied as a series of constraints on the parameters of the Regge models.

We make the following observations from the analysis:

1) The F.E.S.R. suggest small multi-Pomeron cut contributions insufficient to give the levelling of σ_T^+ at Serpukhov energies.

2) Dipole contributions appear consistent with the F.E.S.R. and are large enough to give the levelling of σ_T^+.

3) σ_T^- is not inconsistent with dipole contributions in the negative signature amplitude but there is insufficient evidence to make a conclusive statement on the possible violation of the Pomeranchuk theorem.

We comment briefly on similar results by Violini and Schiff[86,87] and the significance of logarithmically increasing total cross section.

Conventional Regge pole models in terms of the P,P' and ρ poles give an adequate description of the pion-nucleon total cross-section data up to 20 GeV/c but extrapolations of these contributions to the momentum range 20-70 GeV/c do not account for the Serpukhov total cross-section data.

The Serpukhov data revealed unexpected features that may lead to revised ideas about asymptotic behaviour.

a) Total cross-sections $[\sigma_T(\pi^{\pm}p)]$ appear to be constant or rising slightly in the momentum range 25-70 GeV/c.

b) $\sigma_T(\pi^{\pm}p)$ appear compatible with asymptotic equality but they do not exclude the possibility of Pomeranchuk theorem violation

$$\text{i.e.} \quad \sigma_T(\pi^-p) - \sigma_T(\pi^+p) \neq 0$$

$$\text{energy} \to \infty$$

We separate the analysis into the discussion of the contributionsto the sum and difference of the $\pi^{\pm}p$ total cross-sections denoted by σ_T^+, σ_T^- respectively. These cross-sections are simply related to the even and odd signatured amplitudes $A'^{\pm}(\nu,0)$ by the optical theorem

$$\sigma_T^{\pm} = \tfrac{1}{2}\{\delta_T(\pi^-p) \pm \delta_T(\pi^+p)\}$$

$$A'^{\pm}(\nu,0) = (\nu^2-\mu^2)^{1/2}\,\sigma_T^{\pm} \qquad 6.1$$

where μ is the pion mass and ν is the pion total lab. energy.

The amplitudes $A^{\pm}(\nu,0)$ are parameterised in terms of the P,P',ρ Regge poles and other contributing terms which are Regge cuts and dipoles. These additional terms appear in both the even and odd signatured amplitudes and their net effect used to account for the 'new' features of the Serpukhov data. We summarise the significance of each term in their respective amplitudes below.

EVEN SIGNATURE EXCHANGES

Phenomenologically we wish to introduce a term within the framework of Regge theory to account for the apparent change in the behaviour of σ_T^+ at Serpukhov energies which from a) appears to be constant or rising slightly.

1) For constant asymptotic total cross-sections the leading term must be Pomeron like i.e.

$$A'^+(\nu,0) \sim i\,\gamma_p\,\nu/\nu' \qquad 6.2$$

2) Secondary trajectories, the P' yields a contribution

$$A'^+(\nu,0) \sim -\gamma_s\, e^{-i\pi\alpha/2} \left(\nu/\nu'\right)^{\alpha} \qquad 6.3$$

where γ_p, γ_s are the Pomeron and P' residues respectively. The P' contributions give the rapid fall in the total cross-sections at low energies and since $\alpha < 1$ in the absence of other effects

$$\sigma_T^+ \underset{\nu\to\infty}{\to} \gamma_p$$

3) The addition of multi-Pomeron cuts to the conventional Regge poles can give rise to the observed qualitative charge in behaviour of σ_T^+. The cut contribution is parameterised according to

$$A'^+(\nu,0) = i\,\gamma_c\,\frac{\nu}{\nu'}\left[\ln \nu/\nu' - i\pi/2\right]^{-1-\lambda} \qquad 6.4$$

λ small $\sim$ 0.0 - 0.1

Asymptotically σ_T^+ still tends to γ_p but since the cut contribution is only decreasing logarithmically then it will dominate over secondary poles for large ν. Hence if γ_c is negative we may expect σ_T^+ to fall initially, then to level out and finally rise to its asymptotic limit. In effect the

multi-Pomeron cuts displace the region of constant total cross-section to higher energies.

c) Another possibility is to allow logarithmically increasing total cross-sections, then the leading term will have

$$\begin{aligned} &\mathrm{Im}\, A'^{+} \sim \gamma\, \nu \ln \nu \\ &\sigma_T^{+} \to \infty \\ &\nu\to\infty \end{aligned} \qquad 6.5$$

The simplest Regge term which expresses this unconventional asymptotic behaviour is an even signature Regge dipole at t = 0 [Equation 2.59].

$$A'^{+} = i\, \gamma_0\, \nu/\nu' \left[\ln \nu/\nu' - i\pi/2\right] \qquad 6.6$$

and obviously such terms will dominate over Regge poles and cuts at asymptotic energies.

ODD SIGNATURE EXCHANGES

We construct models to describe the difference of the $\pi^{\pm}p$ total cross-section σ_T^{-} under the two assumptions.

1) $\sigma_T^{-} \to 0$ as $\nu \to \infty$

2) $\sigma_T^{-} \not\to 0$ as $\nu \to \infty$

Assumption 2) corresponds to a violation of the Pomeranchuk theorem[88] which asserts the asymptotic equality of particle and anti-particle total cross-sections. It is important to note that a violation of the Pomeranchuk theorem would not violate any basic theoretical principle since the proof of the Pomeranchuk theorem involves an ad hoc assumption about the phase of the forward scattering whose validity has not been established from any basic

axiom.

1) A single odd signature ρ Regge pole gives a contribution to the amplitude of the form

$$A'^{-}(\nu,0) \simeq i\,\gamma_\rho\, e^{-i\pi\alpha/2}\left(\nu/\nu'\right)^{\alpha} \qquad 6.6$$

Consequently a pole or sum of poles cannot give non vanishing σ_T^- asymptotically. Similarly the addition of Regge cuts whilst decreasing slower than the pole terms, will still be compatible with zero σ_T^- at high energies.

2) Pomeranchuk theorem violation requires a contribution to the A'^- amplitude such that

$$\mathrm{Im}\, A'^{-}(\nu,0) \underset{\nu\to\infty}{\sim} \gamma_L\,\nu \qquad 6.7$$

We cannot invoke an odd signature pole with $\alpha(0) = 1$ since the amplitude would be purely real. Given this asymptotic form the Re A' can be determined from the Phagmen-Lindeloff theorem and with reference to the Regge model this term corresponds to an odd signature dipole at $t = 0$

$$A'^{-}(\nu,0) = \gamma_L\left(\nu/\nu'\right)\left[\ln \nu/\nu' - i\,\frac{\pi}{2}\right] \qquad 6.8$$

If $\sigma_T(\pi^{\pm}p)$ do tend to separate limits at asymptopia then from the above term, the real part of the amplitude will dominate over the imaginary part for large ν and in order that the elastic cross-section remains bounded by the unitarity requirement,

$$\sigma_T > \sigma_{el}$$

89

we must have $(\ln \nu)^2$ shrinkage of the forward diffraction peak. However if

dipoles are present in the A'^{+} amplitude such that $\sigma_T^{+} \to \ln \nu$ asymptotically then ($\ln \nu$) shrinkage of the forward peak is sufficient.

THE ANALYSIS

The simultaneous analysis of the pion nucleon scattering data and the C.M.S.R. over a large range of t involves a large information input and if we are able to account for all the predominat features of both types of data with a few physical trajectories then we can regard the model as adequate.

In the analysis of the total cross-section data our information input is considerably reduced and we are interested in the details of the amplitudes. We know the P,P',ρ model is good up to 20 GeV/c but at energies greater than 20 GeV/c we have to include 'extra terms', outlined in the previous sections, to account for the deviations of the Serpukhov data from the P,P',ρ model extrapolations. Obviously the more terms we introduce the greater is our parameter freedom in fitting the data and hence the better the description of the data.

We can improve the input information by the use of the F.E.S.R. to exploit the analytic properties of the scattering amplitude and although the F.E.S.R. are constructed from the same high energy total cross-sections as used in the various fits of the parameterisations, they weight the data in a different way and as such yield added important information.

For any of the parametric forms, which by their choice fit the data we can predict the left hand side of the F.E.S.R. and compare the predictions with the l.h.s. calculated from the integral over the total cross-sections or we can include the F.E.S.R. in the analysis and fit simultaneously the sum rules and the data. The important point in both these types of approach is deciding the relative importance between the F.E.S.R. and the total cross-section data with the consequent assignment of errors to the

F.E.S.R.

An alternative approach, which we pursue in the following, is to give a large weight to the sum rules in the analysis by introducing them as constraint equations between the various contributions to the total cross-sections and seeing if we are still able to produce a good description of the data.

PARAMETERISATIONS

a) There are many ambiguities in the choice of the parameterisations. Whether one should use p_{LAB}, T_{LAB}, or ν etc. as the variable, which differ in magnitude by up to 10% at 10 GeV and when we are considering variations of 1 or 2mb. in total cross-sections this is appreciable. The general parameterisations of the Imaginary parts of the amplitude $A^{\pm}(\nu,0)$ are written

$$\text{Im } A'^{+}(\nu,0) = \gamma_D \nu \ln\nu + \gamma_p \nu + \gamma_s \text{Sin}\pi\alpha/2\ \nu^{\alpha} + \gamma_c \frac{\nu}{\log\nu/\nu'}$$

$$\text{Im } A'^{-}(\nu,0) = \gamma_\rho \text{Cos}\pi\alpha/2\ \nu^{\alpha} + \gamma_{\rho'} + \gamma_L \nu \qquad 6.9$$

where γ_i are the residue functions defined in the preceding sections. The scaling factors ν' do not appear explicitly in the parameterisations, except in the cut contribution. They are absorbed in the residue function or other terms in the parameterisation {e.g. such a term in the even signature dipole will be absorbed in the Pomeron contribution}.

b) These parameterisations of Im $A^{\pm}(\nu,0)$ lend themselves very easily to use in the F.E.S.R. which are written:

$$\int_0^{\nu} d\nu\, \nu^n \,\mathrm{Im}\, A'^{+}(\nu,0) = \gamma_D \frac{\nu^{n+2}}{n+2}\left\{\ln\nu - \frac{1}{n+2}\right\} + \gamma_P \frac{\nu^{n+2}}{n+2} + \gamma_s \,\mathrm{Sin}\pi\alpha/2 \frac{\nu^{\alpha+n+1}}{\alpha+n+1}$$

$$+ \gamma_c \,\mathrm{Im}\left\{E_i\left[(n+2)\left[\ln\left(\nu/\nu'\right) - i\pi/2\right]\right]\right\} \quad (E_i \text{ is the exponential integral})$$

$$n = 1,3,5 \ldots$$

$$\int_0^{\nu} d\nu\, \nu^n \,\mathrm{Im}\, A'^{-}(\nu,0) = \gamma_\rho \,\mathrm{Cos}\pi\alpha/2 \frac{\nu^{\alpha+n+1}}{\alpha+n+1} + \gamma_{\rho'} \frac{\nu^{n+1}}{n+1} \quad \gamma_L \frac{\nu^{n+2}}{n+2}$$

$$n = 0,2,4 \ldots$$

The cut off values for the integrals were chosen at 20 GeV and 15 GeV and the left hand sides for the first three moments are given in table X.

c) Assuming $\sigma_T \geq$ constant for $\nu \to \infty$ the forward dispersion relation for the even signature amplitude A'^{+} will require one subtraction such that the real part of A'^{+} is determined by the parameter γ_i etc. of the Imaginary part with one subtraction constant only.*

Similarly the forward dispersion relation for the odd signature amplitude A'^{-} is given with one subtraction constant if the dipole term is contributing or if the amplitude is given by poles only such that $\nu^{-1}\,\mathrm{Im}\, A'^{-}(\nu,0)$ tends to zero sufficiently fast then the subtraction constant is zero.

DATA AND CALCULATION

The ambiguities in the choice of the parameterisations are comparable to those in the data interpolation. The $\pi^{\pm}p$ total cross-sections are not measured at coincident momenta and it is necessary to interpolate the data to construct the symmetric and antisymmetric combinations $A'^{\pm}$.

We considered two different data interpolations as a check that the errors in the interpolations did not account for any of the observations. The interpolations were taken from a) refs.DATA4-1,2,3 and b) Hohler et al.

* This is just the P'' contribution ($\alpha(0)=0$).

refs.DATA4.4. These interpolations are very similar for the amplitude A'^{+} but there are noticable differences in the interpolation for the A'^{-} amplitude which is due to a certain amount of in-built theoretical high energy information in b).

For each model under consideration we construct a set of constraint equations from the F.E.S.R. evaluated at 20 GeV/c at integer moments and apply them as successive constraints on the parameters of the model which are determined by fitting the high energy total cross-section data. For each model we compare the results from the fit unconstrained by the F.E.S.R. with the constrained solution and we predict the real parts of the amplitude from our parameterisations which are compared to those taken from ref. DATA4.5. The parameters of the fits to the total cross-section data are given in tables XI, XII and the results for the amplitudes $A'^{\pm}$ are summarised below.

EVEN SIGNATURE EXCHANGES

a) Fig.1 illustrates the P,P' contributions to σ_T^+ and the qualitative change in behaviour is apparent at 20 GeV/c. The constrained and unconstrained solutions are similar and it is difficult to envisage any known trajectory raising the asymptotic P,P' projection to the Serpukhov data.

(Rarita suggests a 'N' pole trajectory intercept $\alpha(0) = 0.8$ and negative residue but the analysis away from the forward direction gives no evidence for such a trajectory).[90]

b) The addition of multi-Pomeron cuts to the leading Regge poles improves the fit to the Serpukhov data Fig.2 and the cut has the conventional negative residue corresponding to a Regge eikonal prescription. The constrained fits indicate much smaller cut contributions which are insufficient to give the apparent levelling of the total cross-section data at Serpukhov

energies.

We can understand this result from the χ^2 distribution of the unconstrained fits which show that the parameters for this solution give a very poor fit to the (5-10 GeV) total cross-section data, for which the experimental errors are small. It is not surprising then that this solution also fails to satisfy the constraints provided by the F.E.S.R. which are constructed from the total cross-section data < 20 GeV.

3) The dipole model gives a good fit to the data and both the constrained and unconstrained fits show the levelling of the total cross-section in the range 20-70 GeV Fig.3 but unfortunately the predictions for the real parts are very poor even allowing for the large experimental errors on the Re A'^{+} data.

ODD SIGNATURE EXCHANGES

1) The interpolation a) is fitted with a single ρ pole and there is some evidence for a divergence of the ρ extrapolation from the Serpukhov measurements Fig.4a although the errors on the data are very large.

2) For comparison the interpolation b) is fitted with a single ρ pole and in this interpolation there is no evidence for a rise in δ_T^- at Serpukhov energies Fig.4b.

3) The dipole term in the A'^{-} amplitudes gives the best description of the data Fig.5 both for the constrained and unconstrained fits. The Re A'^{-}, without a subtraction constant, are also described well by the dipole and pole terms. However the small increase in χ^2 for this fit over the single pole fit and the uncertainty in the data prevent a stronger conclusion than that a dipole in the odd signature amplitude is not inconsistent with the data.

DISCUSSION

The relative sizes of the multi-Pomeron cuts necessary to satisfy the F.E.S.R. compared to those suggested by the Serpukhov data relate to the different requirements of the low and intermediate energy cross-sections compared to the Serpukhov total cross-sections. The question is how much are we willing to destroy the low energy fit where the errors on the data are particularly small in order to improve the high energy fit.

The energy dependence of the cut contributions $\nu/\ln \nu$ can be simulated by the function $\nu^{0.5}$ in the range 5-20 GeV which means that the cut acts like a negative residue P' contribution. The fit to the Serpukhov data is achieved by the cancellation of the P' with the cut contribution such that the flat Pomeron contribution is dominant, sufficient to give the levelling of the total cross-sections at these energies. It is this large cancellation which destroys the low energy fit where the size of the P' contribution is well determined by the data.

An alternative approach proposed by Höhler is to introduce a low lying trajectory $\alpha < 0$ to replace the P' which will give a sharper drop off with energy of the 5-20 GeV fit to the total cross-sections. The cuts for such a model will be smaller because of the smaller cancellations necessary in the range 20-70 GeV/c to give the flatness of the data. Even in this description we have the problem of the low energy data which has very small errors and clearly favours the conventional P' contribution.

It is interesting to note that in a recent more detailed analysis with respect to χ^2 of the F.E.S.R. and the total cross-section data Schiff and Violini[86] demonstrated that the inclusion of cuts improved the description of the high energy data (10-25 GeV) but they too observed that the cuts were insufficient to account for the Serpukhov data.

Compatibility between the low energy data and the Serpukhov total cross-

sections suggest a term which increases logarithmically with energy. It is not surprising that such a function satisfies both the F.E.S.R. and the total cross-section data, since it can account for the Serpukhov data without giving a large contribution in the range $\nu \sim 5.0 - 7.0$ GeV.

The dipoles are the simplest forms which violate conventional asymptotics but we do not envisage that these Regge dipoles correspond to physical particles and prefer to regard them as an 'interference effect' between poles or poles and cuts. Srivastava noted the possibilities of such a description and that the inclusion of multi-pomeron cuts with the common condensation point $\alpha(0) = 1$ could invalidate the pole dominance idea. This behaviour at $t = 0$ saturates the Froissart bound and since it is widely believed that strong forces are as strong as they can be, the simple Regge pole is insufficient.

The description of the Serpukhov data is still an open question, we have not found an adequate description in the extensive literature of both the low energy and Serpukhov total cross-section data assuming conventional asymptotics and if we are forced to consider unconventional asymptotics we encounter a whole new series of problems much more complex than the original explanation of the Serpukhov data.

TABLE X

	n	15.0 GeV	20.0 GeV
$\int_0^\nu \nu^n A'^+ d\nu$	1	2.84×10^2	6.66×10^4
	3	3.79×10^6	15.9×10^6
	5	6.09×10^8	45.5×10^8
$\int_0^\nu \nu^n A'^- d\nu$	0	1.38×10^2	2.05×10^2
	2	1.63×10^4	3.65×10^4
	4	2.52×10^6	8.8×10^6

TABLE XI

MODEL		γ_0	γ_P	γ_c	γ_s $\alpha_{P'}=0.4$
P + P'	constrained		21.76		27.34
	unconstrained		21.87		27.6
P + P' + Cut	constrained		22.8	- 2.8	26.7
	unconstrained		26.2	-19.8	35.8
Dipole + P + P'	constrained	1.6	15.5		43.9
	unconstrained	1.6	15.3		44.8

TABLE XII

MODEL		$\alpha_\rho = 0.5$ γ_ρ	γ_L
ρ	Interpolation a)	4.3	
	Interpolation b)	3.9	
ρ + Dipole	constrained	4.15	0.02
	unconstrained	3.72	0.1

FIGURE CAPTIONS - CHAPTER 6

FIG.1 P,P' fit to δ_T^+ and from the parameters of the fit the prediction for Re A'^+. The continuous line denotes the unconstrained solution and the dashed curve the constrained solutions.

FIG.2 P,P' and multi-Pomeron cut fit to δ_T^+ and from the parameters of the fit the prediction for Re A'^+ [cf. ref.Fig.1].

FIG.3 P,P' and dipole fit to δ_T^+ and prediction for Re A'^+ [cf. ref. Fig.1].

FIG.4 a) Single ρ pole fit to δ_T^- taken from [refs. DATA4.1,2,3].

b) Single ρ pole fit to δ_T^- taken from [refs. DATA4.4].

c) Predictions for the above fits to Re A'^-.

FIG.5 ρ + dipole fits to δ_T^- taken from refs. (DATA4.1,2,3) and the predictions for Re A'^-.

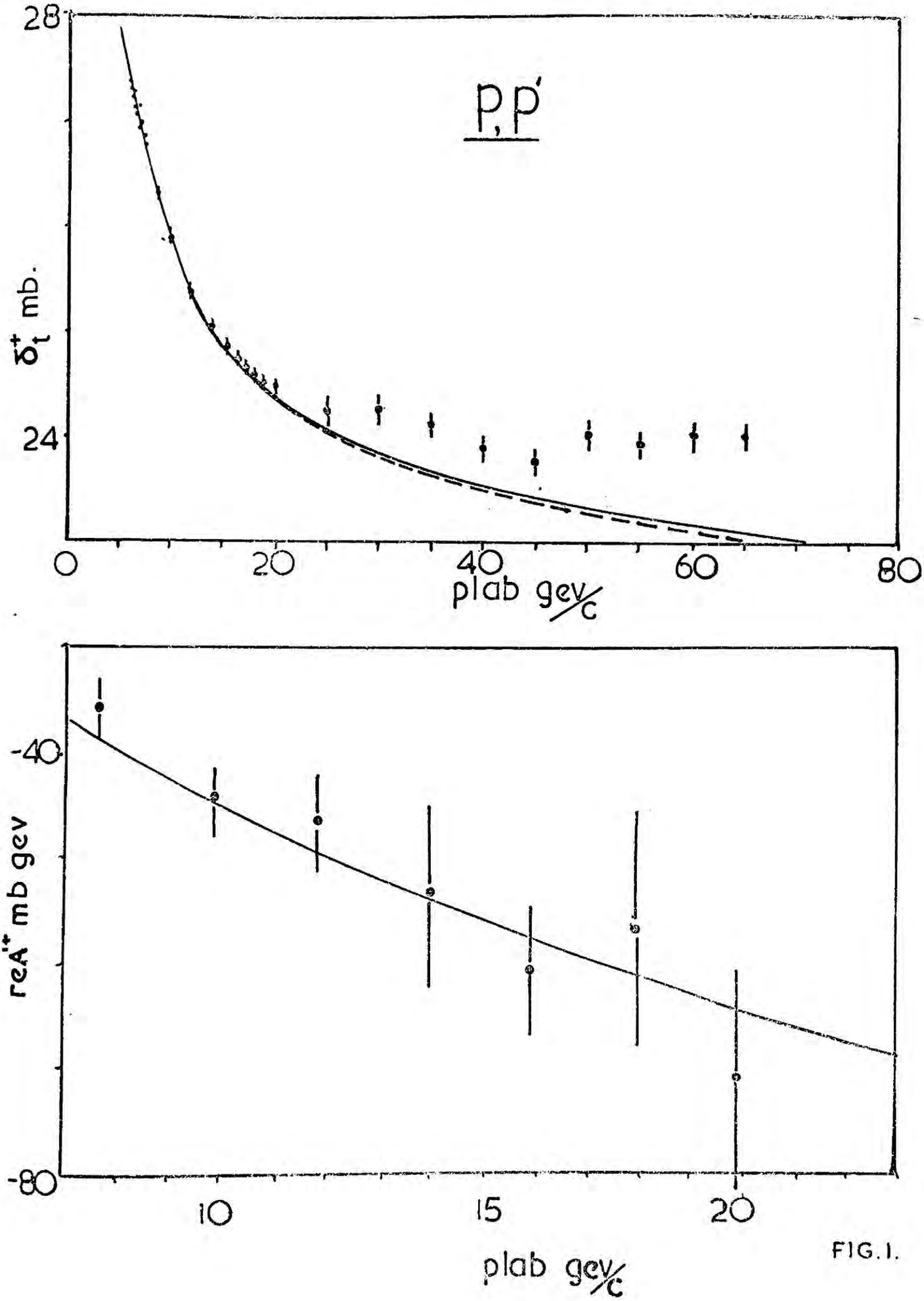
P, P'
28
24
σ_t^+ mb.
0
20
40
60
80
plab gev/c
-40
-80
$re A'^+$ mb gev
10
15
20
plab gev/c

FIG. 1.

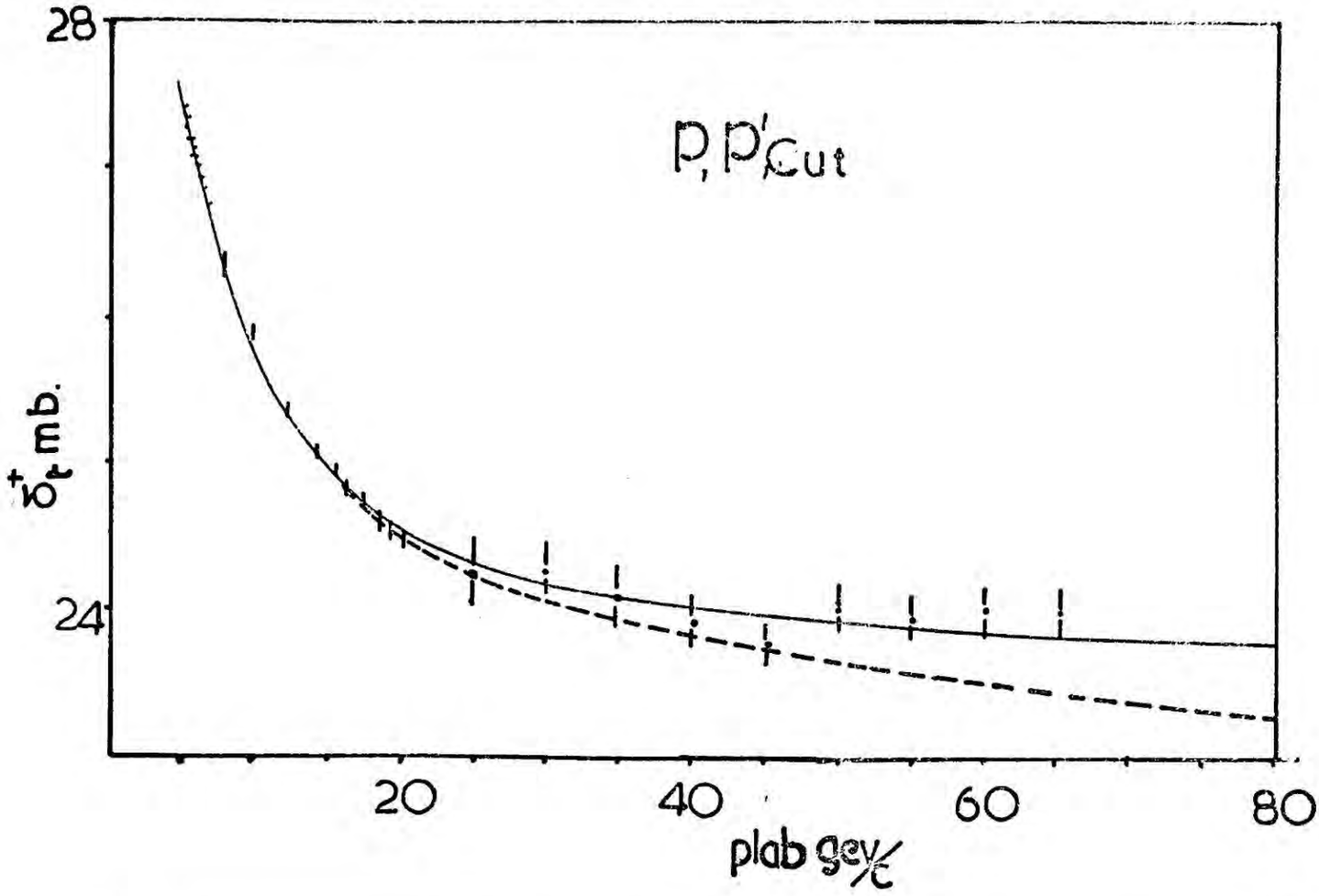
28
24
δ_t^+ mb.
P, P' Cut
20
40
60
80
plab gev/c

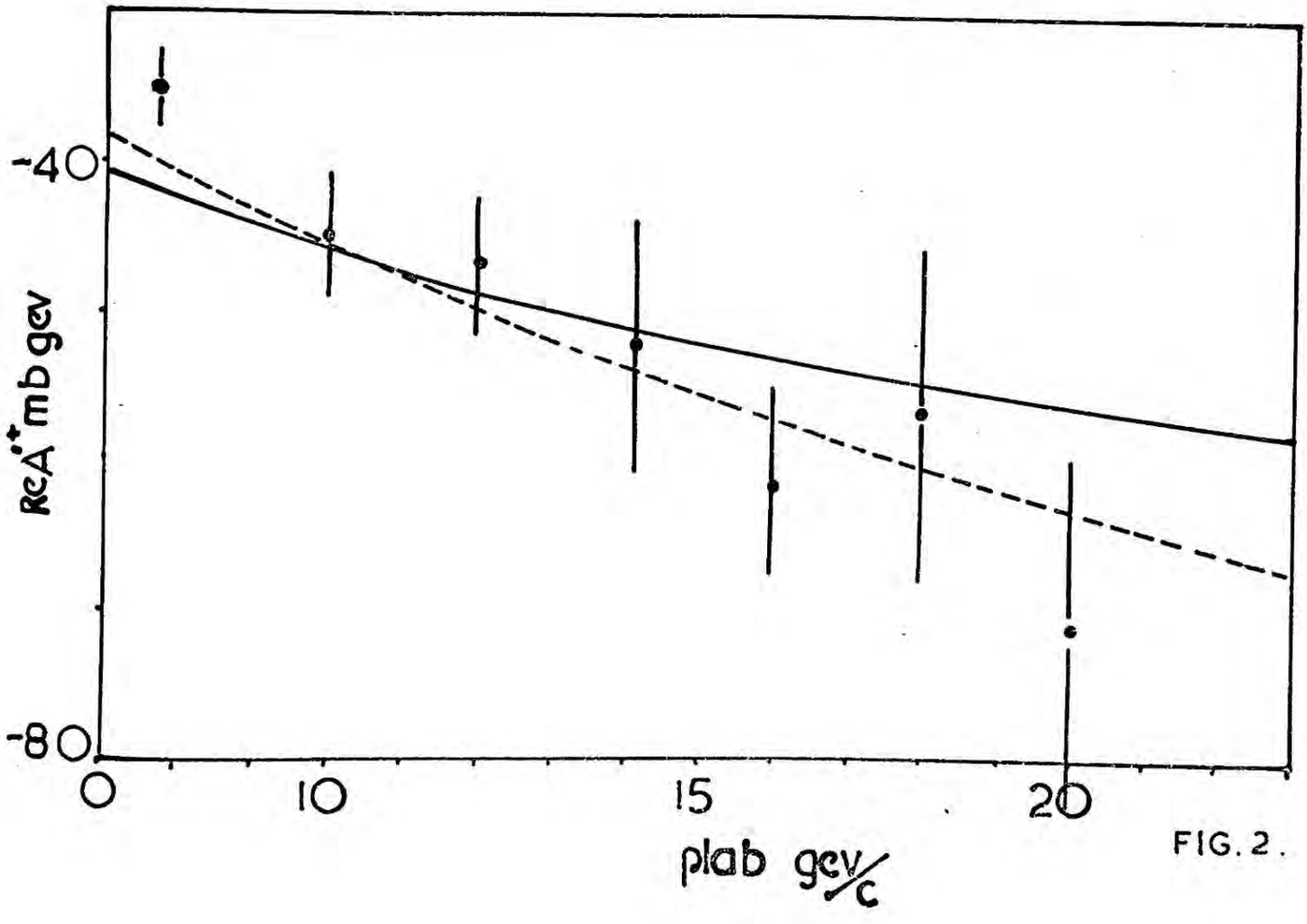
-40
-80
$Re A^{++}$ mb gev
0
10
15
20
plab gev/c

FIG. 2.

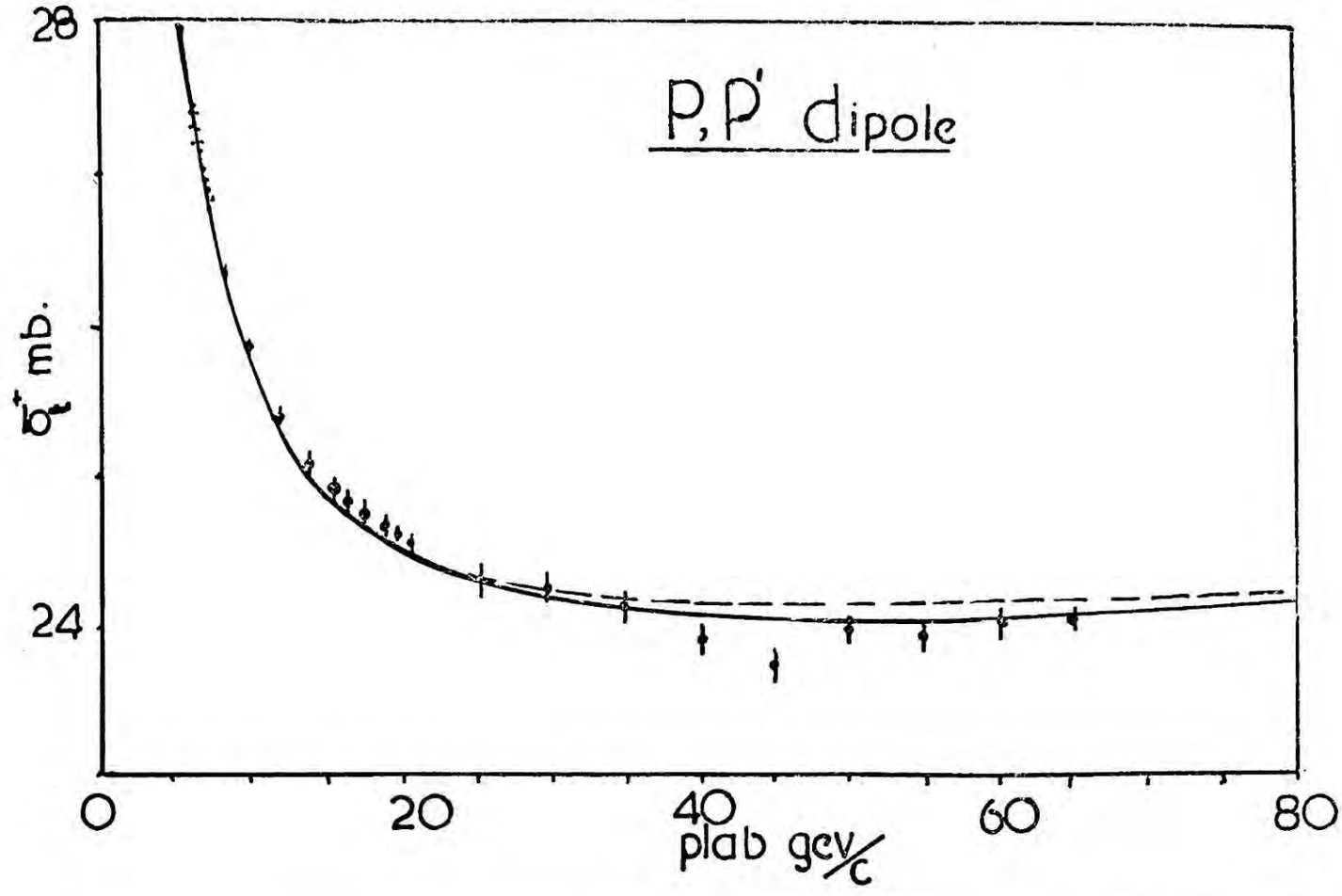
P, P' dipole
28
24
σ_t^+ mb.
0
20
40
60
80
plab gev/c

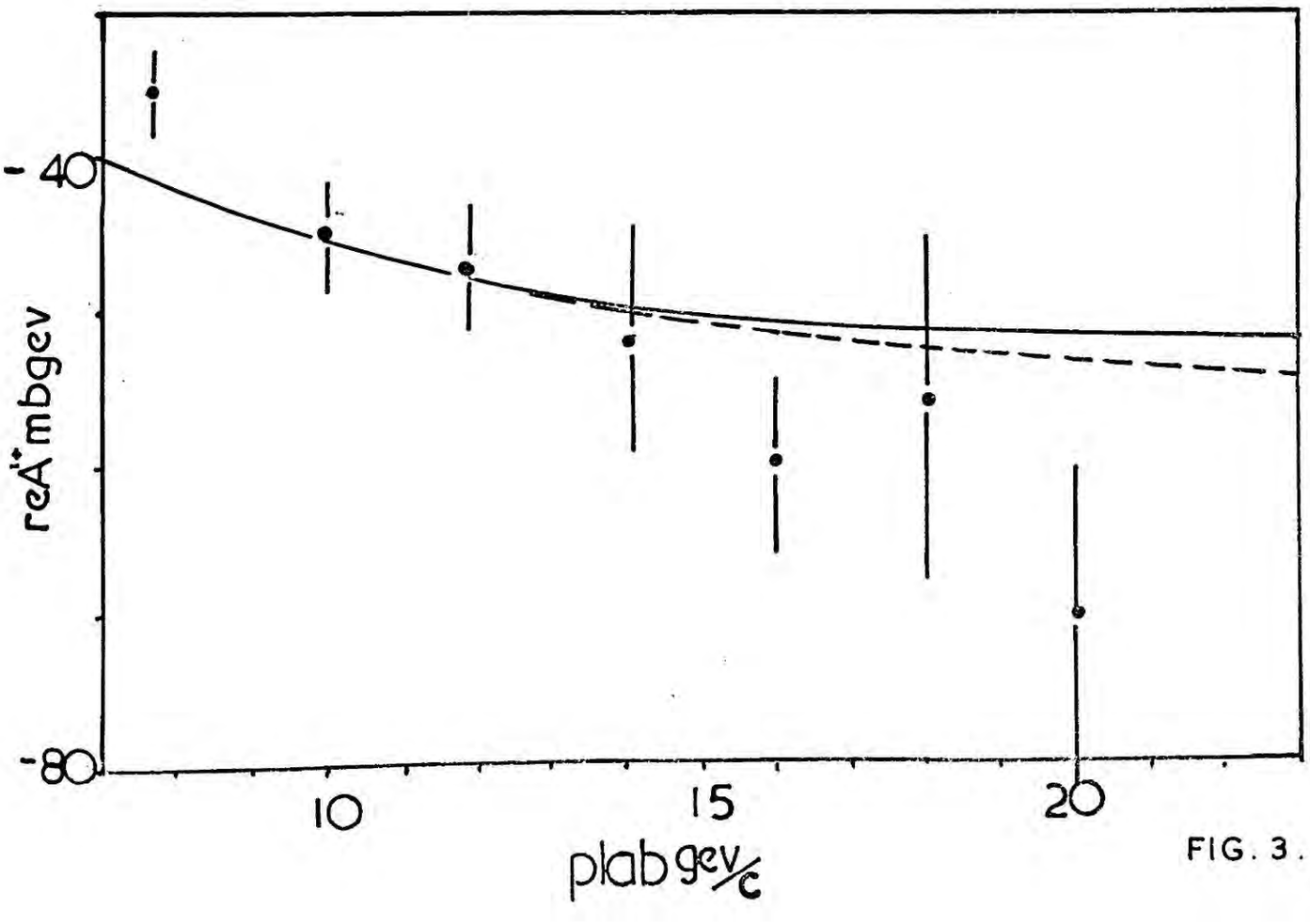
-40
-80
reA+mbgev
10
15
20
plab gev/c

FIG. 3.

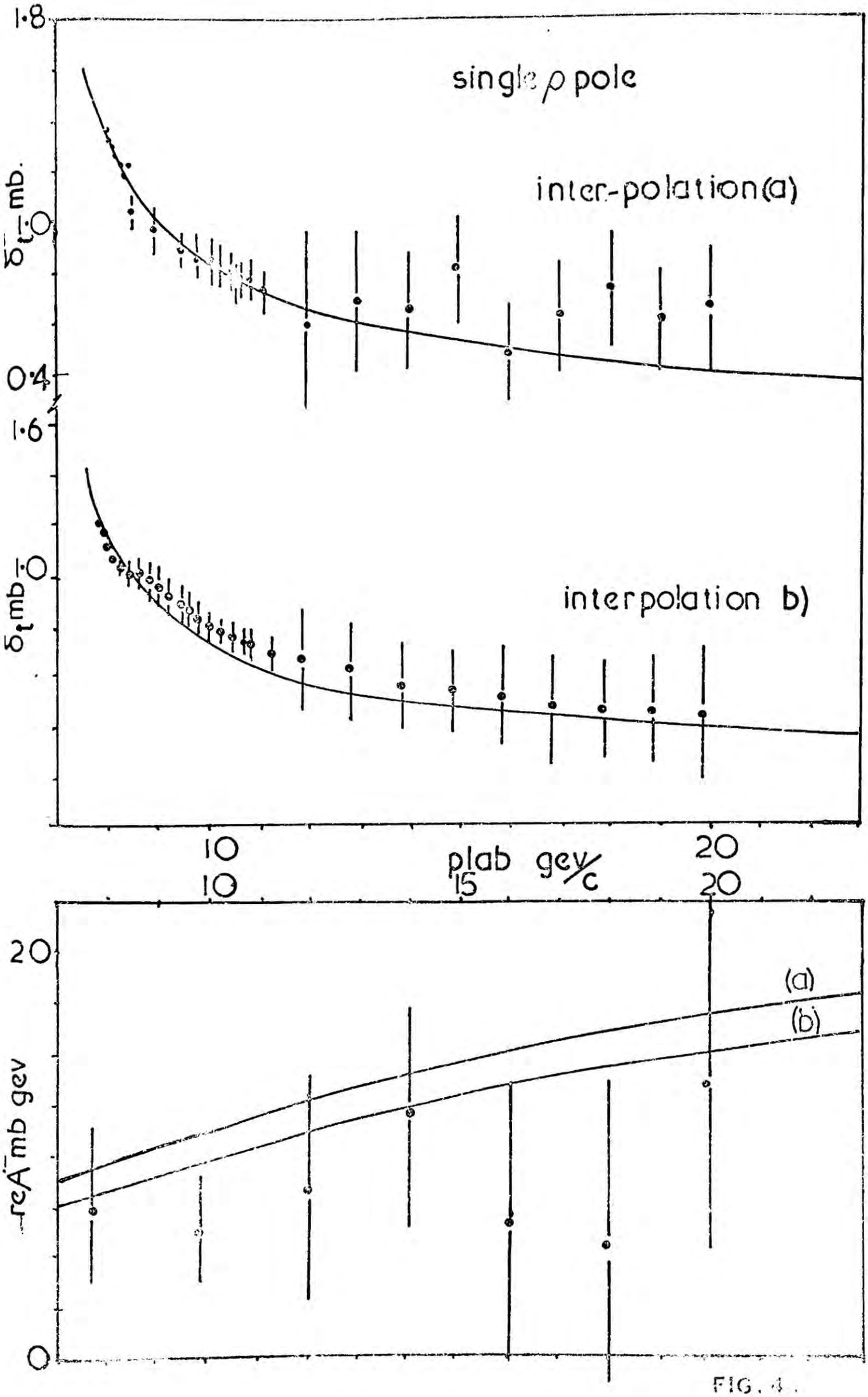
single ρ pole
inter-polation(a)
interpolation b)
σ_t mb
1·8
1·6
1·0
0·4
10
15
20
plab gev/c
$\mathrm{re}\bar{A}$ mb gev
(a)
(b)
0
20

FIG. 4.

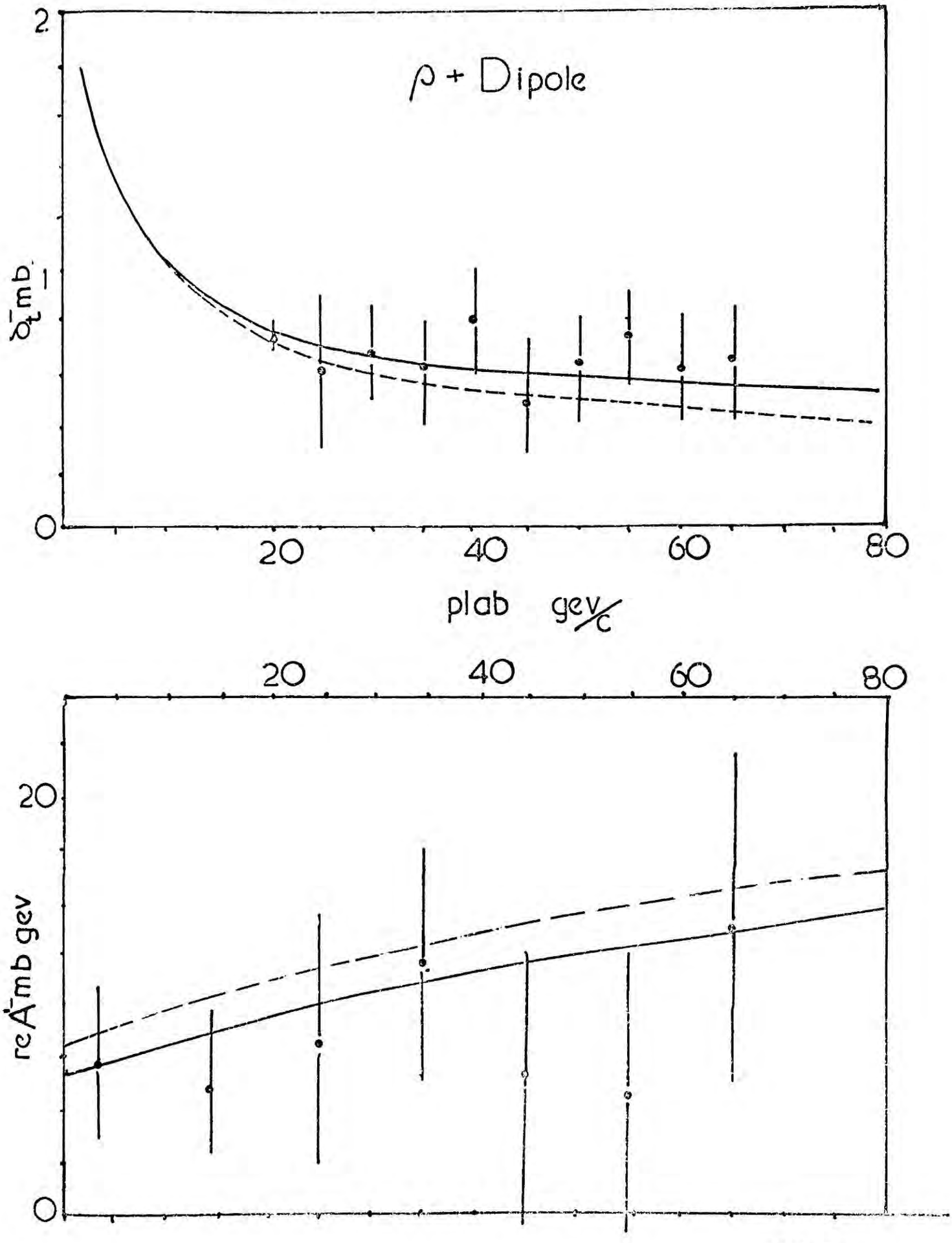
ρ + Dipole
2
1
0
σ_t mb
20
40
60
80
plab gev/c
20
40
60
80
20
0
re $\bar{A}$ mb gev

FIG. 5.

APPENDIX A

The two particle cut contribution to the partial amplitude due to the exchange of a Regge pole and a Pomeron is written (see equation 2.38).

$$F^J_{fi}(s) = i\, k_{ii}(s)\, P^J_{ii}(s)\, R^J_{fi}(s) \qquad A1$$

where $k_{ii}(s) = \frac{q_s}{8\pi\sqrt{s}}$ and $P^J_{ii}(s)$, $R^J_{fi}(s)$ are the Pomeron and Regge pole partial amplitudes respectively.

The total amplitude is written by summing over the partial amplitudes and writing out the helicities explicitly (fig. A1)

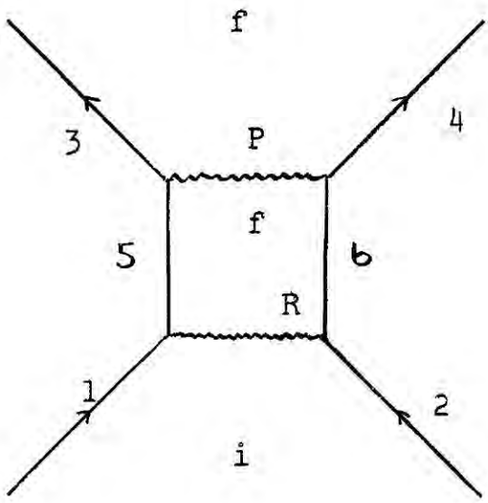

FIG.A1

$$F^{cut}_{\lambda'\lambda}(s,t) = i\, k(s) \sum_J (2J+1) \sum_{\lambda5\lambda6} P^J(s)_{\lambda1\lambda2\lambda5\lambda6}\, R^J(s)_{\lambda5\lambda6\lambda3\lambda4}\, d^J_{\lambda\lambda'}(z_s) \qquad A2$$

where $\lambda = \lambda1 - \lambda2$

$\lambda' = \lambda3 - \lambda4$

Performing the individual partial wave projections of the amplitudes $P^J(s)$,

$R^J(s)$ we can write:

$$P^J_{\lambda_1\lambda_2\lambda_5\lambda_6}(s) = \tfrac{1}{2}\int_{-1}^{+1} P_{\lambda_1\lambda_2\lambda_5\lambda_6}(s,z_1)\, d^J_{\lambda',\lambda''}(z_2)\, dz_1$$

$$R^J_{\lambda_5\lambda_6\lambda_3\lambda_4}(s) = \tfrac{1}{2}\int_{-1}^{+1} R_{\lambda_5\lambda_6\lambda_3\lambda_4}(s,z_2)\, d^J_{\lambda''\lambda'}(z_2)\, dz_2 \qquad \text{A3}$$

where $\lambda'' = \lambda_5 - \lambda_6$

z_1 and z_2 are the cosines of the scattering angles between the initial and intermediate and intermediate and final states respectively. The cosines are related by the following addition theorem:

$$z_1 = z_s z_2 + (1-z_s^2)^{1/2}\,(1-z_2^2)^{1/2}\,\cos\phi_1$$

where ϕ_1 is the azimuthal angle between the directions of motion in the initial and intermediate states. The d^J functions satisfy the relation:

$$\sum_J (2J+1)\, d^J_{\lambda\lambda'}(z_s)\, d^J_{\lambda\lambda''}(z_1)\, d^J_{\lambda''\lambda'}(z_2) = \frac{2}{\pi}\,\frac{\theta(\delta)}{\delta^{1/2}}\,\cos(\lambda\phi_1+\lambda'\phi_2+\lambda''\phi_5) \qquad \text{A5}$$

where δ is defined by:

$$\delta = 1 - z_s^2 - z_1^2 - z_2^2 - 2z_s z_1 z_2$$

and the azimuthal angles satisfy the relations:

$$e^{i\phi_1} = (z_1 - z_s z_2 + i\delta^{1/2})\,(1-z_2^2)^{-1/2}\,(1-z_s^2)^{-1/2}$$

$$e^{i\phi_2} = (z_2 - z_s z_1 + i\delta^{1/2})\,(1-z_s^2)^{-1/2}\,(1-z_1^2)^{-1/2} \qquad \text{A6}$$

$$e^{i\phi_5} = (-z_s + z_1 z_2 - i\delta^{1/2})\,(1-z_1^2)^{-1/2}\,(1-z_2^2)^{-1/2}$$

Equation A2 is then simplified to:

$$F^{cut}_{\lambda'\lambda}(s,t) = \sum_{\lambda 5\lambda 6} \frac{i\,k(s)}{\pi} \int_{-1}^{1} dz_1 \int_{-1}^{1} dz_2 \; P(s,z_1)_{\lambda 1\lambda 2\lambda 5\lambda 6} \; R(s,z_2)_{\lambda 5\lambda 6\lambda 3\lambda 4} \; \frac{\theta(\delta)}{\delta^{1/2}}$$

$$\cos(\lambda\phi_1+\lambda'\phi_2+\lambda''\phi_3) \qquad \text{A7}$$

Hence, given the pole amplitudes we can derive the cut due to the exchange of a Regge pole and Pomeron.

If the scattering angle z_1, z_2 are written:

$$z_1 = 1 + \frac{t_1}{2q_s^2} \qquad z_2 = 1 + \frac{t_2}{2q_s^2}$$

then equation A7 can be further simplified to read:

$$F^{cut}_{\lambda'\lambda}(s,t) = \sum_{\lambda 5\lambda 6} \frac{i\,k(s)}{4\pi q_s^2} \int_{-4q_s^2}^{0} dt_1 \int_{-4q_s^2}^{0} dt_2 \; P(s,t_1)_{\lambda 1\lambda 2\lambda 5\lambda 6} \; R(s,t_2)_{\lambda 5\lambda 6\lambda 3\lambda 4} \; \frac{\theta(\delta)}{\delta^{1/2}}$$

$$\cos(\lambda\phi_1+\lambda'\phi_2+\lambda''\phi_3) \qquad \text{A8}$$

which is comparable with equation 2.48 as derived in the Regge-eikonal model.

APPENDIX B

The relativistic electromagnetic amplitudes for first order in α are

$$f_1^{rem}(\pi^{\pm}p) = \frac{\mp\alpha}{2W(1-\cos\theta)}\left[\frac{W-M}{p_o-M}+\frac{W+M}{p_o+M}\cos\theta-(\mu_p-1)\frac{q_o}{M}(1-\cos\theta)\right.$$
$$\left.-\mu_p-1\ \frac{p_o-M}{2M}\sin^2\theta\right]$$

$$f_2^{rem}(\pi^{\pm}p) = \frac{\pm\alpha\sin\theta}{2W(1-\cos\theta)}\left[\frac{W+M}{p_o+M}+(\mu_p-1)\frac{W+q_o+M}{2M}+(\mu_p-1)\frac{p_o-M}{2M}\cos\theta\right]$$

where the pion total cm energy is $q_o = (k^2+\mu^2)^{1/2}$, k is pion c.m. momentum and $p_o = (k^2+M^2)^{1/2}$ is the proton total c.m. energy.

The total energy is $W = p_o + q_o$ and $\mu_p = 27925$ is the proton magnetic moment in nuclear magnetons.

The non relativistic electromagnetic (Coulomb) amplitudes correct to all order in α are

$$f_1^{coul}(\pi^{\pm}p) = \frac{\mp\alpha(q_op_o+k^2)}{k^2W(1-\cos\theta)}\exp\left[\mp i\frac{\alpha(q_op_o+k^2)}{kW}\left(\frac{1-\cos\theta}{2}\right)\right]$$

$$f_2^{coul}(\pi^{\pm}p) = 0$$

To first order in α the Coulomb amplitudes are

$$f_1^{coul\ \alpha}(\pi^{\pm}p) = \frac{\mp\alpha(q_op_o+k^2)}{k^2W(1-\cos\theta)}$$

$$f_2^{coul\ \alpha}(\pi^{\pm}p) = 0$$

BOOKS

GENERAL

G.F. Chew	S Matrix theory of Strong Interactions
G.F. Chew and M. Jacob	S Matrix theory of Strong Interactions
G.F. Chew and M. Jacob	Strong Interaction Physics
R.J. Eden	High Energy Collisions of Elementary Particles
S.C. Frautschi	Regge Poles and S Matrix theory
R.J. Newton	The Complex J-Plane
R.L. Omnes and M. Froissart	Mandelstam theory and Regge Poles
E.J. Squires	Complex Angular Momenta and Particle Physics

REFERENCES

[1] P.D.B. Collins and E.J. Squires, Regge Poles in Particle Physics.

[2] Martin and Spearman, Elementary Particle Theory.

[3] S. Mandelstam, Phys. Rev. 112 (1958) 1344.

[4] Chew, Goldberger, Low and Nambu, Phys. Rev. 106 (1957) 1337.

[5] Jacob and Wick, Ann. of Phys. 115 (1959) 1741.

[6] J. Hamilton, Strong Interaction of High Energy Physics (Scottish Universities Summer School).

[7] Singh, Phys. Rev. 129 (1963) 1889.

[8] Frazer, Regge Pole Theory in:- Proceedings of International School of Physics, Enrico Fermi 1968.

[9] V.D. Barger and D.B. Cline, Phenomenological Theories of High Energy Scattering (Frontiers in Physics).

[10] A Sommerfeld, Partial Differential Equations in Physics, p.282 (1964).

[11] E.C. Titchmarsh, The theory of functions (1950) p.186.

[12] T. Regge, Nuovo Cimento 14 (1959) 951.
Nuovo Cimento 18 (1960) 947.
V.D. Alfaro and T. Regge, Potential Scattering (North Holland Publishing Company 1965).

[13] See Collins and Squires, ref. [1] page 56.

[14] A. Erdelyi, Bateman Manuscript - 'Higher transcendental functions'.

[15] S. Mandelstam, Ann. of Phys. 19 (1962) 254.

[16] L. Van Hove, Phys. Lett. 24B (1967) 183.

[17] L. Durand, Phys. Rev. 161 (1967) 1610.

[18] Chew and Frautschi, Phys. Rev. Lett. 8 (1968) 41.

[19] A.H. Rosenfeld et al., Data on particles and resonant states.

[20] Chew and Frautschi, Phys. Rev. Lett. 7 (1961) 394.

[21] R. Oehme, Phys. Rev. Lett. 16 (1966) 60.

[22] L. Bertocchi, Heidelberg Conference Report (1967).

[23] S. Mandelstam, Nuovo Cimento 30 (1963) 1127, 1148.

[24] D. Amati et al., Phys. Lett. 1 (1962) 29.

[25] V.N. Gribov et al., Phys. Rev. 139 (1965) B185.

[26] J.B. Bronzan and C.E. Jones, Phys. Rev. 160 (1967) 1494.

[27] J.D. Jackson, Rev. Mod. Phys. 37 (1965) 484.

[28] H.D.D. Watson, Phys. Rev. Lett. 17 (1965) 72.

[29] R.J. Rivers, Nuovo Cimento 63A (1969) 697.

[30] N.J. Sopkovich, Nuovo Cimento 26 (1962) 186.

[31] P.D.B. Collins, Phys. Report 1 (1971) 130.

[32] R.C. Arnold, Phys. Rev. 153 (1967) 1523.

[33] T.T. Chou and C.N. Yang, "High Energy Physics and Nuclear Structure" (1967).

[34] D. Branson, Phys. Rev. 199 (1969) 1608.

[35] V. Barger and R.J.N. Phillips, Madison preprint COO 262 (1970).

[36] K. Igi and S. Matsudu, Phys. Rev. Lett. 18 (1967) 625.

[37] A.A. Logunov et al., Phys. Lett. 24B (1967) 181.

[38] R. Dolen, D. Horn and C. Schmid, Phys. Rev. Lett. 19 (1967) 402.

[39] R. Dolen, D. Horn and C. Schmid, Phys. Rev. 166 (1968) 1768.

[40] V.A. Mesticheriakov et al., Phys. Lett. 25B (1967) 341.

[41] e.g. Chan Hong Mo, Proceedings of 1969 Cern School of Physics.

[42] L.A.P. Balazas and J.M. Cornwall, Phys. Rev. 160 (1967) 1313. This use of the F.E.S.R. is closest in spirit to the original superconvergence calculation of V. de Alfaro et al. ref. [43].

[43] V. de Alfaro, S. Fubini, G. Furlan and G. Rossetti, Phys. Lett. 21 (1966) 576.

[44] V.J. Barger and R.J.N. Phillips, Phys. Lett. 26B (1968) 730.

[45] V.J. Barger and R.J.N. Phillips, Rutherford Lab. Report (1968).

[46] Y.C. Lin and S. Okubo, Phys. Rev. Lett. 19 (1967) 190.

[47] M.G. Olsson, Phys. Rev. 171 No.5 (1968) 1681.

[48] A. Della Selva, L. Masperi and R. Odorico, Nuovo Cimento 55A (1968) 602.

[49] W. Rarita, R.J. Ridell, C.B. Chiu and R.J.N. Phillips, Phys. Rev. 165 (1965) 1615.

[50] V. Barger and R.J.N. Phillips, Phys. Rev. 187 (1969) 2210.

[51] L.K. Chavda,

[52] J.H. Schwarz, Phys. Rev. 159 (1967) 1268.

[53] J.E. Mandula and R.C. Slansky, Phys. Rev. Lett. 20 (1968) 1404.

[54] G.F. Chew and A. Pignotti, Phys. Rev. Lett. 20 (1968) 1078.

[55] M. Jacob, General review of duality - lecture notes at the Schladmig Winter School, Cern Preprint T.H. 1010, 1969.

[56] C. Schmid, Phys. Rev. Lett. 20 (1968) 689.

[57] C. Lovelace, Proceedings of Heidelberg Conf. (1967).

[58] P.D.B. Collins and E.J. Squires, Phys. Lett. 27B (1968) 23.

[59] Chiu and Kotanski, Nucl. Phys. 7 (1968) 615.

[60] Chiu and Kotanski, Nucl. Phys. 8 (1969) 553.

[61] H. Harari, Phys. Rev. Lett. 20 (1968) 1395.

[62] P.G.O. Freund, Phys. Rev. Lett. 20 (1968) 235.

[63] V. Barger and D. Cline, Phys. Rev. Lett. 16 (1966) 913.

[64] V. Barger and D. Cline, Phys. Rev. 155 (1967) 1792.

[65] D.J. Herndon, π-N Partial Wave Compilation UCRL 200-30 π-N

[66] R.H. Dalitz, Ann. Rev. Nucl. Sci. 13 (1963) 339.

[67] P. Baryere, C. Bricman and G. Villet, Phys. Rev. 165 (1968) 1730.

[68] R.K. Roychoudhury, R. Perrin and B.H. Bransden, Nucl. Phys. B16 (1970) 461.

[69] R.K. Roychoudhury, R. Perrin and B.H. Bransden, Nucl. Phys. B22 (1970) 573.

[70] B.H. Bransden and P.J. Ogden, Nucl. Phys. B26 (1971) 511.

[71] A. Donnachie, R.J. Kirsopp and C. Lovelace, Phys. Lett. 26B (1966) 161.

[72] A. Donnachie, 14 ICT Conf. on High Energy Physics, Vienna (1968).

[73] R. Ayed et al., Phys. Lett. 31B (1970) 598.

[74] Roper et al., Phys. Rev. 138 (1965) 13190.

[75] R. Arnott and M.H. Macgregor, Methods in Computational Physics, 16 (1966) 253.

[76] A. Horsley and J.B. Barker, Aldermaston Report (1967).

[77] R.E. Cutkosky, Argonne National Lab. preprint 1970.

[78] V. Barger and R.J.N. Phillips, Phys. Rev. Lett. 21 (1968) 865.

[79] V. Barger and R.J.N. Phillips, Phys. Lett. 26B (1968) 730.

[80] V. Barger and R.J.N. Phillips, Phys. Rev. 187 (1969) 2210.

[81] Ferro, Fontan, R. Ordorico, Nuovo Cimento 58A (1968) 534.

[82] M.G. Olsson, Nuovo Cimento 57A (1968) 420.

[83] L.K. Chavda, Phys. Rev. 186 (1969) 1463.

[84] V. Barger R.J.N. Phillips, Phys. Rev. Lett 24 (1970) 6

[85] V. Barger R.J.N.Phillips, Phys. Lett. 31B (1970) 643

[86] Schiff and Violini University of Rome (preprint)

[87] Ferrari and Violini Nuovo Cimento 69A (1970) 375

[88] R.J. Eden Phys. Rev.D (1970) 529

[89] J. Finkelstein Phys. Rev. Lett. 24(1970) 172

[90] W. Rarita Phys. Rev. D (1970) 11

DATA REFERENCES

DATA1

Total cross sections $\pi^{\pm}p$

(1) A.N. Diddens et al., Phys. Rev. Lett. 10 (1963) 262.

(2) A.A. Carter et al., Phys. Rev. 168 (1968) 1457.

(3) A. Citron et al., Phys. Rev. 144 (1966) 1101.

(4) F.E. James et al., Phys. Rev. 142 (1966) 896.

(5) G. Giacomelli, Stonybrook Conf. (1966).

Elastic and charge-exchange angular distributions $\pi^{\pm}p$

(6) C.T. Coffin et al., Phys. Rev. 159 (1967) 1169.

(7) V. Cook et al., Phys. Rev. 130 (1963) 762.

(8) M.A. Wahlig et al., Phys. Rev. 168 (1968) 1515.

(9) A.S. Carroll et al., Phys. Rev. 177 (1969) 2047.

(10) D.E. Damouth et al., Phys. Rev. Lett. 11 (1963) 287.

(11) W. Busza et al., Phys. Rev. 180 (1969) 1339.

(12) F.E. James et al., Phys. Lett. 19 (1965) 72.

(13) T. Dobrowolski et al., Phys. Lett. 24B (1967) 203.

(14) W.F. Baker et al., Phys. Lett. 25B (1967) 361.

(15) A.S. Carroll et al., Phys. Rev. Lett. 20 (1968) 607.

(16) A. Yokosana et al., Institute report Efins-66-29.

Recoil nucleon polarisation inelastic and charge-exchange scattering

(17) C.H. Johnson, Ph.D. Thesis, U.C.R.L. 17683 (1967).

(18) D. Drobnis et al., Phys. Rev. Lett. 15 (1965) 560.

(19) S. Suna et al., Phys. Rev. Lett. 15 (1965) 560.

(20) C.R. Cox et al., Phys. Rev. to be published.

(21) C.R. Cox, Rutherford Lab. Report R.H.E.L. M137 (1968).

(22) M.J. Hansroul, Ph.D. Thesis, University of California Radiation Lab. report U.C.R.L.-17263, unpublished.

DATA2

Charge exchange differential cross sections

(1) Stirling et al., Phys. Rev. Lett. 14 (1965) 763.

(2) Sonderegger et al., Phys. Lett. 20 (1966) 75.

(3) Wahling et al., Phys. Rev. 168 (1968) 1515.

Charge exchange polarisation measurements

(4) Drobnis et al., Phys. Rev. Lett. 20 (1968) 274.

(5) Bona et al., Nucl. Phys. B16 (1970) 335.

(6) Sonderegger, Cern 1971 unpublished.

DATA3

Total Cross Section $\pi^{\pm}p$

(1) Citron et al., Phys. Rev. 144 (1966) 1101.

(2) Foley et al., Phys. Rev. Lett. 19 (1967) 193.

Elastic Scattering differential cross sections

(3) Rust et al., Phys. Rev. Lett. 24 (1970) 1361.

(4) Foley et al., Phys. Rev. Lett. 11 (1963) 423.

(5) Harting et al., Nuovo Cimento 38 (1965) 60.

(6) Coffin et al., Phys. Rev. 159 (1967) 1169.

(7) Brandt et al., Phys. Rev. Lett. 10 (1967) 413.

Elastic Scattering polarisation measurement

(8) Borghini et al., Phys. Lett. 24B (1967) 77.
Borghini et al., Phys. Lett. 31B (1970) 405.
Bell et al., Vienna Conf. (1968).

DATA4

Total Cross Section Measurement

Interpolation (a)

(1) Citron et al., Phys. Rev. 144 (1966) 1101.

(2) Foley et al., Phys. Rev. Lett. 19 (1967) 193.

(3) IHEP-Cern, Phys. Lett. 30B (1969) 500.

Interpolation (b)

(4) G. Hohler et al., Tables of Pion Nucleon Amplitudes (October 1970).

Real Parts of Pion Nucleon Amplitudes

(5) Foley et al., Phys. Rev. 181 (1969) 1775.